

**SYNTHESIS AND CHARACTERIZATION OF PHOTOPOLYMERIZABLE
HYDROGELS FOR BIOMEDICAL APPLICATIONS**

by

Prutha Joshi

A dissertation submitted to the Graduate Faculty of
Auburn University
in partial fulfillment of the
requirements for the degree of
Doctor of Philosophy

Auburn, Alabama
August 8, 2020

Keywords: Hydrogels, poly (ethylene glycol) dimethacrylate, polysaccharides, double networks,
photopolymerization

Copyright 2020 by Prutha Joshi

Approved by

Dr. Maria L. Auad,
Chair, Associate Dean for Graduate Studies and Faculty Development, Director of Center for
Polymers and Advanced Composites, Professor of Chemical Engineering
Dr. Bryan Beckingham,
Committee member, Assistant Professor, Chemical Engineering
Dr. Xinyu Zhang,
Committee member, Associate Professor, Chemical Engineering
Dr. Soledad Peresin,
Committee member, Assistant Professor, School of Forestry & Wildlife Sciences

Abstract

Hydrogels are polymeric materials widely used in medicine due to their similarity with the biological components of the body. These biocompatible materials have the potential to promote cell proliferation and tissue support because of their hydrophilic nature, porous structure, and elastic properties. The hydrophilicity, mechanical properties and cell responsivity of modified polysaccharides can be tuned by controlling the chemical and molecular structure for different tissue engineering applications. The results show that there is a range of elastic modulus and degradation rate of hydrogels, which can be targeted for various biomedical applications.

In chapter two, we focused on the synthesis of different varieties of poly(ethylene glycol) dimethacrylate (PEGDMA) formulated from poly(ethylene glycol) (PEG) of different molecular weights and further photocured in the presence of a photoinitiator (Irgacure 184). Chemical, thermal, mechanical, rheological, and morphological characteristics were studied, as well as biodegradability. The ability of these hydrogels as material for cell growth was investigated for application towards tissue engineering.

In chapter three, the focus was on the incorporation of methacrylate functionality in gelatin and chitosan polysaccharides. The modified gelatin and chitosan were synthesized by controlling the degree of methacrylation of primary amine groups present in polysaccharides. Further, the effects of various varieties of hydrogels on swelling, mechanical, and rheological properties were investigated. The hydrogels were prepared by UV photocuring of modified polysaccharides in the presence of a photoinitiator Irgacure 184 (365nm wavelength).

In chapter four, we combine the properties of poly(ethylene glycol) dimethacrylate (PEGDMA) macromer and polysaccharides in double networks (DN) for synergistic effects of unique properties of both components resulting in the interpenetrating polymeric network for making it functional for replacement of injured tissues inside the human body.

In the final chapter, the research is based on how the synthesized hydrogels can also be 3D printed to obtain cellular structures for tissue engineering applications. The stereolithography (SLA) 3D printing was carried out with the macromer and double network of macromer systems to get variety in properties of the hydrogel to make it a complex-structured scaffold for tissue engineering.

Altogether, the biomaterial hydrogel properties open the way for applications in the field of medicine.

Acknowledgments

Ever since I came to Auburn University as a graduate student, I had a dream to learn more about my research and gain knowledge in the field. However, I had no idea how the journey towards the end of a doctoral degree will flow. Although there were few ups and downs over the years, the support of all the people who had immense faith in me kept me going in the pursuit of my doctoral degree. It is important, therefore, to show my gratitude for all the people who boosted my confidence and helped me rise in my journey to success.

First and foremost, I express sincere gratitude towards my advisor, Dr. Maria L. Auad, for her immense support, patience, advice, and encouragement. Thank you for believing in me and supporting and guiding me during crucial times. Her work ethic, coupled with her excellent teaching skills, served as a constant source of inspiration for me over these years. Also, the financial support to attend various regional, national and international level conferences help me expand my presentation skills and grow my professional network.

I am thankful to the funding agencies NSF-CREST, USDA, CPAC that provided financial support for various projects during this research. I am incredibly grateful to all the staff and faculty members of the Department of Chemical Engineering for supporting me and creating a happy environment to work. Special thanks to Elaine Manning and Naomi Gehling for their support. I would like to thank my colleagues in the department who were a great support system at times. My sincere gratitude to all my friends for treating me as a family over the years. The special thanks

to my friend and one of the best persons of my life, Kavita Kadu for your encouragement and support.

Besides, I appreciate the love and support of my family and my in-laws who have stood by me in tough times. My parents- Prashant and Radhika Joshi; grandparents- Sudhakar and Sunita Joshi, served as a source of encouragement every single day. They stood firm in the times of failures and boosted my confidence to make me what I am today. They have ingrained in me all the values and principles that have created my image today. They have the biggest smiles when I achieve my goals and show immense support when I failed. Words won't be enough to describe their contribution to my life. I owe my success to them. My sister, Swara Joshi always put a smile on my face, and I would forget about all my struggles whenever I spoke to her. Also, I would like to thank my father-in-law (Ravindra Mulay), mother-in-law (Meena Mulay) and sister-in-law (Gayatri Mulay) for supporting and believing in me. They believed in me more than I believed in myself and helped me to stay optimistic throughout the time.

Last but not least, a very special thanks from the bottom of my heart to my lovely husband Nikhil Mulay, for his love and support over these years. Every moment with you motivated me to become a better person. From your support during thick and thins to helping me manage my time and finances, your contribution is undeniable. You are the best thing to have happened to me ever. I am blessed to have you by my side.

Table of Contents

Abstract	ii
Acknowledgements	iv
List of Tables	xi
List of Figures	xii
List of Abbreviations	xv
CHAPTER 1 Introduction	1
1.1 Hydrogels	1
1.2 Chemistry of Hydrogels	2
1.3 Classification of Hydrogel	5
1.4 Hydrogels for Biomedical Applications	7
1.5 Hydrogels for Tissue Engineering	11
1.6 Challenges of Hydrogels for Tissue Engineering Applications.....	12
1.7 Overcoming Challenges of Hydrogels.....	16
1.7.1 Design an Interpenetrating Polymer Network (IPN) Hydrogels with superior mechanical performance	16
1.7.2 Use of Polysaccharides, such as gelatin and chitosan, to improve the biodegradability	18
1.7.3 Hydrogel scaffolds as cell carriers in tissue engineering.....	21
1.7.4 Hydrogels as Drug Delivery system	22

1.7.5 Hydrogels Based Bio-Inks for 3D Printing.....	23
1.8 Research Objectives.....	25
1.9 References.....	28
CHAPTER 2 Synthesis and Characterization of Photopolymerizable Hydrogels based on Poly (ethylene glycol) for Biomedical Applications	46
2.1 Introduction.....	46
2.2 Materials and Methods.....	48
2.2.1 Materials	48
2.2.2 Methods.....	49
2.2.2.1 Preparation of PEGDMA by chemical modification of PEG	49
2.2.2.2 Preparation of PEGDMA hydrogel.....	50
2.2.2.3 Characterization of PEGDMA samples	52
2.2.2.4 Cell attachment and growth on the hydrogel scaffolds.....	55
2.3 Results and Discussion	56
2.3.1 Characterization of the PEGDMA samples	56
2.3.2 Proliferation of fibroblast cells in the presence of the hydrogels	65
2.4 Conclusion	67
2.5 References.....	68
CHAPTER 3 Synthesis of polysaccharide-based hydrogels for biomedical applications....	73
3.1 Introduction.....	73

3.2 Materials and Methods.....	75
3.2.1 Materials	75
3.2.2 Methods.....	76
3.2.2.1 Preparation of gelatin methacrylate	76
3.2.2.2 Preparation of chitosan methacrylate.....	77
3.2.2.3 Preparation of hydrogel using modified polysaccharide	78
3.2.2.4 Characterization of polysaccharide hydrogels samples	79
3.2.2.5 Fibroblast cell attachment and proliferation on the hydrogel scaffolds.....	82
3.3 Results and Discussion	83
3.3.1 Characterization of hydrogels	83
3.3.2 Cell growth and proliferation on the hydrogel scaffolds	91
3.4 Conclusion	93
3.5 References.....	94
CHAPTER 4 Formulation of the polymeric double networks (DNs) for biomedical applications with physicochemical properties to resemble a biological tissue	99
4.1 Introduction.....	99
4.2 Materials and Methods.....	101
4.2.1 Materials	101
4.2.2 Methods.....	102
4.2.2.1 Preparation of hydrogel based on double networks (DN)	102

4.2.2.2 Characterization of double networks	103
4.2.2.3 Fibroblast cell attachment and proliferation on the hydrogel scaffolds.....	106
4.3 Results and Discussion	107
4.3.1 Characterization of double networks	107
4.3.2 Cell growth and proliferation on the hydrogel scaffolds	114
4.4 Conclusion	115
4.5 References.....	117
CHAPTER 5 Design and synthesis of stereolithography (SLA) 3D printed poly (ethylene glycol) diacrylate (PEGDMA) based hydrogels for biomedical applications.....	122
5.1 Introduction.....	122
5.2 Materials and Methods.....	122
5.2.1 Materials	124
5.2.2 Methods.....	125
5.2.2.1 Preparation of the bioink formulation.....	125
5.2.2.2 SLA 3D printing	127
5.2.2.3 SLA 3D printed Samples	128
5.2.2.4 Characterization of 3D printed samples.....	129
5.3 Results and Discussion	130
5.3.1 FTIR.....	130
5.3.2 Mass Swelling.....	132

5.3.3 Tensile Modulus.....	132
5.4 Conclusion	133
5.5 References.....	134
CHAPTER 6 General Conclusions and Future Work	138

List of Tables

Table 1.1 Classification of hydrogel.....	5
Table 1.2 Hydrogel chemistries for specific biomedical applications	10
Table 1.3 FDA approval check for a few biomaterials.....	20
Table 2.1 Gel permeation chromatography of different varieties of PEGDMA.....	58
Table 2.2: Modulated DSC data for different varieties of PEGDMA	62
Table 2.3: Characterization of the crosslinked PEGDMA hydrogels.....	63
Table 3.1: Characterization of different varieties of modified polysaccharide hydrogels.....	85
Table 4.1: Nomenclature of Double Network hydrogels.....	103
Table 4.2: Comparison of morphology and swelling behavior for DN hydrogels	110
Table 4.3: Characterization of the crosslinked DN hydrogels	111
Table 5.1: Composition of Bioink formulation.....	126
Table 5.2: Characterization of 3D printed hydrogels.....	132

List of Figures

Figure 1.1 General applications of hydrogels	2
Figure 1.2 Hydrophilic macromolecular networks	3
Figure 1.3 Crosslinking in a hydrogel (Reprinted with permission from Ullah et al. 2015) ³³	7
Figure 1.4 Hydrogels for medical applications	8
Figure 1.5 Tissue engineering of cartilage ⁸⁶	11
Figure 1.6 Forces exerted on hydrogel (Reprinted with permission from Li et al. 2018) ¹⁰²	14
Figure 1.7 Differentiation in the interpenetrating polymeric network.....	17
Figure 1.8 Classification of polysaccharides	19
Figure 1.9 3D printing for medical applications	24
Figure 2.1: Microwave-assisted synthesis of PEGDMA.....	49
Figure 2.2 Photo-crosslinking reaction of PEGDMA to obtain the PEGDMA hydrogel via free radical polymerization	51
Figure 2.3: ¹ H-NMR spectra of 8000 Da PEGDMA using microwave-assisted PEG modification. a) PEG and b) PEGDMA	57
Figure 2.4: FT-IR spectrum for a) PEGDMA hydrogel (post-photopolymerized) and.....	60
Figure 2.5: SEM image of PEGDMA hydrogel a) 4000 Da, b) 6000 Da and c) 8000 Da	61
Figure 2.6: Degradation profile of PEGDMA hydrogels.....	64
Figure 2.7: Effect on the morphological characterization after degradation of a hydrogel. a) PEGDMA 4000 at 0th week, b) PEGDMA 4000 after 2 nd week, c) PEGDMA 6000 at 0th week, d) PEGDMA 6000 after 2 nd week, e) PEGDMA 8000 at 0th week, f) PEGDMA 8000 after 2 nd week of degradation.....	65

Figure 2.8: Fibroblast Cell growth on PEGDMA 8000 hydrogels. A) Bright field images of the cells B) Live/Dead Stain images of the cells	66
Figure 2.9: Cell viability of Fibroblast cells by MTT assay	67
Figure 3.1: Methacrylation of a) gelatin and b) chitosan to obtain GelMA and ChMA, respectively.	77
Figure 3.2: Photo-crosslinking of a) GelMA to obtain the GelMA hydrogel, and b) ChMA to ChMA hydrogel via free radical polymerization	79
Figure 3.3: ¹ H-NMR spectra of a) GelMA, b) Gelatin, c) ChMA and d) Chitosan.....	84
Figure 3.4: FT-IR spectrum for a) gelatin and GelMA and b) chitosan and ChMA	86
Figure 3.5: SEM image of a) GelMA (7%), b) GelMA (16%), c) GelMA (21%) and d) ChMA (40%) hydrogel	88
Figure 3.6: Degradation rate profile for different varieties of PEGDA with lysozyme	90
Figure 3.7: Effect of enzymatic degradation on the morphology after 2 weeks of enzyme exposure on hydrogels a) GelMA (7%), b) GelMA (16%), c) GelMA (21%), d) ChMA (40%).	91
Figure 3.8: Fibroblast Cell growth on GelMA (21%) and ChMA (40%). A) Bright field images of the cells B) Live/Dead Stain images of the cells	92
Figure 3.9: Cell viability of Fibroblast cells by MTT assay	93
Figure 4.1: Photopolymerization reaction to obtain DN hydrogels	103
Figure 4.2: FT-IR spectrum for a) GelMA (21%), PEGDMA (8000 Da) and PEGDMA-GelMA DN, b) ChMA (40%), PEGDMA (8000 Da) and PEGDMA-ChMA DN	108
Figure 4.3: SEM image of a) P4G21%, b) P6G21%, c) P8G21% and d) P8C40% DN hydrogels	109
Figure 4.4: Degradation rate profile for different varieties of DN hydrogels with lysozyme	113

Figure 4.5: Effect on the morphology after 3 weeks of degradation of following DN hydrogels a) P4G21%, b) P6G21%, c) P8G21%, and d) P8C40%	114
Figure 4.6: Cell viability of Fibroblast cells by MTT assay	115
Figure 5.1: Bioink formulation for SLA 3D printing.	127
Figure 5.2: 3D printed structures. a) cellular ring (using Type 2 bioink), b) cellular structure (using Type 2 bioink), c) human ear (using Type 2 bioink), and d) rectangular strips (using Type 3 bioink)	128
Figure 5.3: FT-IR spectrum for a) Type 1 (PEGDA) and Type 2 (PEGDMA-PEGDA) bioink formulations, b) Type 3 (PEGDMA-PEGDA-GelMA) bioink, c) Type 4 (PEGDMA-PEGDA-ChMA) bioink formulation	131

List of Abbreviations

AA	Acrylic Acid
ASTM	American Society for Testing and Materials
ATR	Attenuated Total Reflection
BHT	Butylated hydroxy toluene
ChMA	Chitosan methacrylate
CD ₃ COOH	Deuterated Acetic acid
DCM	Dichloromethane
DIW	Direct Ink Writing
DMA	Dynamic Mechanical Analysis
DMEM	Dulbecco's Modified Eagle Medium
DMSO-d ₆	deuterated dimethyl sulfoxide
DN	Double Network
DSC	Differential Scanning Calorimetry
DPBS/PBS	Dulbecco's Phosphate Buffer Saline
D ₂ O	Deuterated Water
ECM	Extra Cellular Matrix
FBS	Fetal Bovine Serum
FDA	Food and Drug Administration
FDM	Fused Deposition Modeling
FTIR	Fourier Transform Infrared
GPC	Gel Permeation Chromatography
GelMA	Gelatin Methacrylate

HPLC	High Performance Liquid Chromatography
IPN	Interpenetrating Polymer Network
LIFT	Laser Induced Forward Transfer
MTT	(3-(4,5-Dimethylthiazol-2-yl)-2,5-Diphenyltetrazolium Bromide) salt
MA	Methacrylic Anhydride
NMR	Nuclear Magnetic Resonance
PDI	Poly Dispersity Index
PEG	Poly(ethylene glycol)
PEGDA	Poly(ethylene glycol) diacrylate
PEGDMA	Poly(ethylene glycol) dimethacrylate
PI	Photoinitiator
PS	Polystyrene
SAPs	Super Absorbent Polymers
SEM	Scanning Electron Microscopy
SLA	Stereolithography
SLS	Selective Laser Sintering
THF	Tetrahydrofuran
TMS	Tetramethyl silane
TT	Trimethylolpropane Triacrylate
UV	Ultraviolet
3D	Three Dimensional

CHAPTER 1

Introduction

1.1 Hydrogels

Hydrogels, by their nature, are soft materials that can swell in a solvent and are comprised of a crosslinked, three-dimensional network^{1,2}. Since the late 1970s, there have been several reports published in the scientific community about the physicochemical structures and innovative applications of hydrogels³.

In recent years, applications of hydrogels have grown exponentially, particularly as drug delivery systems, superabsorbent materials, microfluidics devices, contact lenses, etc⁴⁻⁹ (Figure 1.1). Superabsorbent polymers (SAPs) are lightly crosslinked hydrogels that can absorb large volumes of water or an aqueous medium (up to 2000 g/g). These polymeric hydrogels are currently used in a variety of applications, such as hygienic and biological applications (sanitary napkins and diapers); agrochemical uses (soil remediation and controlled release of agrochemicals); pharmaceutical applications; separation membranes; fibers and textiles; soft actuators and valves; packaging; artificial snow; sludge dewatering; and fire extinguisher gels. They have also been extensively studied for tissue engineering and regenerative medicine applications due to their stimuli-responsive properties⁴, biocompatibility^{7,10-13}, and elastic properties^{10,14-16}. The current global SAPs market is approximately 1.3 million metric tons. Despite the large number of SAPs being produced, there are few companies producing natural-based SAPs that are both biocompatible and biodegradable^{17,18}.

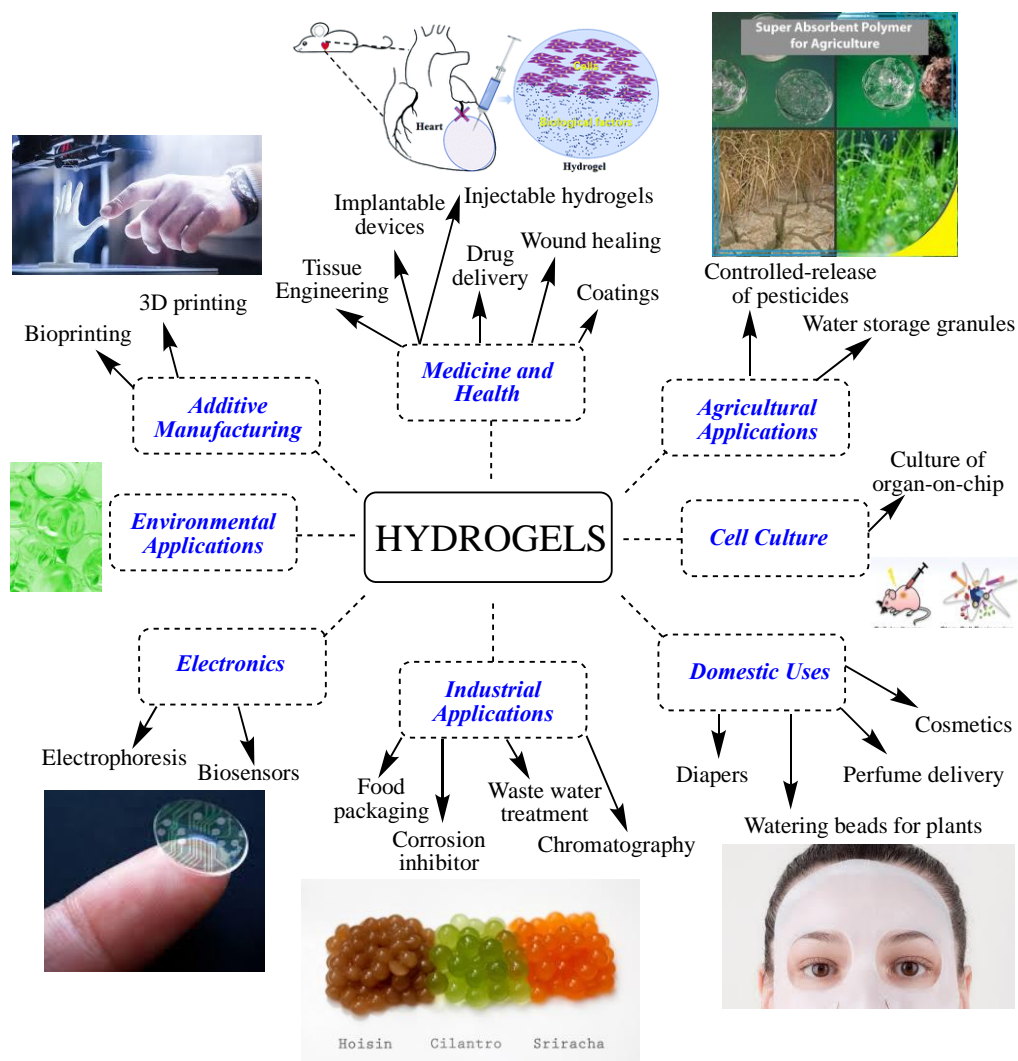


Figure 1.1 General applications of hydrogels

1.2 Chemistry of Hydrogels

In general, the hydrogel network is formed by either physical^{19,20} or chemical^{8,21,22} crosslinks. These 3D structures are able to swell in aqueous solutions until the thermodynamic force of swelling and the elastic and retractile force exerted by the crosslinks are at equilibrium. The amount of aqueous solution retained in the mesh of the hydrogel network depends on the structure of the polymer network and the environmental conditions, such as temperature²³, pH²⁴,

crosslinking agent^{25,26}, and ionic strength²⁷ of the solution. The volume or mass swelling ratio of a hydrogel is the most important property to be evaluated for given environmental conditions. Figure 1.2 describes the nature of a SAP hydrogel. It can be seen that the macromolecular chains involved in network formation acquire a coil-like conformation in the dry state. However, the crosslinked hydrogel in an aqueous medium absorbs a solution to form a swollen macromolecular network, and the structure significantly expands. The most important properties of SAP hydrogels are absorption capacity, absorption rate, and the swollen gel strength. The hydrogel strength in the swollen form depends on the crosslinking density or the number of crosslinking points^{17,18}.

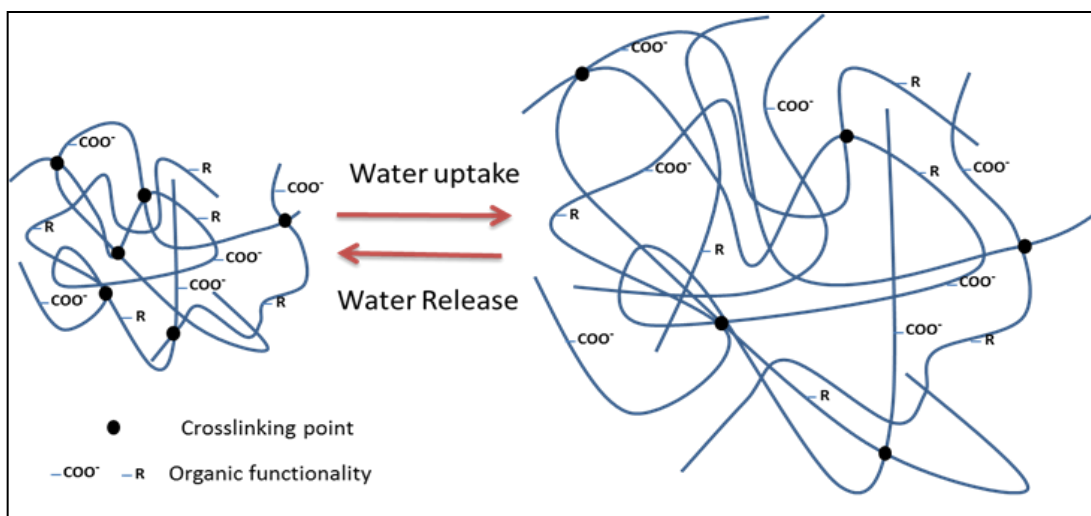


Figure 1.2 *Hydrophilic macromolecular networks*

The hydrophilic nature of hydrogels provides the moisture and controls drug permeation from hydrogel drug assembly as the hydrogel comes in contact with water, the polar groups solvate and it results in the appearance of primarily bound water. Further, when non-polar hydrophobic groups are exposed to water, they form secondary bound water. The combination of the primary and secondary bound water molecules creates bound water, which leads to the completion of the

hydration process. Lastly, an additional amount of water is absorbed, and infinite dilution is restricted due to covalent and physical crosslinks. Bulk water, also known as free water, is the equilibrium water uptake that fills the centers of large pores, macropores, or voids present in the hydrogel network³. The mass swelling ratio can be calculated from Equation 1.

$$\text{Mass Swelling (\%)} = \left(\frac{W_w - W_d}{W_d} \right) * 100 \quad \text{Equation 1}$$

Where W_w and W_d are the weight of hydrogel in its wet and dry state, respectively.

Crosslinking via free-radical polymerizations is the most common technique used to synthesize hydrogels by reacting hydrophilic monomers with multifunctional cross-linkers. Due to the increased usage of hydrogels, other crosslinking technique, such as photopolymerization, have become a standard technique. In photopolymerization, as the initiator is exposed to UV light, it dissociates into radicals that react with different functional groups, like C=C, to propagate the polymer chains until it forms a crosslinked network.

Some advantages of the photopolymerization process over traditional techniques³ are additional process control, faster curing rates at physiological temperatures (~37°C), and minimal heat production. Additionally, the photopolymerization technique minimizes health risks to the patient^{3,28,29} compared to those associated with any traditional surgery.

1.3 Classification of Hydrogel

With the growing multidisciplinary research fields on hydrogels and their revolutionized diversity, they can be classified in different ways based on paramount parameters. Table 1.1 highlights the most important classifications of hydrogels.

Table 1.1 Classification of hydrogel

Criterion	Classes of Hydrogel	Reference
<i>Origin</i>	Natural, Synthetic, Hybrid	3,30
<i>Charge</i>	Cationic, Anionic, Neutral, Amphoteric	3,4
<i>Crosslinking</i>	Physical, Chemical	3,19,31
<i>Structure and Composition</i>	Amorphous, Semi-Crystalline, Supramolecular, Hydrocolloidal Aggregations, Homopolymer, Copolymer, IPNs (or Double Network)	3,32,33

The most important classification of hydrogels is based on their origin; they can be natural, synthetic, or hybrid. Hydrogels, based on biopolymers that are obtained from nature, such as starch and polysaccharides, offer several advantages such as biodegradability, biocompatibility, easy availability, and low cost. Synthetic hydrogels are formed from non-renewable monomers and are favored due to their superior performance in mechanical strength, but they are difficult to degrade. Hybrid hydrogels are a combination of monomers obtained from renewable and synthetic sources. Another important classification is based on the nature of the charge on side groups. Hydrogels are either cationic, like chitosan, anionic, like alginate, neutral, like cellulose, or amphoteric, which is when positive as well as negatively charged species are present, like zwitterionic ionic hydrogels. Based on crosslinking, hydrogels can either be physically or chemically crosslinked. This can be observed in Figure 1.3³³. If the polymer chains are covalently bonded via a crosslinking

agent, it is a chemical crosslinking. Whereas, in physical crosslinking, there are hydrogen bonds, physical domain junctions, hydrophobic interaction, or ionic complexation. M_c is defined as the molecular weight of polymer chains between the crosslinking points³². Based on their structure and physical properties of hydrogel can be amorphous, semi-crystalline, supra-molecules, or hydrocolloidal aggregations³³. Finally, they can be classified based on their molecular arrangement during the preparation of hydrogels as either homopolymer, copolymers, or interpenetrating polymer networks³³. Homopolymer hydrogels are crosslinked networks formed from a single kind of monomer. Copolymer hydrogels, on the other hand, are produced by the crosslinking of two different monomer units, at least one of which must be hydrophilic to render them swellable. Interpenetrating polymeric network hydrogels are produced by fully or partially interlacing two or more polymer networks so that they cannot be separated unless chemical bonds are broken.

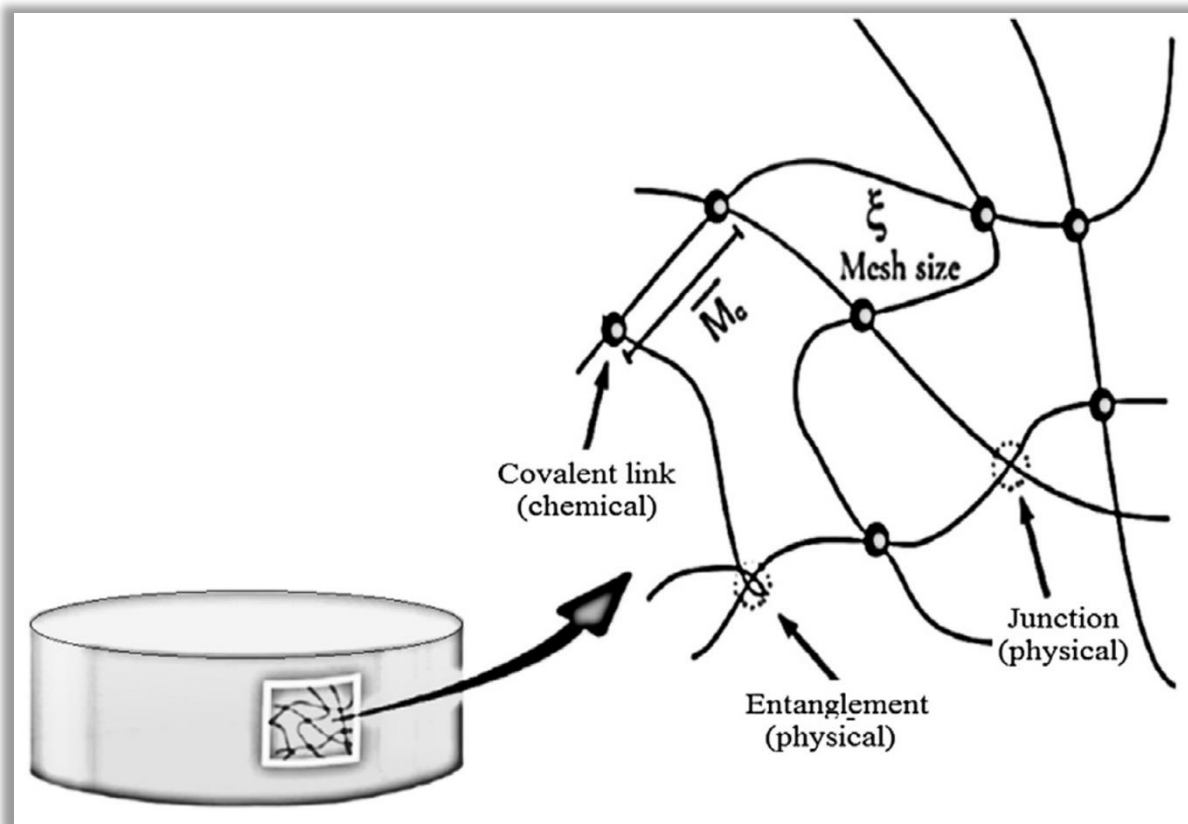


Figure 1.3 Crosslinking in a hydrogel (Reprinted with permission from Ullah et al. 2015)³³

1.4 Hydrogels for Biomedical Applications

Since the 1950s, hydrogels have gained applications in numerous biomedical disciplines, like in ophthalmology as contact lenses and surgery as absorbable sutures and wound dressings. Besides, hydrogels have been used in a plethora of different areas in clinical practice to recover from various illnesses such as diabetes mellitus³⁴, osteoporosis³⁵, asthma³⁶, heart diseases³⁷, and neoplasms^{38,39}.

Figure 1.4 illustrates the major medical applications of hydrogels.

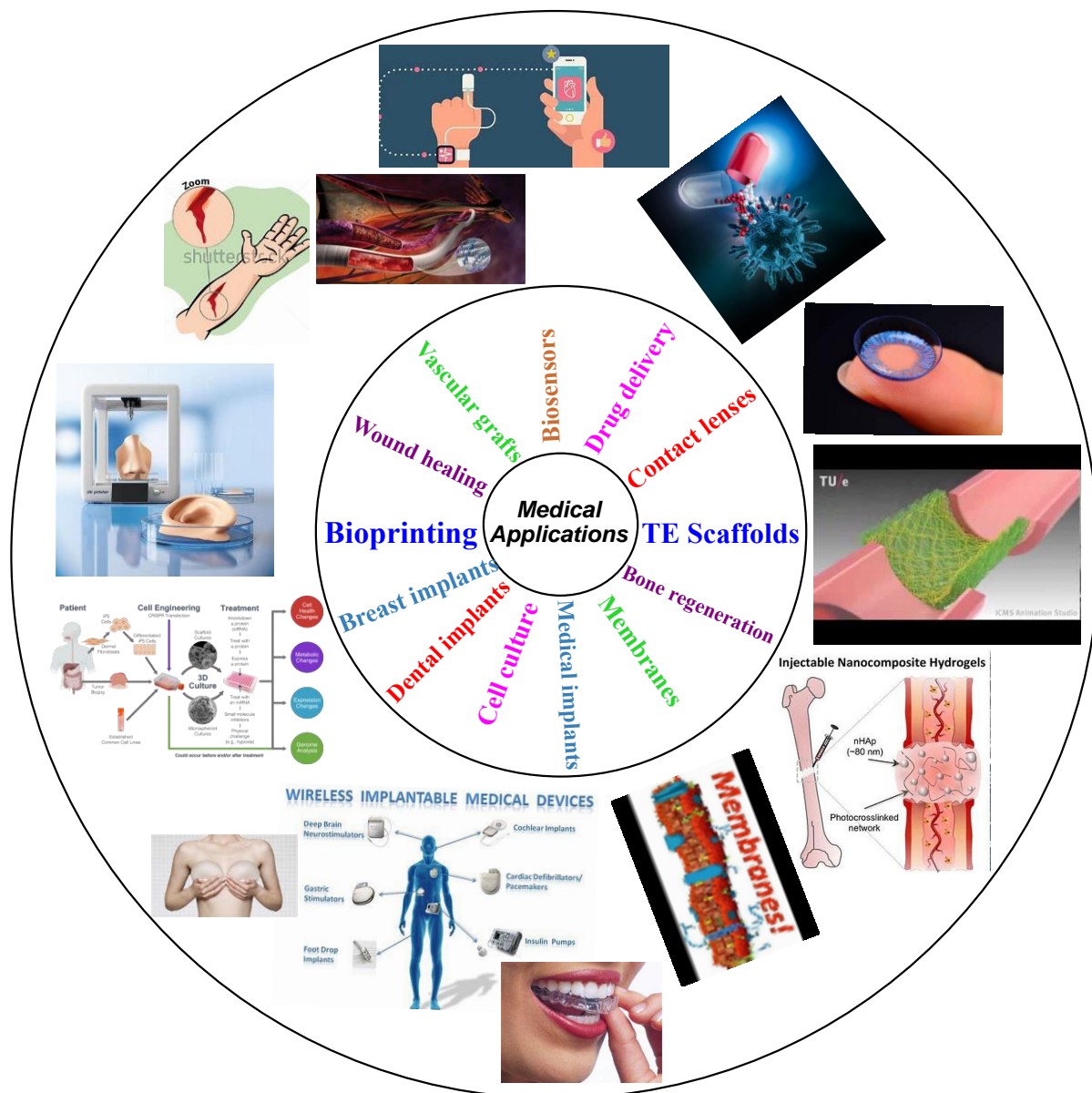


Figure 1.4 Hydrogels for medical applications

In the 1980s, Lim et al.⁴⁰ studied calcium alginate-based microcapsules for cell engineering and Yannas et al.⁴¹ modified synthetic hydrogels with natural substances, such as collagen and shark cartilage to obtain new artificial wound dressings, providing optimal conditions for healing burns.

To design a wound dressing for a patient, it is required to understand the condition of a patient's wound, the effect of material used in dressing on the wound and the healing process¹³.

Since the 2000s⁴², the applications of hydrogels in the field of biomedicine have been especially advancing in regenerative medicine and tissue engineering. Cell culture and injectable hydrogels are evolving with new materials considering safety and toxicity issues. The current trends of applications of hydrogels as bio-inks in three-dimensional printing of objects are favorable in stem cell research, cancer research, and tissue engineering. Bioprinting is an extensively researched field for aiming the production of engineered tissue or organ in a mechanized, optimized, and organized manner. Table 1.2 further illustrates the specific polymers suitable for a particular medical application of a hydrogel.

Table 1.2 Hydrogel chemistries for specific biomedical applications

Medical Applications	Systems	References
<i>Drug Delivery</i>	Poly(hydroxyethyl methacrylate), Hyaluronic Acid, Polysaccharides, PEG-Diacrylate, PEG-Acrylates	43–49
<i>Wound dressing/ Wound Healing</i>	Gelatin, Hyaluronic Acid, Cellulose, Alginate, Chitosan, Poly(vinyl pyrrolidone), Poly(vinyl alcohol)	13,34,41,42,50–54
<i>Contact Lenses</i>	Poly(hydroxyethyl methacrylate), Poly(vinyl alcohol),	3,54–57
<i>Tissue Engineering Scaffolds</i>	Hyaluronic Acid, Chitosan, Alginate, PEG, PEG-Acrylate, PEG-Diacrylate, Cellulose, Collagen, Gelatin, Dextran, Polycaprolactone, Poly(vinyl alcohol), Agarose, Acrylic Acid, Methacrylamide	19,38,47,58–61
<i>Injectable Hydrogels</i>	PEG, PEG-Diacrylate, Polysaccharides, Hyaluronic Acid, Gellan Gum	42,62–67
<i>Implants</i>	PEG, Poly(acryl amide), Poly(vinyl alcohol), HEMA, Acrylic Acid, PEG-Acrylate	68–70
<i>Biosensors and diagnostics</i>	Poly(ethylene oxide), Potassium Poly(acrylate), Poly(vinyl alcohol), Gelatin	42,71
<i>Bioprinting</i>	Hyaluronic Acid, Chitosan, Alginate, PEG, PEG-Acrylate, PEG-Diacrylate, Cellulose, Collagen, Gelatin, Polycaprolactone, Poly(vinyl alcohol), Acrylic Acid	72–79
<i>Vascular Grafts</i>	Hyaluronic Acid, PEG, PEG-Acrylate, PEG-Diacrylate, Collagen, Polycaprolactone, Poly(vinyl alcohol), Acrylic Acid, Methacrylamide	6,80–83
<i>Bone Regeneration</i>	Alginate, Fibrin, Chitosan, Hyaluronic Acid	35,42

1.5 Hydrogels for Tissue Engineering

Tissue engineering is a multifaceted field that combines engineering and life sciences to fabricate biological substitutes that can restore, support, or improve tissue function^{80,84}. Tissue engineering can be either be used in a *therapeutic application*, where new tissue is cultured in-vivo or in-vitro for transplantation, as seen in Figure 1.5, or in *diagnostic applications*, where the tissue is cultured in-vitro and used for determining drug metabolism, uptake, toxicity, and pathogenicity^{82,85}.

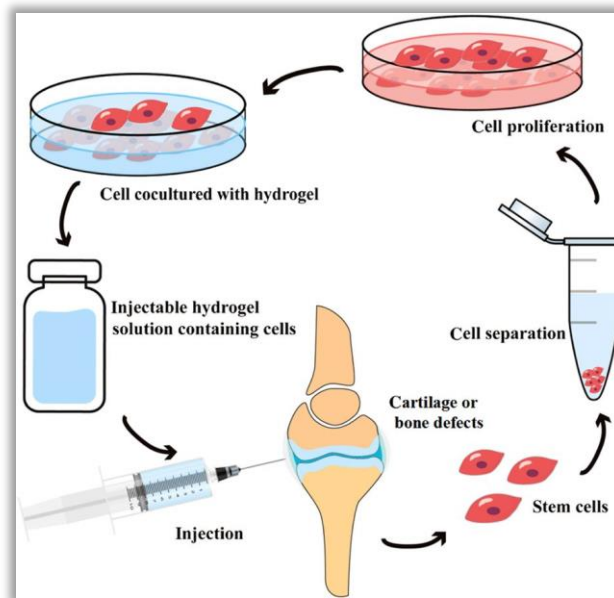


Figure 1.5 Tissue engineering of cartilage⁸⁶

Hydrogels have played an essential role in the field of tissue engineering and regenerative medicine^{20,49}. Recent developments of hydrogels include hydrogels derived from a variety of natural polymers like dextran^{11,42}, pectin⁸⁷, collagen⁹, cellulose⁸⁸, hyaluronic acid⁸⁹, alginate⁸⁸, chitosan⁹⁰, and many others. The main applications of hydrogels for tissue engineering applications are as space-filling agents, drug delivery assemblies for bioactive molecules, three-

dimensional structures to organize cells and present stimuli for desired tissue formation, and tissue adhesives. Hydrogels, due to their inbuilt properties, can reproduce the structure of the extracellular matrixes (ECM) and allow for cell adhesion and proliferation.

Kim et al.⁹¹ elaborate on the in-depth analysis of the tissue engineering market space with 49 publicly listed tissue-engineering companies in the United States. Out of 49 companies, 21 of them had sales of \$9 billion in tissue engineering related products during 2017. Also, biomaterial-based companies are the primary contributor to the tissue engineering market in the United States. Stem cell companies have the highest share of R&D expenses among tissue engineering companies in the US. Kim et al.⁹¹ reported that a large amount of the tissue engineering-related clinical trials, around 77% of the total tests, were sponsored by the industry. In comparison, category wise tissue engineering market contribution is 79.5%, 60%, and 87.5% for biomaterials (cells and biomaterials), and stem cells, respectively. The survey⁹¹ by Kim et al. suggests that there is continued interest from industry to grow and push tissue engineering products onto the market.

1.6 Challenges of Hydrogels for Tissue Engineering Applications

A structurally strong, biodegradable, and porous hydrogel plays a critical role in tissue engineering^{82,92}. Hydrogel scaffolds not only needs to provide a tissue template, but it also needs to support cell attachment, proliferation, and differentiation. Therefore, the chemical composition, physical structure, and biological functionality are influential aspects of tissue engineering applications^{93,94}. A perfect hydrogel scaffold must be biocompatible and biodegradable with tunable degradation rates and nontoxic by-products. It should have a three-dimensional structure

and a highly absorptive and interlacing pore network to expedite the nutrient and waste transport. It should have good mechanical properties to support the reconstruction process, and it should have the relevant surface chemistry and surface contour to interact with the cells^{82,95,96} easily. Keeping the above criterion in mind, the main challenges of hydrogels are: *i) mechanical strength, ii) degradation, iii) cell carriers for tissue engineering, iv) drug delivery, and v) complex shape and geometry.*

Mechanical Strength

The lack of mechanical strength is a concern in most of the synthetic hydrogel as compared with the hydrogel-like bio-tissues such as cartilage⁹, tendon⁹⁷, muscle⁹⁸, and blood vessel^{99,100}. Natural bio-tissues have outstanding mechanical characteristics. For example, cartilage tissue possesses a high toughness, good shock-absorbance, and low sliding friction, as reported by Fung et al.¹⁰¹. On the contrary, classical polymeric hydrogels can have non-uniform networks, which can lead to lower mechanical strength. Matricardi et al. studied polysaccharide hydrogels, and stated that the main reason for the failure of the hydrogels sample at high forces is due to concentration of stresses around short polymer chains²⁰. Li et al.¹⁰² studied the double network hydrogels to substitute load-bearing, degenerated soft tissue. They found that compression failure is the major issue for hydrogels used as a tissue-engineered scaffold. The hydrogels are required to withstand a variety of forces like folding, pushing, or pulling for targeted applications inside a human body. This can be observed in Figure 1.6. Therefore, developing new artificial substitutes of tissues with polymeric hydrogels has been a challenging task.

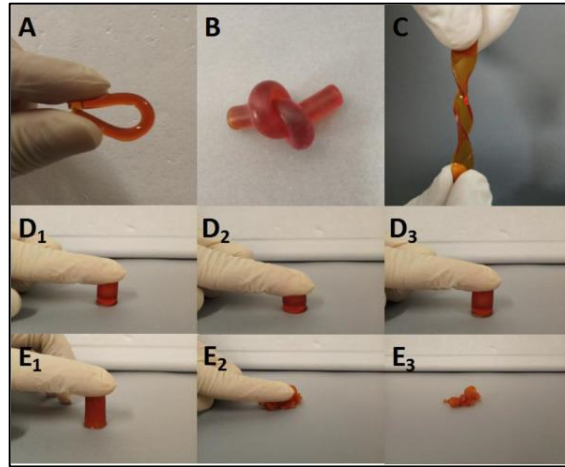


Figure 1.6 Forces exerted on hydrogel (Reprinted with permission from Li et al. 2018)¹⁰²

Degradation

A hydrogel-based scaffold needs to undergo degradation after performing any application inside the body. The biodegradation of hydrogels, as well as the rate at which it degrades, are considered important designer factors¹². During the process, the by-products or exudates must be nontoxic¹⁰³. The degradation rate of the scaffold, rate of cell growth, and rate of removal of decomposition products are the three crucial factors for determining the biodegradation of a scaffold hydrogel. The biodegradation of hydrogels can be catalyzed using acid, free radical degradation, oxidation-reduction depolymerization, or enzymatic degradation¹². The enzymatic degradation profile of hydrogels can be studied to simulate the physiological conditions found in the human body. It is reported in the literature^{12,103} that the rate at that the hydrogel degrades should match the rate of tissue formation to ensure that there is no hindrance in tissue remodeling. Thus, the degradation is a pivotal property of engineered constructs with an ability to mimic the structure of the extracellular matrix, making it suitable for drug or cell delivery, space-filling agents, and other tissue engineering applications.

Cell carrier for tissue engineering

Hydrogels, in regenerative medicine, do have limitations specifically when it comes to their role as a cell carrier in tissue engineering applications^{98,104–106}. Because the aim is to restore or replace damaged tissues using a combination of cells, scaffolding materials, and growth factors, scaffolding material temporarily acts as an extracellular matrix. The challenges¹⁰⁷ involved in this are- firstly, it must provide a good supporting structure for the cells, and secondly, must have a place that can let the cells to deposit their specific extracellular matrix. The application of cells in tissue engineering robustly depends on the regulation of cell fate, cell morphology, proliferation, differentiation, and adhesion. There is a need for a suitable vehicle for cell delivery to retain the required number of cells and preserve cell phenotype with the matrix support.

Drug delivery

Hydrogels, however, do have several limitations in drug delivery applications^{43,108,109}. The premature dissolution or flow away of the hydrogel from the local targeted site limits its area of effectiveness. The continuous exchange of nutrients, proteins, gases, and waste products into, out of, and within the hydrogel is essential in drug delivery. The hydrogel network structure and the thermodynamic nature of the components of these networks play a crucial role in their diffusional behavior, molecular mesh sizes, and stability¹⁰⁸. The challenges for a hydrogel to function as drug delivery assemblies are control over the network structure and tuning of a drug release mechanism in order to facilitate the delivery of drugs from the delivery site to the target site inside the body.

Complex shape and geometry

Although hydrogels can be formulated in a variety of physical forms^{72,73,110–112}, the control over the complex shape and geometry of hydrogel is needed. Additive manufacturing has been studied to fabricate different shape-specific and application-specific hydrogels. Additive manufacturing is used for precise three-dimensional construction in a layer by layer fashion. This is also defined as 3D printing¹¹³. Recently, different research groups are using this technique for improving the applicability and function of scaffolds. Researchers are exploring different biomaterials with fast crosslinking behavior (as a prerequisite) for 3D printing in the field of tissue engineering. Two important challenges¹¹³ to be considered are the printability of the fabrication process and the cell compatibility and viability. Other minor challenges cannot be ignored, such as stability, crosslinking time and interlayer adhesion of the printed objects.

1.7 Overcoming Challenges of Hydrogels

In this work, we propose the following approaches to overcome the previously listed challenges for a hydrogel in its tissue engineering application.

1.7.1 Design an Interpenetrating Polymer Network (IPN) Hydrogels with superior mechanical performance

Interpenetrating polymer networks^{32,114} (IPN), also called double networks (DNs)³², are comprised of two or more networks of polymeric material which are partially interlaced on a molecular scale but are not bonded with a covalently bond to each other and cannot be separated without breaking the chemical bond. Different types of IPNs, as seen in Figure 1.7, include semi-IPNs, full-IPNs, and graft-IPNs. It can be seen that the crosslinking points increase from left to right in the figure.

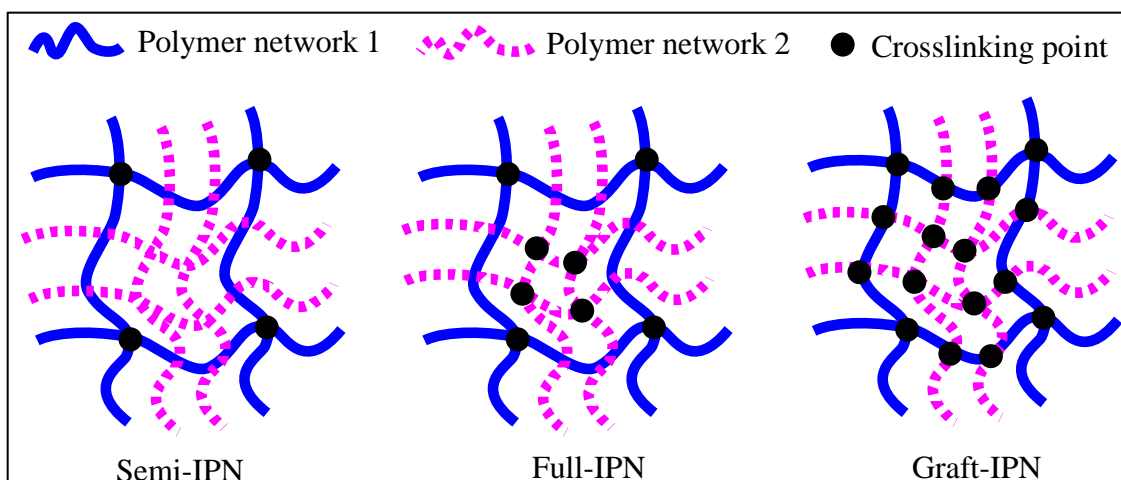


Figure 1.7 Differentiation in the interpenetrating polymeric network

The application of double networks or IPNs will help with the bio-adhesion and tuning of network properties, cell compatibility, biodegradability, and stimuli-responsive behavior. This is because the double network possesses properties from both components of the dual system, which allows for drug delivery and their application as scaffolds for tissue engineering²⁰. The individual polymers that make up the double network hydrogels affect overall properties such as network density, rigidity, molecular weight, and crosslinking density. The reason for exploring double network hydrogels is because of the combination of favorable properties of each constituent polymer leading to new systems with improved properties that are sometimes different from those of the individual polymers components²⁰.

Haque et al.⁹⁹ reported that interpenetrating hydrogels based on poly(2-acrylamido-2-methylpropanesulfonic acid) and polyacrylamide contain about 90wt% water, possess better mechanical performance with an elastic modulus of 0.1-1.0MPa, a failure tensile stress of 1-10MPa at a strain between 1000-2000%, a failure compressive stress of 20-60MPa at strain 90-

95%, and a tearing fracture energy of 100-4400 J.m⁻²⁹⁹. The individual polymeric hydrogels made from poly(2-acrylamido-2-methylpropanesulfonic acid) had a toughness of ~0.1 J.m⁻², and those made from polyacrylamide possess a toughness of ~10 J.m⁻², which shows the need of a double network to get better performance. IPN hydrogel systems synthesized by other researchers⁸⁸ are based on cellulose/gelatin, where the observed Young's modulus of elasticity was ~100 times greater than individual gelatin hydrogel. The above examples show how having a double network system enhances the mechanical performances that had not been observed in individual synthetic or natural hydrogels, and they are comparable to and even exceed some soft loadbearing tissues¹⁰¹.

1.7.2 Use of Polysaccharides, such as gelatin and chitosan, to improve the biodegradability

Polysaccharides are one of the types of biopolymers, which can be seen in Figure 1.8. They consist of multiple small monosaccharides, such as simple sugars like glucose, units bonded together by enzymes or peptides. Polysaccharides, such as cellulose⁸⁸, hyaluronic acid⁸⁹, alginate⁸⁸, chitosan⁹⁰, collagen^{115,116}, gelatin¹⁰⁶, and many others, are commonly used to develop hydrogels with the potential for supporting cell adhesion and function^{47,117,118} for tissue engineering applications^{20,49}.

Polysaccharides are gaining attention due to their abundance, accessibility from renewable sources, and the ability to retain the variable composition and various properties that allow for chemical modifications. The functional groups present along the backbone of polysaccharide can undergo chemical modifications to enhance the properties and make new polymer systems, like obtaining crosslinked chains.

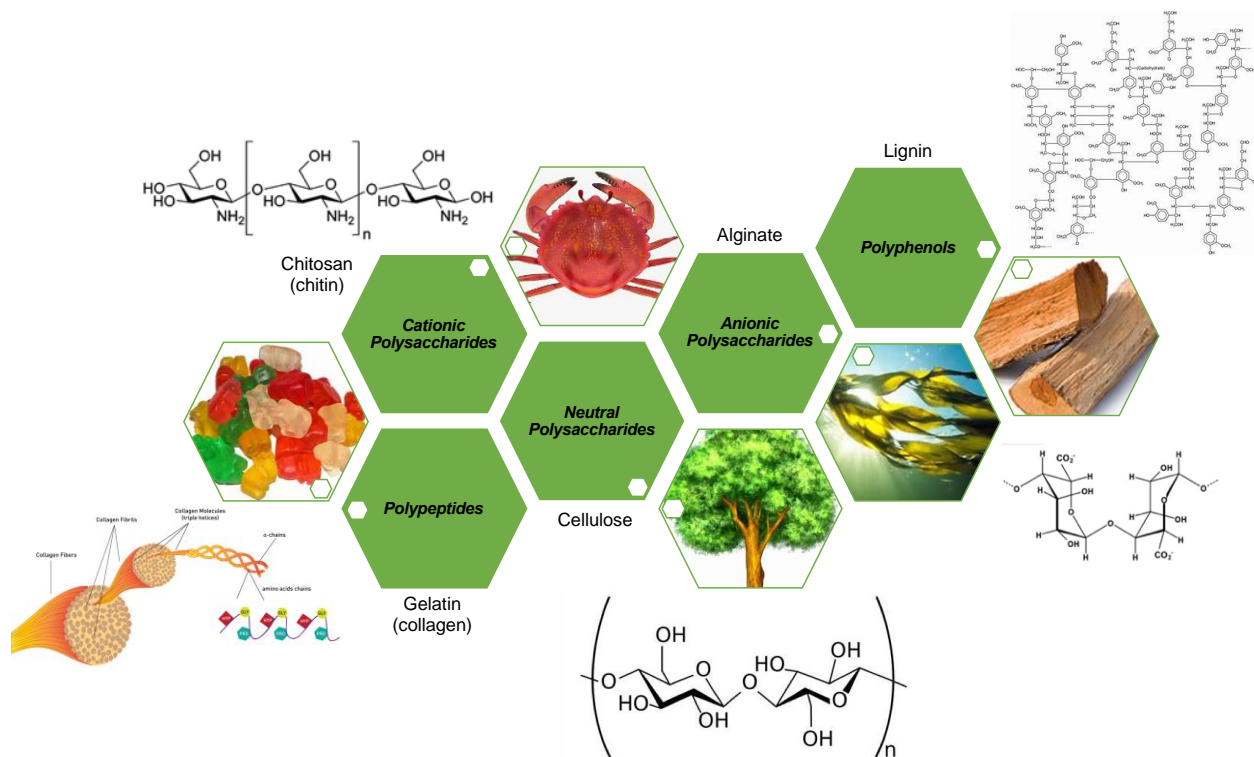
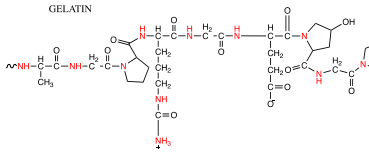
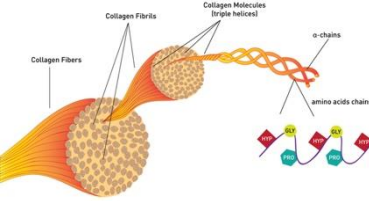
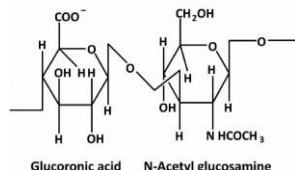
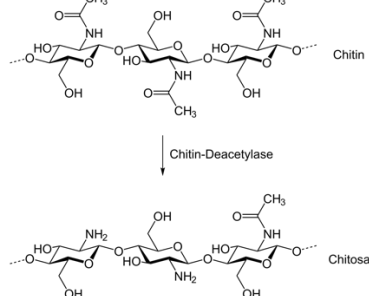
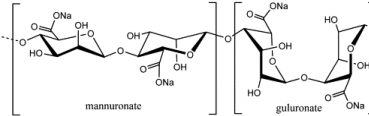
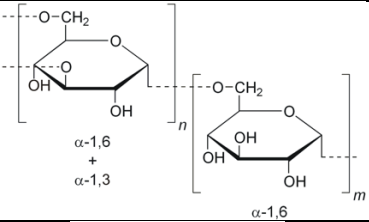
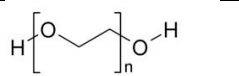
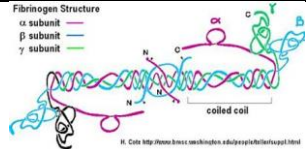
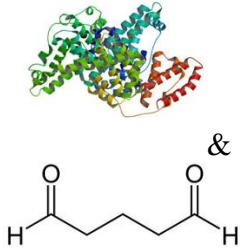
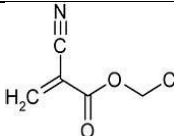


Figure 1.8 Classification of polysaccharides

Because of the characteristics of polysaccharide, like biodegradability and biocompatibility, hydrogels can have properties that allow it to be used as bio-like natural hydrogels inside the body for major biomedical or pharmaceutical applications. The combination of desirable properties by incorporating multiple polymeric networks is the key to have artificial hydrogels mimicking the functions of tissues^{20,49}. Moreover, FDA approval of biomaterial incorporation inside the body during any biomedical applications is essential to verify the safety and toxicity of those polymers. The FDA approved materials can be seen in Table 1.3.

Table 1.3 FDA approval check for a few biomaterials

Biomaterial	Source	Structures	FDA Approval Status	Ref.	
Polysaccharides	Gelatin	Denatured collagen Type A: Porcine; Type B: Bovine		✓	119,120
	Collagen	Extra cellular matrix (ECM)		✓	121
	Hyaluronic Acid	Enclosed in ECM		✓	122
	Chitosan	From chitin of the crustacean skeleton		✓	123
	Alginic Acid	Brown algae		✓	124,125
	Dextran	From digestion of amylopectin		✓	126
	PEG based			✓	127-129

Non-Polysaccharides	Fibrin	Protein		✓	130
	Albumin & Glutaraldehyde	Protein		✓	127,131
	Cyanoacrylate			✓	130,132 -135

1.7.3 Hydrogel scaffolds as cell carriers in tissue engineering

According to the European Commission on Health and Consumer Protection, there should be the synergy of cells, biomolecules, and supporting structures at the appropriate site in tissue engineering¹³⁶. Since the last decade, such hydrogels have been explored as matrices for regenerating and repairing a wide variety of tissues and organs^{19,81,136-138}. Natural or synthetic hydrogels have gained significant interest in cell encapsulation^{29,113,136}. The hydrogel can form chemically stable and biodegradable gels due to its property of hydrophilicity.

The characteristic properties of hydrogels make them especially appealing for repairing and regenerating soft tissue^{19,54,137,138}. The hydrogel can play the multiple roles to be a tissue-engineered scaffold, such as defining a space that molds the regenerating tissue, the temporary substitution of tissue functioning, and guide for tissue ingrowth. Therefore, there is an utmost need for hydrogel to fulfill the basic requirements of scaffold designing. Hydrogels, with (i) high

porosity (for interconnectivity for optimal nutrient/waste flow and tissue ingrowth); (ii) relevant internal geometry and pore dimensions (5-10 times the cell diameter); biodegradable nature; (iii) maintaining the mechanical integrity; and (iv) having suitable cell-biomaterial interactions can be easy to manufacture the targeted cell-laden scaffolds¹³⁶.

1.7.4 Hydrogels as Drug Delivery system

The first hydrogel based on hydroxyethyl methacrylate was formulated for contact lenses production^{3,54-57}. The significant advantages found in these hydrogels were their stability under varying pH and temperature conditions. Hydrogels have been extensively used as intelligent carriers for peptides, proteins, or drug delivery^{36,39,42,43,139,140}. They have been used to regulate drug release in controlled systems or as carriers for controlled release devices¹⁰⁹. The physical and chemical properties of a hydrogel can be tuned to optimize permeability, surface functionality, biodegradability, and surface recognition sites for acting like the drug delivery assemblies. Drug release can be triggered using one or more of the following: control over swelling properties, encapsulation, temperature, pH, enzymatic response, and molecular recognition³⁰.

Polymeric hydrogels with interpenetrating networks (or double networks) have the capability for drug delivery systems because of their improved physical properties⁴³⁻⁴⁵. Gaining control over the number of active chains between crosslinks in the matrix and the affinity to water can promise high porosity¹³. The porous structure of hydrogels allows the loading of drugs into the gel matrix and subsequent diffusion of the drugs. The drug delivery applications are for sustained release of

a drug resulting in the maintenance of a high local concentration of an active pharmaceutical ingredient over a prolonged period⁴³.

Indeed, the benefits of hydrogels for drug delivery may be as follows: the creation of formulation through which drugs slowly elute, maintaining a high local concentration of drug in the surrounding tissues over an extended period, and a systemic delivery process.

1.7.5 Hydrogels Based Bio-Inks for 3D Printing

3D printing is an emerging technology that is capable of assembling living as well as non-living biological matrices to form an ideal complex layout for further tissue maturation. It follows the mechanized, organized and optimized pathway to needed fabricate engineered tissue. To establish intricate tissue designs for simulation of the natural structure of organs and tissues present in the human body, a variety of biomaterials and printing techniques are available to print in different shapes, sizes, and resolutions¹¹². With this, the emphasis is given on the production of tissue engineering scaffolds with controlled parameters, such as porosity, permeability, and others, to be considered for biomedical devices as well as tissue models^{74,141–145}. Computer-aided design (CAD) using the specific and complex geometrical data obtained from the medical imaging techniques, such as X-ray imaging, magnetic resonance imaging, and micro computerized tomography scan, helps in fabricating tissue structures that can be successfully printed. 3D printing in the field of medical and health science promises the following benefits: the advancement of personalized patient-specific 3D engineered-objects, high precision, and economic and production-on-demand creation of complicated structures within a limited time-frame^{146,147}.

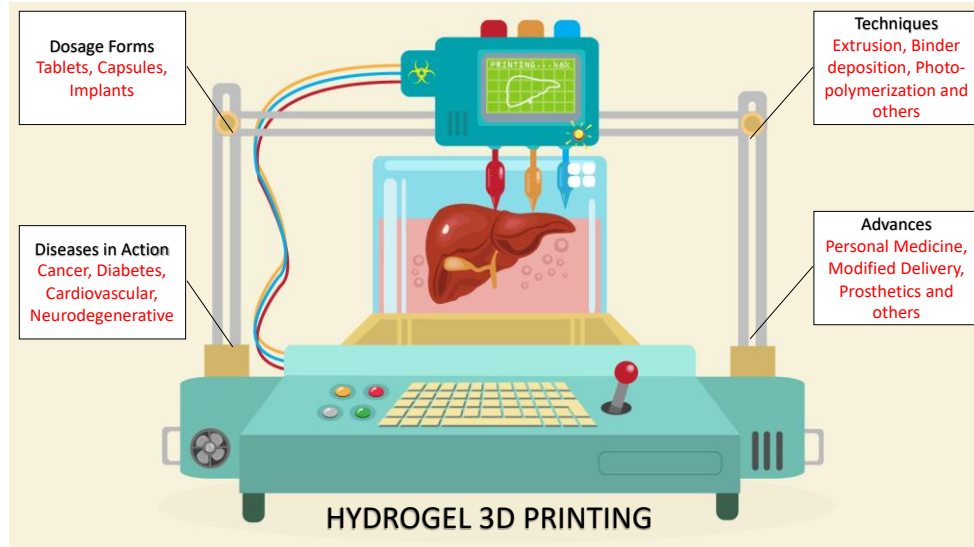


Figure 1.9 3D printing for medical applications

The popular 3D printing technologies include fused deposition modeling (FDM), direct ink writing (DIW), inkjet bioprinting, selective laser sintering (SLS), stereolithography (SLA), and laser-induced forward transfer (LIFT)^{74,75,77}. In the case of DIW, extrusion of highly viscous polymeric solutions or cell suspensions is essential to obtain 3D structures¹⁴⁴. In inkjet bioprinting, less viscous solutions such as suspensions or colloidal solutions can be deposited as droplets having a high rate of shear^{74,148–150}. Whereas, for the SLA method, the photocuring process is typically not affected by viscosity and occurs without degrading the bio-ink^{10,74,151,152}. Other methods, such as acoustic bio-printing, microwave bio-printing, electro-hydrodynamic bio-printing, and pneumatic bio-printing are currently studied and practiced for bioprinting of tissues and organs^{74,79}. Although 3D printing has numerous benefits in biomedicine, more research in bio-ink designing is required for proper commercialization.

1.8 Research Objectives

Considering the biomedical applications of hydrogels, the research objectives for this Ph.D. thesis are:

Objective 1: Synthesis and characterization of photopolymerizable hydrogels based on poly(ethylene glycol) for biomedical applications

Hydrogels are polymeric materials widely used in medicine due to their similarity with the biological components of the body. Hydrogels are biocompatible materials that have the potential to promote cell proliferation and tissue support because of their hydrophilic nature, porous structure, and elastic mechanical properties. In this work, we demonstrate the microwave-assisted synthesis of three molecular weight varieties of poly(ethylene glycol) dimethacrylate (PEGDMA) with different mechanical and thermal properties and the rapid photocuring of them using 1-hydroxy-cyclohexyl-phenyl-ketone (Irgacure 184) as UV photoinitiator. The effects of the poly(ethylene glycol) molecular weight and degree of acrylation on swelling, mechanical, and rheological properties of hydrogels were investigated. The biodegradability of the PEGDMA hydrogels, as well as the ability to grow and proliferate cells were examined for its viability as a scaffold in tissue engineering. Altogether, the biomaterial hydrogel properties open the way for applications in the field of regenerative medicine for functional scaffolds and tissues.

Objective 2: Synthesis of polysaccharide-based hydrogels for biomedical applications

The traditional hydrogel materials have reported low cell-responsivity and have limited biodegradability. Polysaccharides possess potentially useful biological as well as physicochemical

properties. To obtain biocompatible hydrogels for use as tissue engineering scaffolds, polysaccharides like gelatin and chitosan were modified to get methacrylate functionality to make it a photo-polymerizable system. Methacrylation was verified by $^1\text{H-NMR}$. The degree of methacrylation varied from 7%-40% by changing the molar ratio of polysaccharide to methacrylic anhydride and the type of polysaccharide. After modification by methacrylation reaction, free radical polymerization reaction occurs to obtain a polysaccharide-based hydrogel in the presence of UV light and Irgacure 184 as a photoinitiator. The physical, chemical and mechanical properties of the hydrogels were further characterized. By controlling the degree of methacrylation of the respective polysaccharides, it can be observed that the hydration and mechanical properties of modified polysaccharides can be tuned to different biomedical applications. The biodegradability of the polysaccharide hydrogels was investigated for its viability as a scaffold in tissue engineering along with cell culturing with stem cells. Fibroblasts seeded directly onto the hydrogel surface, populated the entirety of the hydrogel, and remained viable for up to one week.

Objective 3: Formulation of the polymeric double networks (DNs) for biomedical applications with physicochemical properties to resemble a biological tissue

In the current objective, we synthesized the hydrogel with double networks (DN) by combining the poly(ethylene glycol) dimethacrylate (PEGDMA) macromer and polysaccharides as the two components. The DN possess synergy of unique properties of individual components resulting in the interpenetrating polymeric network. This makes it suitable for the replacement of injured tissues inside the human body. The hydrogels were characterized for physical properties like swelling ratio, mechanical properties like tensile and compressive modulus, rheological behavior, the chemical composition was studied using FTIR, and thermal properties using DSC experiments.

Biodegradability and mechanical strength, both are gained using double networks (DN), thus making it resemble more like living tissues. The ability of the cell to culture on DN hydrogels was examined for its viability as a scaffold in tissue engineering. Furthermore, these properties may allow their application as tissue-engineered scaffolds.

Objective 4: Design and synthesis of stereolithography (SLA) 3D printed poly (ethylene glycol) diacrylate (PEGDMA) based hydrogels for biomedical applications

Previous objectives have mainly focused on the preparation of material for hydrogel to be used in the biomedical field. In the current objective, we considered the customizability factor for making the hydrogel scaffolds. The idea of three-dimensional printing makes it easy for patient-specific applicability of hydrogel scaffolds. We have photocured the macromer and double network of macromer systems to get variety in properties of the hydrogel. The photocuring process takes into account of stereolithography (SLA) technique. It occurs in a layer by layer fashion where each of its layers gets cured as the printing proceeds resulting in an end product which is a scaffold matrix.

1.9 References

- (1) Haque, M. A.; Kurokawa, T.; Gong, J. P. Super Tough Double Network Hydrogels and Their Application as Biomaterials. *Polymer*. Elsevier Ltd April 17, 2012, pp 1805–1822. <https://doi.org/10.1016/j.polymer.2012.03.013>.
- (2) Anseth Kristi S., B. C. N. and B.-P. L. Mechanical Properties of Hydrogels and Their Experimental Determination. *Biomaterials* **1996**, *17*, 1647–1657.
- (3) Gibas, I.; Janik, H. Review: Synthetic Polymer Hydrogels For Biomedical Applications. *Chem. Chem. Technol.* **2010**, *4* (January 2010), 297–304.
- (4) Ahmed, E. M. Hydrogel: Preparation, Characterization, and Applications: A Review. *J. Adv. Res.* **2015**, *6* (2), 105–121. <https://doi.org/10.1016/j.jare.2013.07.006>.
- (5) Sergeeva, A. S.; Gorin, D. A.; Volodkin, D. V. In-Situ Assembly of Ca-Alginate Gels with Controlled Pore Loading/Release Capability. *Langmuir* **2015**, *31* (39), 10813–10821. <https://doi.org/10.1021/acs.langmuir.5b01529>.
- (6) Melchels, F. P. W.; Domingos, M. A. N.; Klein, T. J.; Malda, J.; Bartolo, P. J.; Hutmacher, D. W. Additive Manufacturing of Tissues and Organs. *Prog. Polym. Sci.* **2012**, *37* (8), 1079–1104. <https://doi.org/10.1016/j.progpolymsci.2011.11.007>.
- (7) Escudero-Castellanos, A.; Ocampo-García, B. E.; Domínguez-García, M. V.; Flores-Estrada, J.; Flores-Merino, M. V. Hydrogels Based on Poly(Ethylene Glycol) as Scaffolds for Tissue Engineering Application: Biocompatibility Assessment and Effect of the Sterilization Process. *J. Mater. Sci. Mater. Med.* **2016**, *27* (12). <https://doi.org/10.1007/s10856-016-5793-3>.
- (8) Berger, J.; Reist, M.; Mayer, J. M.; Felt, O.; Peppas, N. A.; Gurny, R. Structure and

- Interactions in Covalently and Ionically Crosslinked Chitosan Hydrogels for Biomedical Applications. *Eur. J. Pharm. Biopharm.* **2004**, *57* (1), 19–34.
[https://doi.org/10.1016/S0939-6411\(03\)00161-9](https://doi.org/10.1016/S0939-6411(03)00161-9).
- (9) Yang, X.; Guo, L.; Fan, Y.; Zhang, X. Preparation and Characterization of Macromolecule Cross-Linked Collagen Hydrogels for Chondrocyte Delivery. *Int. J. Biol. Macromol.* **2013**, *61*, 487–493. <https://doi.org/10.1016/j.ijbiomac.2013.07.021>.
- (10) Morris, V. B.; Nimbalkar, S.; Younesi, M.; McClellan, P.; Akkus, O. Mechanical Properties, Cytocompatibility and Manufacturability of Chitosan:PEGDA Hybrid-Gel Scaffolds by Stereolithography. *Ann. Biomed. Eng.* **2017**, *45* (1), 286–296.
<https://doi.org/10.1007/s10439-016-1643-1>.
- (11) Azevedo, H.; Reis, R. Understanding the Enzymatic Degradation of Biodegradable Polymers and Strategies to Control Their Degradation Rate. *Biodegrad. Syst. Tissue Eng. Regen. Med.* **2004**, 177–202. <https://doi.org/10.1201/9780203491232.ch12>.
- (12) Costa-Pinto AR, Martins AM, Castelhana-Carlos MJ, Correlo VM, Sol PC, Longatto-Filho A, Battacharya M, R. R. and N. N. In Vitro Degradation and in Vivo Biocompatibility of Chitosan– Poly(Butylene Succinate) Fiber Mesh Scaffolds. *J. Bioact. Compat. Polym.* **2014**, *29* (2), 137–151.
- (13) Caló, E.; Khutoryanskiy, V. V. Biomedical Applications of Hydrogels: A Review of Patents and Commercial Products. *Eur. Polym. J.* **2015**, *65*, 252–267.
<https://doi.org/10.1016/j.eurpolymj.2014.11.024>.
- (14) Borges, A. C.; Bourban, P. E.; Pioletti, D. P.; Månson, J. A. E. Curing Kinetics and Mechanical Properties of a Composite Hydrogel for the Replacement of the Nucleus Pulposus. *Compos. Sci. Technol.* **2010**. <https://doi.org/10.1016/j.compscitech.2010.07.018>.

- (15) Lih, E.; Lee, J. S.; Park, K. M.; Park, K. D. Rapidly Curable Chitosan-PEG Hydrogels as Tissue Adhesives for Hemostasis and Wound Healing. *Acta Biomater.* **2012**, *8* (9), 3261–3269. <https://doi.org/10.1016/j.actbio.2012.05.001>.
- (16) Bedel, N. S.; Tezcan, M.; Ceylan, O.; Gurdag, G.; Cicek, H. Effects of Pore Morphology and Size on Antimicrobial Activity of Chitosan/Poly(Ethylene Glycol) Diacrylate Macromer Semi-IPN Hydrogels. *J. Appl. Polym. Sci.* **2015**, *132* (43), 1–10. <https://doi.org/10.1002/app.42707>.
- (17) Kabiri, K.; Omidian, H.; Zohuriaan-Mehr, M. J.; Doroudiani, S. Superabsorbent Hydrogel Composites and Nanocomposites: A Review. *Polym. Compos.* **2012**, 277–289. <https://doi.org/10.1002/pc>.
- (18) Mun, G.; Suleimenov, I.; Park, K.; Omidian, H. Superabsorbent Hydrogels. In *Biomedical Applications of Hydrogels Handbook*; 2010; pp 375–391. https://doi.org/10.1007/978-1-4419-5919-5_20.
- (19) Sun, J.; Tan, H. Alginate-Based Biomaterials for Regenerative Medicine Applications. **2013**, 1285–1309. <https://doi.org/10.3390/ma6041285>.
- (20) Matricardi, P.; Di Meo, C.; Coviello, T.; Hennink, W. E.; Alhaique, F. Interpenetrating Polymer Networks Polysaccharide Hydrogels for Drug Delivery and Tissue Engineering. *Adv. Drug Deliv. Rev.* **2013**, *65* (9), 1172–1187. <https://doi.org/10.1016/j.addr.2013.04.002>.
- (21) Pawar, S. N. *Chemical Modification of Alginate*; Elsevier Inc., 2017. <https://doi.org/10.1016/B978-0-12-809816-5/00008-6>.
- (22) Safranski David L, G. K. Effect of Chemical Structure and Crosslinking Density on the Thermo-Mechanical Properties and Toughness of (Meth)Acrylate Shape Memory Polymer

- Networks. *Polymer (Guildf)*. **2008**, *49*, 4446–4455.
- (23) Hahn, S. K.; Park, J. K.; Tomimatsu, T.; Shimoboji, T. Synthesis and Degradation Test of Hyaluronic Acid Hydrogels. *Int. J. Biol. Macromol.* **2007**, *40* (4), 374–380.
<https://doi.org/10.1016/j.ijbiomac.2006.09.019>.
- (24) Wu, J.; Wang, Y.; Yang, H.; Liu, X.; Lu, Z. Preparation and Biological Activity Studies of Resveratrol Loaded Ionically Cross-Linked Chitosan-TPP Nanoparticles. *Carbohydr. Polym.* **2017**, *175*, 170–177. <https://doi.org/10.1016/j.carbpol.2017.07.058>.
- (25) Mudassir, J.; Ranjha, N. M. Dynamic and Equilibrium Swelling Studies: Crosslinked PH Sensitive Methyl Methacrylate-Co-Itaconic Acid (MMA-Co-IA) Hydrogels. *J. Polym. Res.* **2008**, *15* (3), 195–203.
- (26) Ranjha, N. M.; Mudassir, J.; Akhtar, N. Methyl Methacrylate-Co-Itaconic Acid (MMA-Co-IA) Hydrogels for Controlled Drug Delivery. *J. Sol-Gel Sci. Technol.* **2008**, *47* (1), 23–30.
- (27) Rázga, F.; Vnuková, D.; Némethová, V.; Mazancová, P.; Lacík, I. Preparation of Chitosan-TPP Sub-Micron Particles: Critical Evaluation and Derived Recommendations. *Carbohydr. Polym.* **2016**, *151*, 488–499. <https://doi.org/10.1016/j.carbpol.2016.05.092>.
- (28) Williams D. (Ed.). *Concise Encyclopedia of Medical and Dental Materials*, 1st ed.; Williams, D., Ed.; Pergamon Press: Oxford, 1990.
- (29) Truong, N. K.; West, J. L. Photopolymerizable Hydrogels for Tissue Engineering Applications. *Biomaterials* **2002**, *23*, 4307–4314. https://doi.org/10.1007/978-1-4419-5919-5_11.
- (30) Peppas, N. A.; Hilt, J. Z.; Khademhosseini, A.; Langer, R. Hydrogels in Biology and Medicine: From Molecular Principles to Bionanotechnology. *Adv. Mater.* **2006**, *18* (11),

- 1345–1360. <https://doi.org/10.1002/adma.200501612>.
- (31) Patel, P. N.; Smith, C. K.; Patrick, C. W. Rheological and Recovery Properties of Poly(Ethylene Glycol) Diacrylate Hydrogels and Human Adipose Tissue. *J. Biomed. Mater. Res. - Part A* **2005**, *73* (3), 313–319. <https://doi.org/10.1002/jbm.a.30291>.
- (32) Sperling, L. H. *Interpenetrating Polymer Networks and Related Materials*, 1st ed.; Plenum Press: New York, 1981.
- (33) Ullah, F.; Othman, M. B. H.; Javed, F.; Ahmad, Z.; Akil, H. M. Classification, Processing and Application of Hydrogels: A Review. *Mater. Sci. Eng. C* **2015**, *57*, 414–433. <https://doi.org/10.1016/j.msec.2015.07.053>.
- (34) Rahmani, S.; Mooney, D. Tissue-Engineered Wound Dressings for Diabetic Foot Ulcers. In *Contemporary Diabetes*; Veves, A., Giurini, J., Guzman, R., Eds.; Humana, Cham, 2018; pp 247–256. https://doi.org/https://doi.org/10.1007/978-3-319-89869-8_15.
- (35) Tse, J.; Engler, A. Preparation of Hydrogel Substrates with Tunable Mechanical Properties. *Curr Protoc Cell Biol Chapter 10 Unit 10* **2010**.
- (36) Peppas, N. A.; Bures, P.; Leobandung, W.; Ichikawa, H. Hydrogels in Pharmaceutical Formulations. *Eur. J. Pharm. Biopharm.* **2000**, *50*, 27–46.
- (37) Stevens, M.; George, J. Exploring and Engineering the Cell Surface Interface. *Science (80-.)*. **2005**, *310*, 1135–1138.
- (38) Pradhan, S.; Hassani, I.; Seeto, W. J.; Lipke, E. A. PEG-Fibrinogen Hydrogels for Three-Dimensional Breast Cancer Cell Culture. **2016**, No. June, 236–252. <https://doi.org/10.1002/jbm.a.35899>.
- (39) Prabakaran, M. Chitosan-Based Nanoparticles for Tumor-Targeted Drug Delivery. *Int. J. Biol. Macromol.* **2015**, *72*, 1313–1322. <https://doi.org/10.1016/j.ijbiomac.2014.10.052>.

- (40) Lim, F.; Sun, A. Microencapsulated Islets as Bioartificial Endocrine Pancreas. *Science* (80-.). **1980**, *210*, 908–910.
- (41) Yannas, I.; Lee, E.; Orgill, D.; Skrabut, E.; Murphy, G. Synthesis and Characterization of a Model Extracellular Matrix That Induces Partial Regeneration of Adult Mammalian Skin. *Proc Natl Acad Sci US A* **1989**, *86*, 933–937.
- (42) Chirani, N.; Yahia, L.; Gritsch, L.; Motta, F. L.; Chirani, S.; Faré, S. History and Applications of Hydrogels. *J. Biomed. Sci.* **2015**, *04* (02), 1–23.
<https://doi.org/10.4172/2254-609x.100013>.
- (43) Hoare, T. R.; Kohane, D. S. Hydrogels in Drug Delivery: Progress and Challenges. *Polymer (Guildf)*. **2008**, *49* (8), 1993–2007.
<https://doi.org/10.1016/j.polymer.2008.01.027>.
- (44) Vashist, A.; Vashist, A.; Gupta, Y.; Ahmad, S. Recent Advances in Hydrogel Based Drug Delivery Systems for the Human Body. *J. Mater. Chem. B* **2014**, No. 2, 147–166.
- (45) Elviraa, C.; Mano, J.; San Román, J.; Reisa, R. Starch-Based Biodegradable Hydrogels with Potential Biomedical Applications as Drug Delivery Systems. *Biomaterials* **2002**, *23* (9), 1955–1966.
- (46) Bagre, A. P.; Jain, K.; Jain, N. K. Alginate Coated Chitosan Core Shell Nanoparticles for Oral Delivery of Enoxaparin: In Vitro and in Vivo Assessment. *Int. J. Pharm.* **2013**, *456* (1), 31–40. <https://doi.org/10.1016/j.ijpharm.2013.08.037>.
- (47) Lee, C. Y.; Teymour, F.; Camastral, H.; Tirelli, N.; Hubbell, J. A.; Elbert, D. L.; Papavasiliou, G.; Kousar, F.; Malana, M. A.; Chughtai, A. H.; et al. Synthesis and Characterization of Methacrylamide-Acrylic Acid-N-Isopropylacrylamide Polymeric Hydrogel: Degradation Kinetics and Rheological Studies. *Biomed. Mater.* **2018**, *155* (2),

- 1275–1298. <https://doi.org/10.1088/1748-605X/aa9ad2>.
- (48) Pelras, T.; Glass, S.; Scherzer, T.; Elsner, C.; Schulze, A.; Abel, B. Transparent Low Molecularweight Poly(Ethylene Glycol) Diacrylate-Based Hydrogels as Film Media for Photoswitchable Drugs. *Polymers (Basel)*. **2017**. <https://doi.org/10.3390/polym9120639>.
- (49) Coviello, T.; Matricardi, P.; Marianecci, C.; Alhaique, F. Polysaccharide Hydrogels for Modified Release Formulations. *J. Control. Release* **2007**, *119* (1), 5–24. <https://doi.org/10.1016/j.jconrel.2007.01.004>.
- (50) Chen, S. H.; Tsao, C. T.; Chang, C. H.; Lai, Y. T.; Wu, M. F.; Liu, Z. W.; Chuang, C. N.; Chou, H. C.; Wang, C. K.; Hsieh, K. H. Synthesis and Characterization of Reinforced Poly(Ethylene Glycol)/Chitosan Hydrogel as Wound Dressing Materials. *Macromol. Mater. Eng.* **2013**, *298* (4), 429–438. <https://doi.org/10.1002/mame.201200054>.
- (51) Stashak, T.; Farstvedt, E.; Othica, A. Update on Wound Dressings: Indications and Best Use. *Clin. Tech. Equine Pract.* **2004**, *3* (2), 148–163.
- (52) Jones, V.; Grey, J. E.; Harding, K. G. Wound Dressings. *BMJ* **2006**, *332*, 777.
- (53) Rusanu, A.; Tamaş, A. I.; Vulpe, R.; Rusu, A.; Butnaru, M.; Vereştiuc, L. Biocompatible and Biodegradable Hydrogels Based on Chitosan and Gelatin with Potential Applications as Wound Dressings. *J. Nanosci. Nanotechnol.* **2017**, *17* (7). <https://doi.org/10.1166/jnn.2017.14298>.
- (54) Hoffman Allan S. Hydrogels for Biomedical Applications. *Adv. Drug Deliv. Rev.* **2012**, *64*, 18–23. <https://doi.org/10.1016/B978-0-12-813665-2.00011-9>.
- (55) Prins W., N. W. Hydrogels of Crosslinked Poly(1-glyceryl Methacrylate) and Poly(2-hydroxypropyl Methacrylamide). *J. Appl. Polym. Sci.* **1975**, *19* (7).
- (56) Wichterle O.; Lim D. Hydrophilic Gels in Biologic Use. *Nature* **1960**, *185*, 117.

- (57) Swarbrick J. (Ed.). *Encyclopedia of Pharmaceutical Technology*, 3 rd.; J., S., Ed.; Informa Healthcare: New York, 2006.
- (58) Leach, S. P. Z. and J. B. Hydrolytically Degradable Poly(Ethylene Glycol) Hydrogel Biomacromolecules. *Biomacromolecules* **2011**, *11* (5), 1348–1357.
<https://doi.org/10.1021/bm100137q>.Hydrolytically.
- (59) Singh, B. K.; Sirohi, R.; Archana, D.; Jain, A.; Dutta, P. K. Porous Chitosan Scaffolds: A Systematic Study for Choice of Crosslinker and Growth Factor Incorporation. *Int. J. Polym. Mater. Polym. Biomater.* **2015**, *64* (5), 242–252.
<https://doi.org/10.1080/00914037.2014.936596>.
- (60) Fu, Y.; Xu, K.; Zheng, X.; Giacomini, A. J.; Mix, A. W.; Kao, W. J. 3D Cell Entrapment in Crosslinked Thiolated Gelatin-Poly(Ethylene Glycol) Diacrylate Hydrogels. *Biomaterials* **2012**, *33* (1), 48–58. <https://doi.org/10.1016/j.biomaterials.2011.09.031>.
- (61) Moffat, K. L.; Neal, R. A.; Freed, L. E.; Guilak, F. *Engineering Functional Tissues : In Vitro Culture Parameters*, Fourth Edi.; Elsevier, 2014. <https://doi.org/10.1016/B978-0-12-398358-9.00013-6>.
- (62) Pacelli, S.; Paolicelli, P.; Dreesen, I.; Kobayashi, S.; Vitalone, A.; Antonietta, M. International Journal of Biological Macromolecules Injectable and Photocross-Linkable Gels Based on Gellan Gum Methacrylate : A New Tool for Biomedical Application. **2015**, *72*, 1335–1342.
- (63) Fenn, S. L.; Oldinski, R. A. Visible Light Crosslinking of Methacrylated Hyaluronan Hydrogels for Injectable Tissue Repair. **2015**, 1229–1236.
<https://doi.org/10.1002/jbm.b.33476>.
- (64) Tan, G.; Wang, Y.; Li, J.; Zhang, S. Synthesis and Characterization of Injectable

- Photocrosslinking Poly (Ethylene Glycol) Diacrylate Based Hydrogels. *Polym. Bull.* **2008**, *61*, 91–98. <https://doi.org/10.1007/s00289-008-0932-8>.
- (65) Radhakrishnan, J.; Subramanian, A.; Krishnan, U. M.; Sethuraman, S. Injectable and 3D Bioprinted Polysaccharide Hydrogels : From Cartilage to Osteochondral Tissue Engineering. **2017**. <https://doi.org/10.1021/acs.biomac.6b01619>.
- (66) Bhattarai, N.; Gunn, J.; Zhang, M. Chitosan-Based Hydrogels for Controlled, Localized Drug Delivery. *Adv. Drug Deliv. Rev.* **2010**, *62* (1), 83–99. <https://doi.org/10.1016/j.addr.2009.07.019>.
- (67) Qayyum, A. S.; Jain, E.; Kolar, G.; Kim, Y.; Sell, S. A.; Zustiak, S. P. Design of Electrohydrodynamic Sprayed Polyethylene Glycol Hydrogel Microspheres for Cell Encapsulation. *Biofabrication* **2017**, *9* (2). <https://doi.org/10.1088/1758-5090/aa703c>.
- (68) Lončarević, A.; Ivanković, M.; Rogina, A. Lysozyme-Induced Degradation of Chitosan: The Characterisation of Degraded Chitosan Scaffolds. *J. Tissue Repair Regen.* **2017**, *19* (1), 177.
- (69) Gnanaprakasam Thankam, F.; Muthu, J.; Sankar, V.; Kozhiparambil Gopal, R. Growth and Survival of Cells in Biosynthetic Poly Vinyl Alcohol-Alginate IPN Hydrogels for Cardiac Applications. *Colloids Surfaces B Biointerfaces* **2013**, *107*, 137–145. <https://doi.org/10.1016/j.colsurfb.2013.01.069>.
- (70) Kerscher, P. HUMAN DEVELOPING CARDIAC TISSUES FOR SCALE-UP AND DISEASE. **2016**.
- (71) Chai, Q.; Jiao, Y.; Yu, X. Hydrogels for Biomedical Applications: Their Characteristics and the Mechanisms behind Them. *Gels* **2017**, *3* (1), 6. <https://doi.org/10.3390/gels3010006>.

- (72) Kyle, S.; Whitaker, I. S. To Print or Not to Print , That Is the Question : How Close Are We to Clinical Translation of Contemporary Bioinks ? **2018**, *2*, 1–3.
- (73) An, J.; Ee, J.; Teoh, M.; Suntornnond, R.; Chua, C. K. 3D Printing — Review Design and 3D Printing of Scaffolds and Tissues. *Engineering* **2015**, *1* (2), 261–268.
<https://doi.org/10.15302/J-ENG-2015061>.
- (74) Gopinathan, J.; Noh, I. Recent Trends in Bioinks for 3D Printing. *Biomaterials Research*. BioMed Central Ltd. April 6, 2018. <https://doi.org/10.1186/s40824-018-0122-1>.
- (75) Gudapati, H.; Dey, M.; Ozbolat, I. A Comprehensive Review on Droplet-Based Bioprinting: Past, Present and Future. *Biomaterials* **2016**, *102*, 20–42.
- (76) Bioprinting, T.; Skardal, A.; Sc, B.; Zhang, J.; Ph, D.; McCoard, L.; Sc, B.; Xu, X.; Ph, D. Photocrosslinkable Hyaluronan-Gelatin Hydrogels. **2010**, *16* (8).
<https://doi.org/10.1089/ten.tea.2009.0798>.
- (77) Ozbolat, I.; Peng, W.; Ozbolat, V. Application Areas of 3D Bioprinting. *Drug discov today* **2016**, *21* (8), 1257–1271.
- (78) Markstedt, K.; Mantas, A.; Tournier, I.; Ha, D.; Gatenholm, P. 3D Bioprinting Human Chondrocytes with Nanocellulose – Alginate Bioink for Cartilage Tissue Engineering Applications. **2015**. <https://doi.org/10.1021/acs.biomac.5b00188>.
- (79) Holzl, K.; Lin, S.; Tytgat, L.; Van Vlierberghe, S.; Gu, L.; Ovsianikov, A. Bioink Properties before, during and after 3D Bioprinting. *Biofabrication* **2016**, *8* (3), 032002.
- (80) Khademhosseini, A.; Langer, R. Microengineered Hydrogels for Tissue Engineering. *Biomaterials* **2007**, *28* (34), 5087–5092.
<https://doi.org/10.1016/j.biomaterials.2007.07.021>.
- (81) Miri, A. K.; Khalilpour, A.; Cecen, B.; Maharjan, S.; Shin, S.-R.; Khademhosseini, A.

- Multiscale Bioprinting of Vascularized Models. *Biomaterials* **2018**.
<https://doi.org/10.1016/j.biomaterials.2018.08.006>.
- (82) Baolin, G.; Ma, P. X. Synthetic Biodegradable Functional Polymers for Tissue Engineering: A Brief Review.
- (83) Nijst, C. L. E.; Bruggeman, J. P.; Karp, J. M.; Ferreira, L.; Zumbuehl, A.; Bettinger, C. J.; Langer, R. Synthesis and Characterization of Photocurable Elastomers from Poly(Glycerol-Co-Sebacate). *Biomacromolecules* **2007**, *8* (10), 3067–3073.
<https://doi.org/10.1021/bm070423u>.
- (84) Langer, R.; Vacanti, J. Tissue Engineering. *Science (80-.)*. **1993**, *260*, 920–926.
- (85) Guo X, Wang W, Wu G, Zhang J, Mao C, D. Y. et al. Controlled Synthesis of Hydroxyapatite Crystals Templated by Novel Surfactants and Their Enhanced Bioactivity. *New J Chem*. **2011**, *35*, 663–671.
- (86) Liu, M.; Zeng, X.; Ma, C.; Yi, H.; Ali, Z.; Mou, X.; Li, S.; Deng, Y.; He, N. Injectable Hydrogels for Cartilage and Bone Tissue Engineering. **2017**, No. November 2016.
<https://doi.org/10.1038/boneres.2017.14>.
- (87) Munarin, F.; Guerreiro, S.; Grellier, M.; Tanzi, M.; Barbosa, M. Pectin-Based Injectable Biomaterials for Bone Tissue Engineering. *Biomacromolecules* **2011**, *12*, 568–577.
- (88) Arnold, M. P.; Daniels, A. U.; Ronken, S.; García, H. A.; Friederich, N. F.; Kurokawa, T.; Gong, J. P.; Wirz, D. Acrylamide Polymer Double-Network Hydrogels : Candidate Cartilage Repair Materials with Cartilage-Like Dynamic Stiffness and Attractive Surgery-Related Attachment Mechanics. **2011**. <https://doi.org/10.1177/1947603511402320>.
- (89) Fallacara, A. Hyaluronic Acid in the Third Millennium. **2018**.
<https://doi.org/10.3390/polym10070701>.

- (90) Miguel, S. P.; Ribeiro, M. P.; Brancal, H.; Coutinho, P.; Correia, I. J. Thermoresponsive Chitosan-Agarose Hydrogel for Skin Regeneration. *Carbohydr. Polym.* **2014**, *111*, 366–373. <https://doi.org/10.1016/j.carbpol.2014.04.093>.
- (91) Kim, Y. S.; Mikos, A. G.; Smoak, M. M.; Melchiorri, A. J. An Overview of the Tissue Engineering Market in the United States from 2011 to 2018. **2019**, *25*, 1–8. <https://doi.org/10.1089/ten.tea.2018.0138>.
- (92) Ma, P. X. Biomimetic Materials for Tissue Engineering. *Adv. Drug Deliv. Rev.* **2008**, *60*, 184–198.
- (93) Liu, X. .; Holzwarth, J. .; Ma, P. . Functionalized Synthetic Biodegradable Polymer Scaffolds for Tissue Engineering. *Macromol. Biosci.* **2012**, *12*, 911–919.
- (94) Chen, G. .; Ushida, T.; Tateishi, T. Scaffold Design for Tissue Engineering. *Macromol. Biosci.* **2002**, *2*, 67–77.
- (95) Yang, S.; Leong, K.; Du, Z.; Chua, C. The Design of Scaffolds for Use in Tissue Engineering-Part 1 (Traditional Factors). *Tissue Eng.* **2001**, *7*, 679–689.
- (96) Holzwarth, J. .; Ma, P. X. 3D Nanofibrous Scaffolds for Tissue Engineering. *J. Mater. Chem.* **2011**, *21*, 10243–10251.
- (97) Horn, M. M.; Martins, V. C. A.; de Guzzi Plepis, A. M. Influence of Collagen Addition on the Thermal and Morphological Properties of Chitosan/Xanthan Hydrogels. *Int. J. Biol. Macromol.* **2015**, *80*, 225–230. <https://doi.org/10.1016/j.ijbiomac.2015.06.011>.
- (98) Poon, Y. F.; Cao, Y.; Liu, Y.; Chan, V.; Chan-park, M. B. Hydrogels Based on Dual Curable Layer-by-Layer Cell Encapsulation. **2012**, *2* (7). <https://doi.org/10.1021/am1002876>.
- (99) Haque Md. Anamul, Kurokawa Takayuki, G. J. P. Super Tough Double Network

- Hydrogels and Their Application as Biomaterials. *Polymer (Guildf)*. **2012**, 53, 1805–1822.
- (100) Calvert, P. Hydrogels for Soft Machines. *Adv. Mater.* **2009**, 21 (7), 743.
- (101) Fung, Y. *Biomechanics: Mechanical Properties of Living Tissues*, 2nd ed.; Springer-Verlag Inc: New York, 1993.
- (102) Li, H.; Wang, H.; Zhang, D.; Xu, Z.; Liu, W. A Highly Tough and Stiff Supramolecular Polymer Double Network Hydrogel. *Polymer (Guildf)*. **2018**, 153, 193–200.
<https://doi.org/10.1016/j.polymer.2018.08.029>.
- (103) Saraiva Sofia M, Miguel Sonia P, Ribeiro Maximiano P, Coutinho Paula, C. I. J. Synthesis and Characterization of a Photocrosslinkable Chitosan-Gelatin Hydrogel Aimed for Tissue Regeneration. *RSC Adv.* **2015**, 5, 63478–63488.
- (104) Suntornnond, R.; An, J.; Chua, C. K. Bioprinting of Thermoresponsive Hydrogels for Next Generation Tissue Engineering: A Review. *Macromol. Mater. Eng.* **2017**, 302 (1), 1–15. <https://doi.org/10.1002/mame.201600266>.
- (105) Schmidt, J. J.; Rowley, J.; Hyun, J. K. Hydrogels Used for Cell-Based Drug Delivery. *J. Biomed. Mater. Res. - Part A* **2008**, 87 (4), 1113–1122.
<https://doi.org/10.1002/jbm.a.32287>.
- (106) Monteiro, N.; Thirvikraman, G.; Athirasala, A.; Tahayeri, A.; França, C. M.; Ferracane, J. L.; Bertassoni, L. E. Photopolymerization of Cell-Laden Gelatin Methacryloyl Hydrogels Using a Dental Curing Light for Regenerative Dentistry. *Dent. Mater.* **2018**.
<https://doi.org/10.1016/j.dental.2017.11.020>.
- (107) Schuurman, W.; Levett, P. A.; Pot, M. W.; van Weeren, P. R.; Dhert, W. J. A.; Hutmacher, D. W.; Melchels, F. P. W.; Klein, T. J.; Malda, J. Gelatin-Methacrylamide Hydrogels as Potential Biomaterials for Fabrication of Tissue-Engineered Cartilage

- Constructs. *Macromol. Biosci.* **2013**, *13* (5), 551–561.
<https://doi.org/10.1002/mabi.201200471>.
- (108) Peppas, N. A. Hydrogels and Drug Delivery. *Curr. Opin. Colloid Interface Sci.* **1997**, *2* (5), 531–537. [https://doi.org/10.1016/S1359-0294\(97\)80103-3](https://doi.org/10.1016/S1359-0294(97)80103-3).
- (109) Kalshetti, P. P.; Rajendra, V. B.; Dixit, D. N.; Parekh, P. P. Hydrogels as a Drug Delivery System and Applications: A Review. *Int. J. Pharm. Pharm. Sci.* **2012**, *4* (1), 1–7.
- (110) Gopinathan, J.; Noh, I. Recent Trends in Biopinks for 3D Printing. **2018**, 1–15.
- (111) Maxson, E. L.; Young, M. D.; Noble, C.; Go, J. L.; Heidari, B.; Khorramirouz, R.; Morse, D. W.; Lerman, A. In Vivo Remodeling of a 3D-Bioprinted Tissue Engineered Heart Valve Scaffold. *Bioprinting* **2019**, e00059. <https://doi.org/10.1016/j.bprint.2019.e00059>.
- (112) Lee, J. M.; Yeong, W. Y. Design and Printing Strategies in 3D Bioprinting of Cell-Hydrogels: A Review. *Adv. Healthc. Mater.* **2016**, *5* (22), 2856–2865.
<https://doi.org/10.1002/adhm.201600435>.
- (113) Derakhshanfar, S.; Mbeleck, R.; Xu, K.; Zhang, X.; Zhong, W.; Xing, M. 3D Bioprinting for Biomedical Devices and Tissue Engineering: A Review of Recent Trends and Advances. *Bioact. Mater.* **2018**, *3* (2), 144–156.
<https://doi.org/10.1016/j.bioactmat.2017.11.008>.
- (114) Jenkins, A. D.; Kratochvil, P.; Stepto, R. F. T.; Suter, U. W. Glossary of Basic Terms in Polymer Science (IUPAC Recommendations 1996). *Pure Appl. Chem* **1996**, *68*, 2287–2311.
- (115) Tan, F.; Xu, X.; Deng, T.; Yin, M.; Zhang, X.; Wang, J. Fabrication of Positively Charged Poly(Ethylene Glycol)-Diacrylate hydrogel as a Bone Tissue Engineering Scaffold. *Biomed. Mater.* **2012**, *7* (5). <https://doi.org/10.1088/1748-6041/7/5/055009>.

- (116) Deepthi, S.; Nivedhitha Sundaram, M.; Deepthi Kadavan, J.; Jayakumar, R. Layered Chitosan-Collagen Hydrogel/Aligned PLLA Nanofiber Construct for Flexor Tendon Regeneration. *Carbohydr. Polym.* **2016**, *153*, 492–500.
<https://doi.org/10.1016/j.carbpol.2016.07.124>.
- (117) Van Vlierberghe, S.; Dubruel, P.; Schacht, E. Biopolymer-Based Hydrogels as Scaffolds for Tissue Engineering Applications: A Review. *Biomacromolecules* **2011**, *12*, 1387–1408.
- (118) Tate, M.; Falls, T.; McBride, S.; Atit, R.; Knothe, U. Mechanical Modulation of Osteochondroprogenitor Cell Fate. *Int J Biochem Cell Biol* **2008**, *40*, 2720–2738.
- (119) Persson, G.; Salvi, G.; Heitz-Mayfield, L.; Lang, N. Antimicrobial Therapy Using a Local Drug Delivery System (Arestin) in the Treatment of Peri-Implantitis. I: Microbiological Outcomes. *Clin Oral Implant. Res* **2006**, *17* (4), 386–393.
- (120) No Title <https://www.cambridge.org/core/journals/mrs-communications/article/gelatinbased-hydrogels-for-biomedical-applications/C1DA8426E188AEBDBC412B64B7D87BFD/core-read>.
- (121) FDA approval - Collagen <http://collagencomplete.com/how-safe-is-collagen/>.
- (122) No Title. *Acta Biomater* **2013**, *9* (7), 7081–7092.
<https://doi.org/doi:10.1016/j.actbio.2013.03.005>.
- (123) Wedmore, I.; McManus, J.; Pusateri, A.; Holcomb, J. A Special Report on the Chitosan-Based Hemostatic Dressing: Experience in Current Combat Operations. *J Trauma* **2006**, *60*, 655–658.
- (124) No Title [https://www.ams.usda.gov/sites/default/files/media/Alginic Acid TR.pdf](https://www.ams.usda.gov/sites/default/files/media/Alginic%20Acid%20TR.pdf)

- (125) Pollack, S. K. *FDA and the Regulatory Pathway for Biomaterials in Medical Devices*, 2nd ed.; Military Biomaterials Roadmap Workshop Wednesday: New Brunswick NJ.
- (126) FDA approval - Dextran
https://www.accessdata.fda.gov/drugsatfda_docs/label/2009/017441s1711bl.pdf.
- (127) Otani, Y.; Tabata, Y.; Ikada, Y. No Title. *Biomaterials* **1998**, *19*, 2091.
- (128) Spotnitz, W. No Title. *Surgery* **2007**, *142*, S34.
- (129) Peppas, N.; Hilt, J.; Khademhosseini, A.; Langer, R. No Title. *Adv. Mater.* **2006**, *18*, 1345.
- (130) *Tissue Adhesives in Clinical Medicine*; Quinn, J., Ed.; BC Decker Inc: Hamilton, 2005.
- (131) Nakayama, Y.; Matsuda, T. No Title. *ASAIO J.* **1995**, *41*, M374.
- (132) Chafke, N.; Gasser, B.; Lindner, V.; Rouyer, N.; Rooke, R.; Kretz, J.; Nicolini, P.; Eisenmann, B. No Title. *J. Cardiovasc. Surg.* **1996**, *37*, 431.
- (133) *Absorbable and Biodegradable Polymers*; Shalaby, S., Burg, K., Eds.; CRC Press: Boca Raton, 2004.
- (134) Ryan, B.; Stockbrugger, R.; Ryan, J. No Title. *Gastroenterology* **2004**, *126*, 1175.
- (135) Leggat, P.; Kedjarune, U.; Smith, D. No Title. *Ind. Health* **2004**, *42*, 207.
- (136) Billiet, T.; Vandenhaute, M.; Schelfhout, J.; Van Vlierberghe, S.; Dubruel, P. A Review of Trends and Limitations in Hydrogel-Rapid Prototyping for Tissue Engineering. *Biomaterials* **2012**, *33* (26), 6020–6041.
<https://doi.org/10.1016/j.biomaterials.2012.04.050>.
- (137) Choi, J. H.; Choi, O. K.; Lee, J.; Noh, J.; Lee, S.; Park, A.; Rim, M. A.; Reis, R. L.; Khang, G. Evaluation of Double Network Hydrogel of Poloxamer-Heparin/Gellan Gum for Bone Marrow Stem Cells Delivery Carrier. *Colloids Surfaces B Biointerfaces* **2019**, *181* (June), 879–889. <https://doi.org/10.1016/j.colsurfb.2019.06.041>.

- (138) Campos, F.; Bonhome-Espinosa, A. B.; Vizcaino, G.; Rodriguez, I. A.; Duran-Herrera, D.; López-López, M. T.; Sánchez-Montesinos, I.; Alaminos, M.; Sánchez-Quevedo, M. C.; Carriel, V. Generation of Genipin Cross-Linked Fibrin-Agarose Hydrogel Tissue-like Models for Tissue Engineering Applications. *Biomed. Mater.* **2018**, *13* (2).
<https://doi.org/10.1088/1748-605X/aa9ad2>.
- (139) Bloomquist, C. J.; Mecham, M. B.; Paradzinsky, M. D.; Januszewicz, R.; Warner, S. B.; Luft, J. C.; Mecham, S. J.; Wang, A. Z. Controlling release from 3D Printed Medical Devices Using CLIP and Drug- Loaded Liquid Resins. *J. Control. Release* **2018**, *278* (March), 9–23. <https://doi.org/10.1016/j.jconrel.2018.03.026>.
- (140) Kondiah, P. J.; Choonara, Y. E.; Kondiah, P. P. D.; Marimuthu, T.; Kumar, P.; Toit, L. C.; Pillay, V. A Review of Injectable Polymeric Hydrogel Systems for Application in Bone Tissue Engineering. **2016**. <https://doi.org/10.3390/molecules21111580>.
- (141) Murphy, S.; Atala, A. 3D Bioprinting of Tissues and Organs. *Nat. Biotech* **2014**, *32* (8), 773–785.
- (142) Gu, B.; Choi, D.; Park, S.; Kim, M.; Kang, C.; Kim, C. 3-Dimensional Bioprinting for Tissue Engineering Applications. *Biomater. Res.* **2016**, *20* (1), 12.
- (143) Ahn, H.; Khalmuratova, R.; Park, S.; Chung, E.; Shin, H.; Kwon, S. Serial Analysis of Tracheal Restenosis after 3D-Printed Scaffold Implantation: Recruited Inflammatory Cells and Associated Tissue Changes. *Tissue Eng. Regen. Med.* **2017**, *14* (5), 631–639.
- (144) Jakus, A.; Rutz, A.; Shah, R. Advancing the Field of 3D Biomaterial Printing. *Biomed Mater.* **2016**, *11*, 014102.
- (145) Shafiee, A.; Atala, A. Printing Technologies for Medical Applications. *Trends Mol Med.* **2016**, *22* (3), 254–265.

- (146) Guvendiren, M.; Molde, J.; Soares, R.; Kohn, J. Designing Biomaterials for 3D Printing. *ACS Biomater Sci Eng* **2016**, *2* (10), 1679–1693.
- (147) Guillotin, B.; Souquet, A.; Catros, S.; Duocastella, M.; Pippenger, B.; Bellance, S.; Bareille, R.; Remy, M.; Bordenave, L.; Amedee, J.; et al. Laser Assisted Bioprinting of Engineered Tissue with High Cell Density and Microscale Organisation. *Biomaterials* **2010**, *31* (28), 7250–7256.
- (148) Nakamura, M.; Kobayashi, A.; Takagi, F.; Watanabe, A.; Hiruma, Y.; Ohuchi, K.; Iwasaki, Y.; Horie, M.; Morita, I.; Takatani, S. Biocompatible Inkjet Printing Technique for Designed Seeding of Individual Living Cells. *Tissue Eng.* **2005**, *11* (11–12), 1658–1666.
- (149) Mironov, V.; Boland, T.; Trusk, T.; Forgacs, G.; Markwald, R. Organ Printing: Computer-Aided Jet-Based 3D Tissue Engineering. *Trends Biotechnol.* **2003**, *21* (4), 157–161.
- (150) Wislon, W.; Boland, T. Cell and Organ Printing 1: Protein and Cell Printers. *Anat Rec Part A* **2003**, *272* (2), 491–496.
- (151) Wang, Z.; Abdulla, R.; Parker, B.; Samanipour, R.; Ghosh, S.; Kim, K. A Simple and High-Resolution Stereolithography-Based 3D Bioprinting System Using Visible Light Crosslinkable Bioinks. *Biofabrication* **2015**, *7* (4), 045009.
- (152) Elomaa, L.; Pan, C.; Shajani, Y.; Malkovskiy, A.; Seppala, J.; Yang, Y. Three-Dimensional Fabrication of Cell-Laden Biodegradable Poly (Ethylene Glycol-Co-Depsipeptide) Hydrogels by Visible Light Stereolithography. *J. Mater. Chem. B* **2015**, *3* (42), 8348–8358.

CHAPTER 2

Synthesis and Characterization of Photopolymerizable Hydrogels based on Poly (ethylene glycol) for Biomedical Applications

2.1 Introduction

Hydrogels are hydrophilic crosslinked polymer chains that acquire an expanded three-dimensional network when in the swollen state¹. These physical and chemical characteristics allow hydrogels to be valuable materials for a variety of biomedical applications: drug delivery²⁻⁴, tissue engineering⁵⁻⁷, molecular imprinting³, microsensors, medical electrodes, bio-composite scaffolds⁸⁻¹⁰, breast implants, contact lenses, wound healing, 3D cell culture and other biomedical applications¹¹⁻¹⁴.

The crosslinked nature of the hydrogels allows them to possess material characteristics that increase water uptake, simulates the mechanical properties of native biological extracellular matrices (ECM), and propagates diffusion-induced solute transport. Synthetic ECM provides an environment for growing cells, proliferation, migration, and simulation of *in vivo* surfaces, which are of vital importance in cell culture, wound repair, and tissue engineering¹⁵.

In particular, the biodegradation behavior of hydrogels, as well as the rate at which they degrade, are considered essential factors during the tissue regeneration¹⁶. During the process, the by-products or exudates must be non-toxic and should not have any adverse side effects on the human body¹⁷.

As far as tissue engineering applications are concerned, property like cell adhesion to material matrix plays a vital role. Saraiva et al. reported that the capacity of cells to adhere, proliferate, and become internalized within biomaterials are greatly affected by the morphology and structure of the surface material¹⁷.

Hydrogels can be produced by different methods like radiating, annealing, freeze-thawing, chemical, or physical crosslinking. However, UV radiation or photopolymerization is selected for its benefits in lowering the emissions of solvent and fast processability. During this process, a photoinitiator (PI) is required to produce free radicals for the polymerization process within a few minutes, to convert the liquid monomer or macromer into a gel-like hydrogel form¹⁷.

Several studies¹⁸⁻²⁰ have focused on the fabrication of hydrogels based on poly (ethylene glycol) diacrylate (PEGDA). PEGDA hydrogels with N-acryloyl-glucosamine (AGA) and with 2-hydroxyethyl methacrylate (HEMA) have scope to control the swelling behavior as well as the crosslinking density for improving mechanical performance. Poly(ethylene glycol) diacrylate (PEGDA), in itself, can produce hydrogels after photo-crosslinking. Hydrophilic PEGDA macromere possesses end double bonds (-C=C-), which participate in the free-radical polymerization in the presence of UV radiation. Poly(ethylene glycol) (PEG) acrylates²¹, like poly(ethylene glycol) diacrylates (PEGDA) and multi-arm PEG acrylate, are a few of the most utilized macromers used in free radical polymerization reaction for generating scaffolds. PEGDMA and other acrylates are non-toxic, non-immunogenic, and soluble in common solvents like ethanol and water, which makes them the ideal candidates for regenerative medicine. Morris et al. suggested that PEG hydrogels can undergo a variety of modifications to mimic the ECM²¹.

PEGDA with other natural polysaccharides like gelatin, alginate, and chitosan can be synergized to increase its control over biocompatibility²²⁻²⁵ when PEGDA remains the backbone for its mechanical strength.

In this research, we focused on the synthesis of different PEGDMAs formulated from poly(ethylene glycol) (PEG) of different molecular weights (4000, 6000, and 8000 g/mol) and further photocured in the presence of a photoinitiator (Irgacure 184). Chemical, thermal, mechanical, rheological, and morphological characteristics were studied, as well as biodegradability. The ability of these hydrogels as material for cell growth was investigated for application towards tissue engineering.

2.2 Materials and Methods

2.2.1 Materials

In this study, three varieties of linear poly (ethylene glycol) (PEG) were used: PEG (Mw ~ 4000 g/mol) purchased from Bean Town Chemicals (BTC) (US) and PEG (Mw ~ 6000 g/mol) and PEG (Mw ~ 8000 g/mol) purchased from Acros Organics (US). Methacrylic anhydride was purchased from Thermofisher Scientific Inc. (US). Dichloromethane (DCM), HPLC grade tetrahydrofuran (THF) (stabilized with BHT) and anhydrous diethyl ether were purchased from VWR International LLC (US). Photoinitiators, 1-hydroxycyclohexyl phenyl ketone (Irgacure 184), while the UV light source used (UVLS-28 EL Series UV Lamp) was manufactured by Analytik Jena (US). For the degradation studies, lysozyme (chicken egg white) was purchased from Thermofisher Scientific Inc. Deuterated dimethyl sulfoxide (DMSO-D6) (with 0.1 vol. % TMS, 99.9% purity) was

purchased from Magnisolv (Switzerland). Fibroblast cells were brought commercially (CCL 110; ATCC, VA). Cells were cultured in DMEM (Gibco, Gaithersburg, MD) supplemented with 10% v/v fetal bovine serum (Gibco, Gaithersburg, MD). MTT (3-(4,5-Dimethylthiazol-2-yl)-2,5-Diphenyltetrazolium Bromide) salt was brought from vendor (Invitrogen, NY). Live and Dead Double Staining Kit was bought (Abbkine, China).

2.2.2 Methods

2.2.2.1 Preparation of PEGDMA by chemical modification of PEG

Poly(ethylene glycol) dimethacrylate (PEGDMA) was synthesized as described by Van Hoven et al²⁶ (Figure 2.1). Briefly, poly(ethylene glycol) (PEG) was mixed with ten (10) molar excess of methacrylic anhydride into a vial and reacted in a microwave (1100 W) for 5 minutes on maximum power to obtain the PEGDMA samples. During the process, the vials were vortexed every 30 seconds until the end of time. After the PEGDMA samples were cooled to room temperature, they were dissolved in a small amount of dichloromethane (DCM) and precipitated in a 10x excess ice-cold diethyl ether. Finally, the PEGDMA was collected by vacuum filtration using a Büchner funnel and flask and stored overnight in a vacuum chamber to dry. Finally, the PEGDMA was again re-dissolved in DCM and re-precipitated to remove the unreacted methacrylic anhydride.

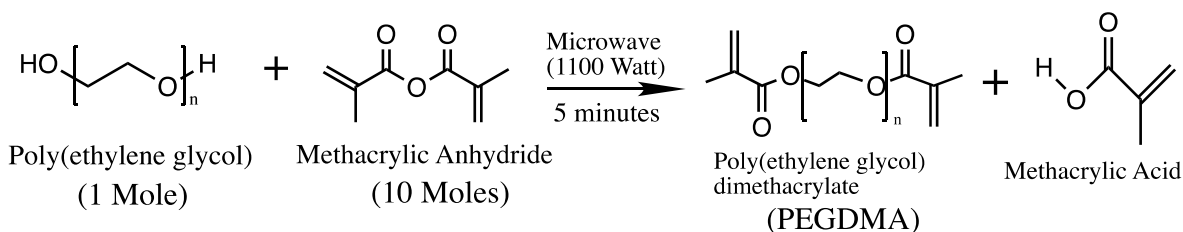
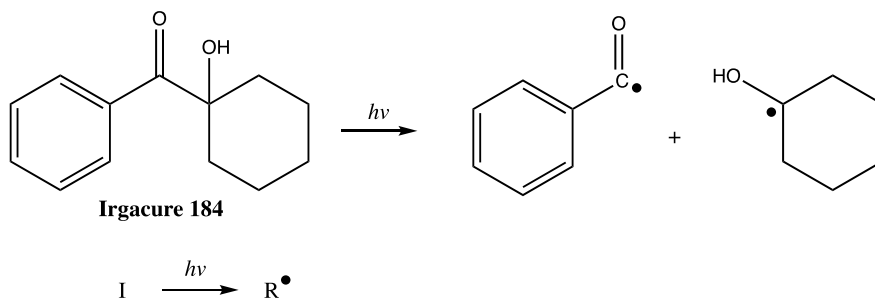


Figure 2.1: Microwave-assisted synthesis of PEGDMA.

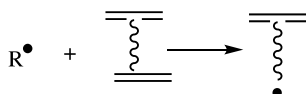
2.2.2.2 Preparation of PEGDMA hydrogel

10% (w/v) vacuum dried PEGDMA macromer was mixed into distilled water containing 2% (w/v) 1-hydroxycyclohexyl phenyl ketone (Irgacure 184) as a photoinitiator at room temperature until fully dissolved. Then, the solution was placed in small aluminum dishes and photo-polymerized under UV-radiation (365 nm) at room temperature for 5-10 mins. Hydrogels were removed after curing and stored in distilled water for further testing. Figure 2.2 summarizes the reaction steps occurring during PEGDMA polymerization. During step 1, the photoinitiator (Irgacure 184) is dissociated into radicals. The radicals interact with $-C=C-$ end bonds to initiate the free radical polymerization reaction in step 2. The polymerization propagates during step 3, forming a crosslinked network. Also, the PEGDMA hydrogels in the presence of water become physically crosslinked via the formation of hydrogen bonds, as shown in Figure 2.2.

Step 1: Dissociation of Initiator (I)



Step 2: Reaction of PEGDMA with radical



Step 3: Network formation among PEGDMA monomer

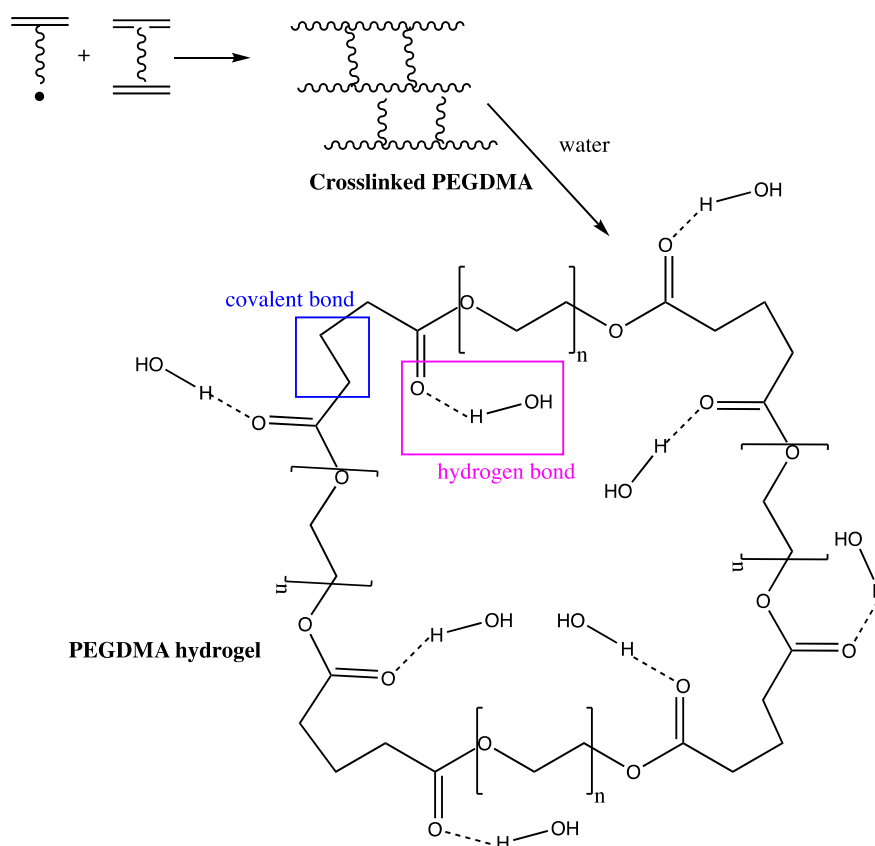


Figure 2.2 Photo-crosslinking reaction of PEGDMA to obtain the PEGDMA hydrogel via free radical polymerization

2.2.2.3 Characterization of PEGDMA samples

Infrared spectra of the starting material- PEGDMA powder and final product-PEGDMA hydrogel were measured by attenuated total reflection (ATR) method using a Thermo Nicolet 6700 Fourier transform infrared spectrometer. The spectrums were analyzed using OMNIC 7.3 software. All spectra were recorded between 400 and 4000 cm^{-1} over 256 scans with a resolution of 4 cm^{-1} .

$^1\text{H-NMR}$ spectra were measured with 400 MHz spectrometer, at room temperature for at least 64 scans. Each spectrum was phase-corrected; the baseline was subtracted and integrated by a Mest Re Nova software. The degree of methacrylation was measured using the following equation:

$$\text{Degree of Methacrylation (\%)} = \left[\frac{\frac{V}{10}}{\frac{V}{10} + \left\{ \frac{O}{4} * \frac{44}{\text{MW of PEG}} \right\}} \right] * 100 \quad \text{Equation 1}$$

Where V (vinylic integrals) is the summation of the peaks 'a', 'b' and 'c', O: the oxyethylene integral is the integral of peak 'd' (refer to Figure 2.3).

Gel permeation chromatography (GPC) was performed on a Malvern OmniSEC Resolve and Reveal system using a refractive index detector and two PL Gel Mixed-C plus guard columns with 5 μm pores were used. The sample of 5 mg was dissolved in 5 mL of tetrahydrofuran (THF) (at 35°C), which was used as the mobile phase with a flow rate of 1.0 mL/min. The column was calibrated using polystyrene (PS) standards²⁷. Average molar masses of samples were obtained using Agilent Cirrus GPC software. Mean values of replicates give us the weight-average molar mass (M_w) and dispersity index (PDI).

The morphological structure of the hydrogels was investigated by scanning electron microscopy (SEM, Zeiss EVO 50 VP-SEM, Carl Zeiss Microscopy, LLC, White Plains, NY) to obtain the topological characteristics of the hydrogels. After photo-crosslinking, swollen hydrogels were lyophilized in a freeze dryer. The fractured surfaces of pre-chilled hydrogels in liquid nitrogen were studied by SEM. The samples were mounted on aluminium support stubs with double stick tape or fingernail polish. Then the stubs were sputtered with gold (EMS Q150R sputter coating device) prior to SEM observations. The average pore size of the samples was quantified using ImageJ software.

The swelling analysis was performed in hydrogel samples lyophilized in a freeze dryer and weighed to obtain dry sample weight (W_d). Then, samples were immersed in distilled water at room temperature for 48 hours to reswell the samples. The swollen hydrogels were removed from the water and after wiping the excess water on the surface were weighed to obtain the weight of the wet sample (W_w). Swelling ratios were calculated using the following equation:

$$\text{Mass Swelling (\%)} = \left(\frac{W_w - W_d}{W_d} \right) * 100 \quad \text{Equation 2}$$

Modulated differential scanning calorimetry (DSC) (modulate $\pm 0.531^\circ\text{C}$ every 60 seconds using a heating rate $5^\circ\text{C}/\text{min}$) was carried out to observe the change in crystallization temperature (T_c), melting temperature (T_m) and enthalpy of melting (ΔH_m) of the polymer networks. Polymer crystallinity can be determined with DSC by quantifying the heat associated with melting (fusion) of the polymer. This heat is reported as percent crystallinity ($\% X_c$)²⁸ by normalizing the observed heat of fusion (ΔH_m) to a 100% crystalline sample of the same polymer ($\Delta H_m^0 = 196.8 \text{ J/g}$)²⁹.

Table 3 gives the quantification of crystallinity (from equation 3) in the PEGDMA based on reversible heat flow.

$$X_c (\%) = [\Delta H_m / \Delta H_m^0] * 100 \quad \text{Equation 3}$$

The mechanical properties of the hydrogels were tested with the help of a dynamic mechanical analyzer (DMA) TA Instrument RSAIII, US. Compression testing analysis was carried out according to the ASTM D695-15³⁰ on the specimens with 5 mm diameter and extension rate -0.067 mm/s at room temperature using the cylindrical compression geometry, performed for 3-6 replicates. From this data, the compression modulus was determined. Rheological measurements were obtained using a TA Instruments Rheology Advantage AR, US, using parallel plate geometry fitted with 25 mm aluminum plate in the presence of air and at room temperature. Cylindrical samples (15 μ m diameter and 1000 μ m thickness) were cut and placed for strain sweep and frequency sweep experiments. From the strain sweep experiment performed at 1Hz, 0.5% strain was selected (in the linear elastic range), which was then used as the constant strain in the oscillatory frequency sweep experiments.

The biodegradation analysis of PEGDMA was performed in distilled water containing 600-900 mg/L of lysozyme^{31,32} at 37°C. Enzymatic degradation was monitored for four (4) weeks, while the enzyme solution was refreshed once. At a predetermined time (1, 2, 3, and 4 weeks), samples were removed from the medium and dried thoroughly. The weight of samples, before (m_1) and after (m_2) in-vitro degradation and degree of degradation (%) was determined relative to respective weight loss to the initial weight of the sample as follows:

$$\text{Degree of Degradation (\%)} = \left(\frac{m_1 - m_2}{m_1} \right) * 100 \quad \text{Equation 4}$$

2.2.2.4 Cell attachment and growth on the hydrogel scaffolds

Fibroblast cells were cultured in DMEM media with 10% FBS and 1% Penicillin-Streptomycin antibiotic solution in a 5% CO₂ incubator at 37°C. The scaffolds were UV sterilized for 30 minutes and placed in sterile tissue culture plates with DMEM-10 media overnight. Following day cells were seeded (50,000/well) on scaffolds. The cellular constructs were maintained in 5% CO₂ incubator at 37°C. The cells were regularly monitored using optical and fluorescent microscope after staining with live/dead stain according to manufacturer protocol at a concentration of 1µl/ml. The scaffolds were incubated with stain at 37°C for 30 minutes, followed by washing with PBS twice and then imaging.

Cell viability of cells grown on scaffolds was measured by MTT (3-(4, 5-dimethyl-thiazol-2-yl)-2,5-diphenyl-tetrazolium bromide) dye reduction. Fibroblast cells were seeded in a 96-well plate at a density of 20,000 cells per well in DMEM containing 10% FBS and grown overnight. At periodic time intervals, 10 µl of MTT (0.5 mg/ml) in sterile-filtered PBS was added to each well and incubated for 3 h to allow the formation of formazan crystals at 37 °C. DMSO (200 µl) was added to each well after incubation to dissolve the MTT formazan crystals and incubated for another 60 min at 37°C. The absorbance of formazan products was measured at 570 nm using a microplate reader (Synergy LX, BioTek). The percentage of live cell death was obtained by the difference between the absorbance of control cells and cells grown on scaffolds.

The seeding efficiency of fibroblast cells on hydrogels was investigated by plating 20,000 cells on the surface of each scaffold in a 48 well cell culture plate in 100µl of media and incubated in 5%

CO₂ incubator at 37 °C. After 30 minutes, an additional 200 µl of media was added and incubated. MTT assay was performed after 2 hours of incubation to calculate the number of seeded cells. A 96-well without scaffold was plated with cells and was used as a control. Seeding efficiency was calculated using the following equation where C is the absorbance of control cells and T is the absorbance of cells on the scaffold.

$$\text{Seeding efficiency (\%)} = \left(\frac{C-T}{C} \right) * 100 \quad \text{Equation 5}$$

2.3 Results and Discussion

2.3.1 Characterization of the PEGDMA samples

The degree of methacrylation of the different molecular weight PEGDMA macromer samples synthesized was determined by proton nuclear magnetic resonance (¹H-NMR) (Figure 2.3).

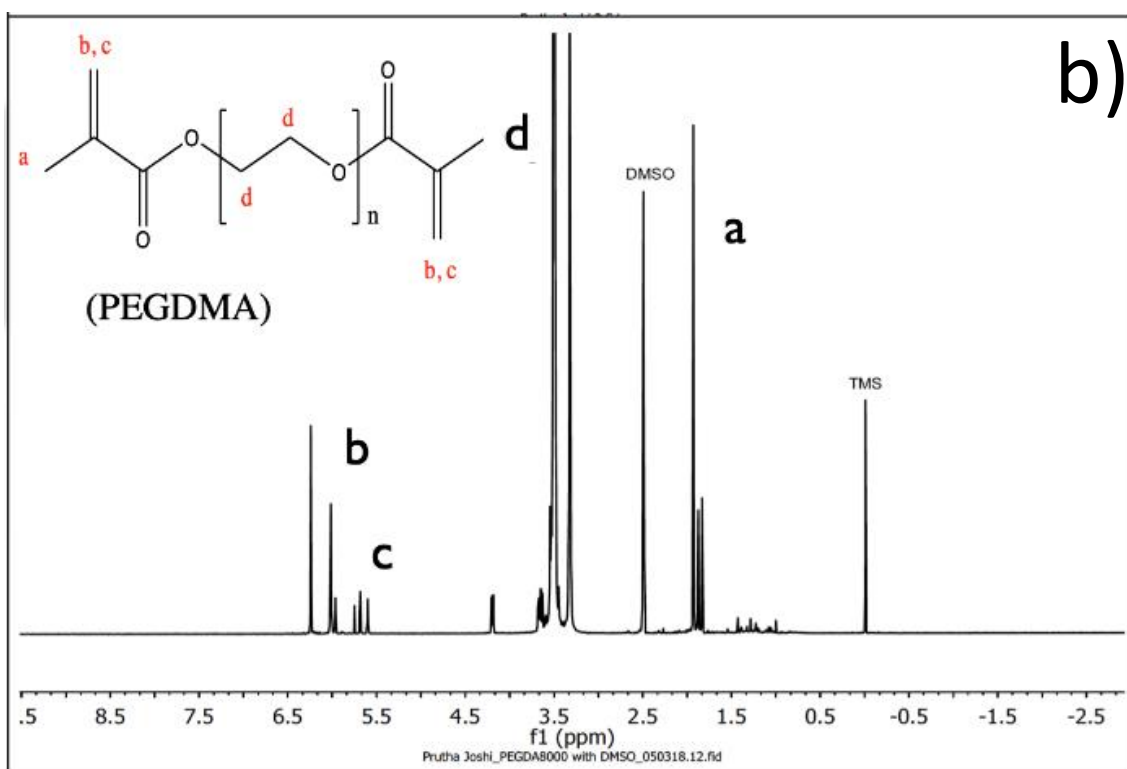
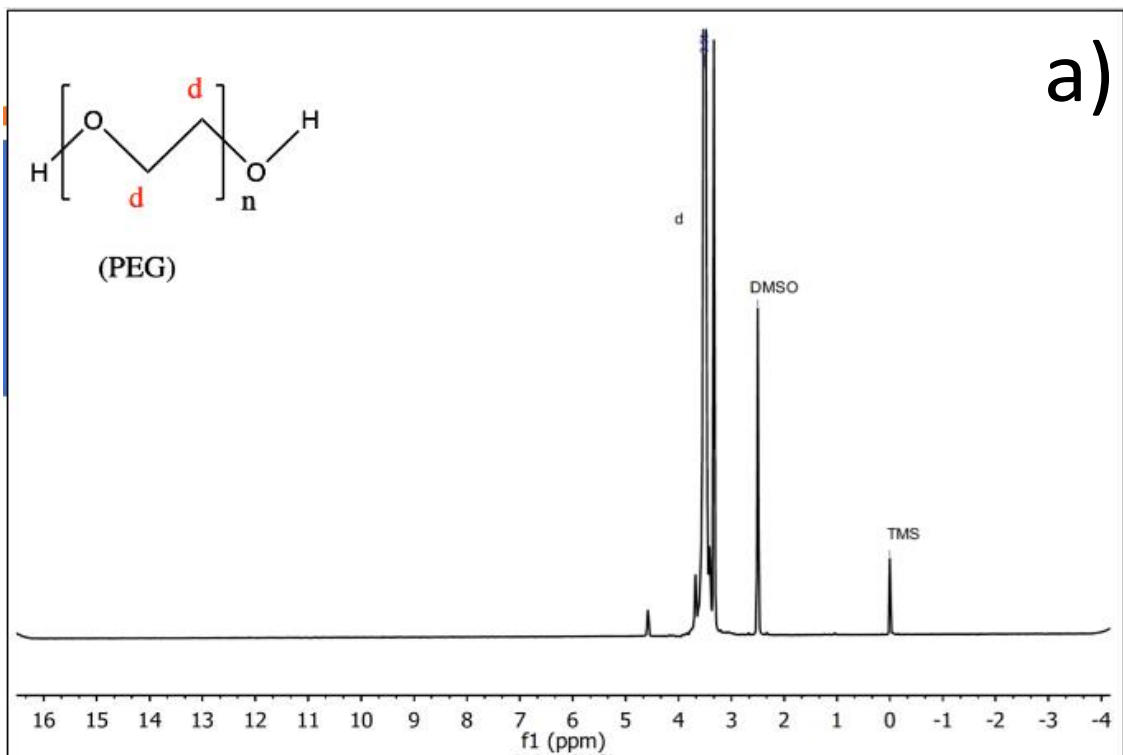


Figure 3.3: $^1\text{H-NMR}$ spectra of 8000 Da PEGDMA using microwave-assisted PEG modification. a) PEG and b) PEGDMA

The degree of methacrylation calculated using equation 1, from the experimental/theoretical ratio of terminal methacrylate protons (a, b and c) to the central PEG protons (d) are reported in Table 2.1. These results are in agreement with the values obtained by Hove and collaborators using a similar procedure²⁶.

Table 2.1 Gel permeation chromatography of different varieties of PEGDMA

PEGDMA samples	MW of commercial PEG (Da)	Degree of Methacrylation (%)	MW of PEGDMA (M_w)(Da)	Dispersity (PDI)
PEGDMA 4000	4000	73	4978	3.56
PEGDMA 6000	6000	77	5604	2.28
PEGDMA 8000	8000	84	6990	1.11

Besides, the weight-average molecular weights and dispersity of the synthesized polymers characterized by gel permeation chromatography (GPC) are also reported in Table 2.1. The dispersity indicates the distribution of individual molecular masses in a batch of polymers. In PEGDMA 8000, the polymer chain lengths have considerably more uniform nature as compared to the other two varieties.

FTIR analysis of the freeze-dried PEGDMA (hydrogels) and PEGDMA (macromer) was performed to characterize and confirm the chemical crosslinking among the different PEGDMA hydrogels after the free radical polymerization. The FTIR spectrum (Figure 2.4) displays the comparison of characteristic bands of PEGDMA powder (pre-photopolymerized) and PEGDMA hydrogel (post-photopolymerized). The strong bands at $\sim 2880\text{ cm}^{-1}$ and $\sim 1466\text{ cm}^{-1}$ were representing $-\text{CH}_2$ bonds^{22,33}. The peak at 1727 cm^{-1} and 1717 cm^{-1} in PEGDMA hydrogel and

PEDGA macromer represent the C=O stretching mode of ester groups^{22,33}. The peak at 1636 cm⁻¹ is assigned to the C=C-H in PEGDMA, which disappears during the curing process, marking the success of the free radical polymerization reaction carried out^{22,34}. The bands at ~1140 cm⁻¹ and ~960 cm⁻¹ represent the asymmetrical C-O-C stretching mode³⁴.

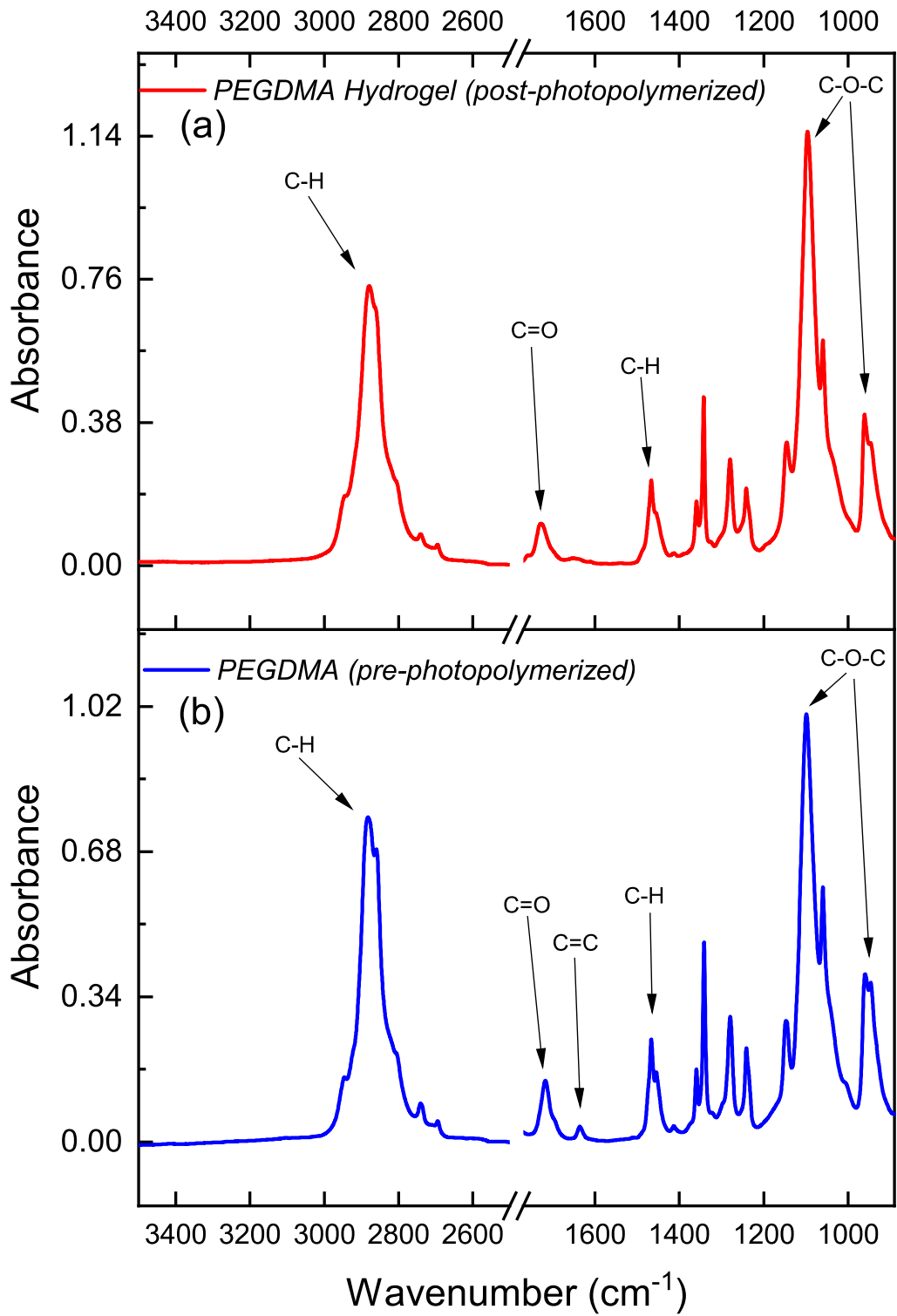


Figure 2.4: FT-IR spectrum for a) PEGDMA hydrogel (post-photopolymerized) and b) PEGDMA (pre-photopolymerized)

Figures 2.5 a, b and c show the SEM micrograph of the freeze-dried PEGDMA hydrogels with different molecular weight. These pictures reveal a well-defined 3D porous network of the hydrogel with an average pore size of 60 μ m, 72 μ m and 87 μ m for 4000Da, 6000Da and 8000Da respectively. As the molecular weight of PEGDMA increases from 4000 Da (Figure 2.5a) to 8000Da (Figure 2.5c), the voids become more prominent. As expected, there is a decrease in the crosslinking density when the molecular weight of PEGDMA is increased, as a consequence of the increased molecular weight between crosslinking points. To exemplify the effect of the crosslinked network, cartoon structures are shown in Table 2.2, evidencing the effect of the molecular weight of the PEGDMA samples and the pore size.

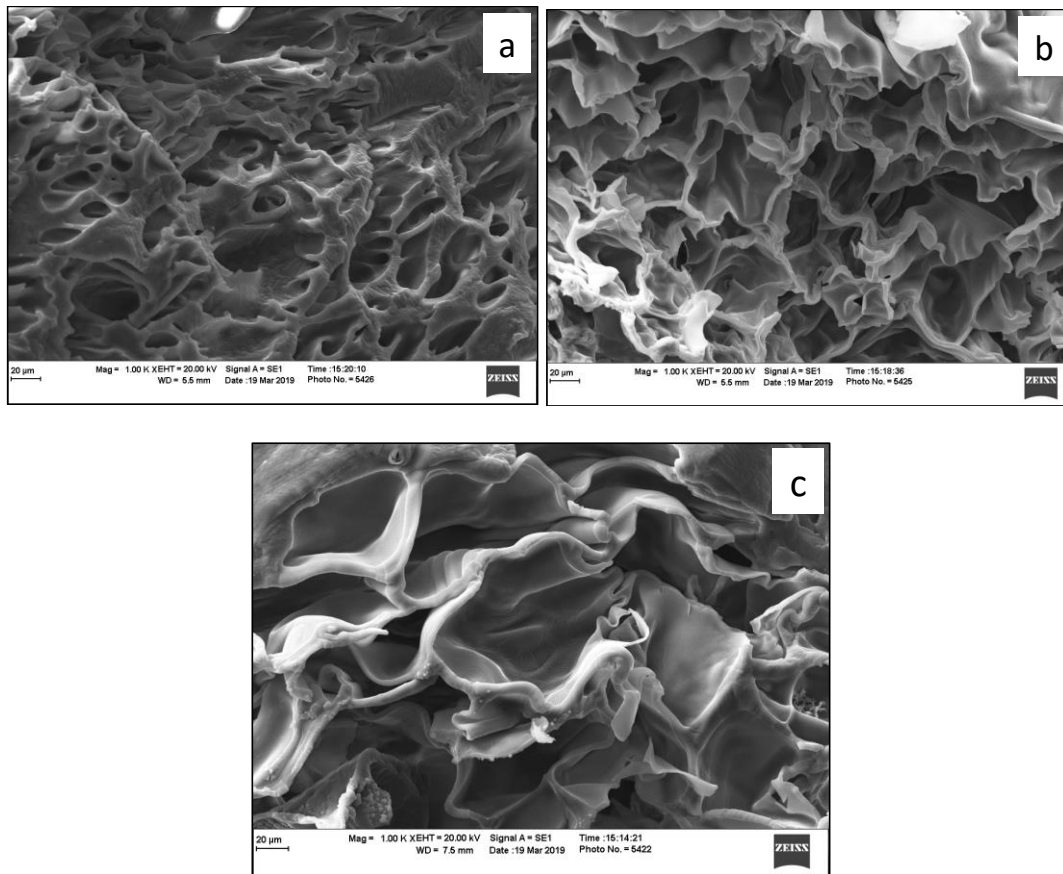


Figure 2.5: SEM image of PEGDMA hydrogel a) 4000 Da, b) 6000 Da and c) 8000 Da

The porous structure is crucial for the cell dwelling, proliferation and cell culture on polymer-based hydrogel; on the other side, this open architecture affects the swelling and mechanical properties of the hydrogel, as can be observed in the following section.

The water uptakes (%) of the synthesized PEGDMA hydrogels were calculated using equation 2. The obtained water uptake percentages are reported as 1420 ± 234 , 1597 ± 64 , and 1937 ± 141 for PEGDMA 4000, 6000 and 8000, respectively. The observed trend shows that as the molecular weight of PEG is increased, the water uptake (or swelling ratio) is also increased. This property also follows the pore size trend explained before. As the molecular weight of PEGDMA increases, there is an increase in the molecular weight between the crosslinking points, which increases the ability to swells.

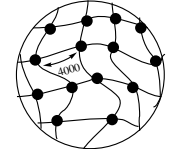
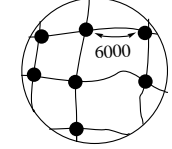
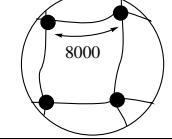
Table 2.2: Modulated DSC data for different varieties of PEGDMA

	Tc (°C)	ΔH_c (J/g)	Tm (°C)	ΔH_m (J/g)	Crystallinity (%)
PEGDMA 4000	27.75	108.1	48.42	70.57	35.9
PEGDMA 6000	37.06	146.4	56.31	109.3	55.5
PEGDMA 8000	41.54	174.2	57.93	151.6	77.0

Table 2.2 summarizes the temperatures of melting (Tm), temperatures of crystallization (Tc), heat of melting (ΔH_m) and heats of crystallization (ΔH_c) of the different PEGDMA hydrogels. As was explained before, the increase of the molecular weight between crosslinking points induces the crystallization of the linear PEG sample. As a result, the heat of melting increases, and the melting

temperature elevates hence increases the tendency to form a crystalline phase reducing the segmental mobility of the network.

Table 2.3: *Characterization of the crosslinked PEGDMA hydrogels*

		Compressive Modulus (kPa)	Shear Modulus (kPa)
PEGDMA 4000		17 ± 7	2.7 ± 0.73
PEGDMA 6000		18.8 ± 6	4.31 ± 0.68
PEGDMA 8000		16.5 ± 4	1.9 ± 0.43

The mechanical behavior of the hydrogels is reported in Table 2.3. It can be observed that the compressive and shear modulus shows an increase followed by a decreased effect, as the molecular weight of PEGDMA is increased. As explained, two factors are affecting modulus of the network, the crosslinking density, and the induced crystallinity. As we increase the molecular weight of PEGDMA, the molecular weight of the linear PEG increases the ability of the linear chains to crystallize, thus, increases the modulus. However, at higher molecular weight, the decrease of the crosslinking densities overpowers the effect of the crystallinity, reducing the modulus.

Figure 2.6 shows the degradation behavior of synthesized hydrogels with degradative weight loss of $23\% \pm 1.1$, $24\% \pm 1.2$ and $28\% \pm 1.4$ for PEGDMA 4000, 6000 and 8000, respectively. In these

experiments, a lysozyme solution served as the medium for biodegradation studies, which is similar to the physiological conditions found in the human body which undergo normal metabolism of degradation. As the exposure to the lysozyme enzyme solution increased, the degree of degradation was also increased. It can be observed in Figure 2.6, the hydrogel with the higher crosslinking density (lower molecular weight between crosslinking points) degrades at a slower rate as compared to PEGDMA 8000 Da. Moreover, having the larger pore size, PEGDMA 8000 allows a higher amount of the lysozyme solution to penetrate and degrade of the hydrogel.

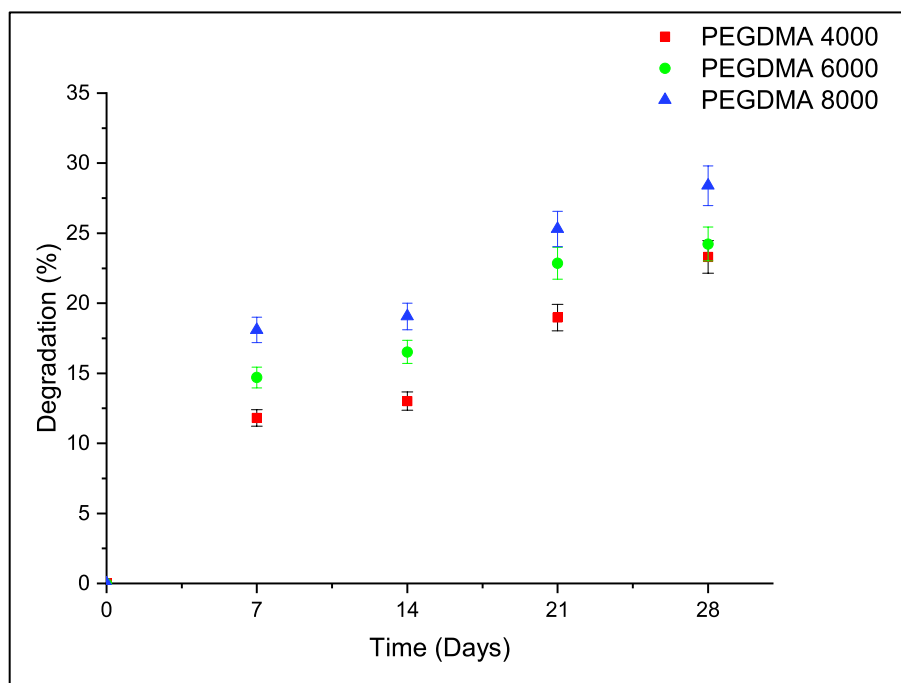


Figure 2.6: *Degradation profile of PEGDMA hydrogels*

Figure 2.7 shows the morphology of hydrogel morphology after 14 days of degradation. From the scanning electron microscopy (SEM), it is possible to observe the effect of the degradation process, as the porous structure collapses and fibrillar structures are formed.

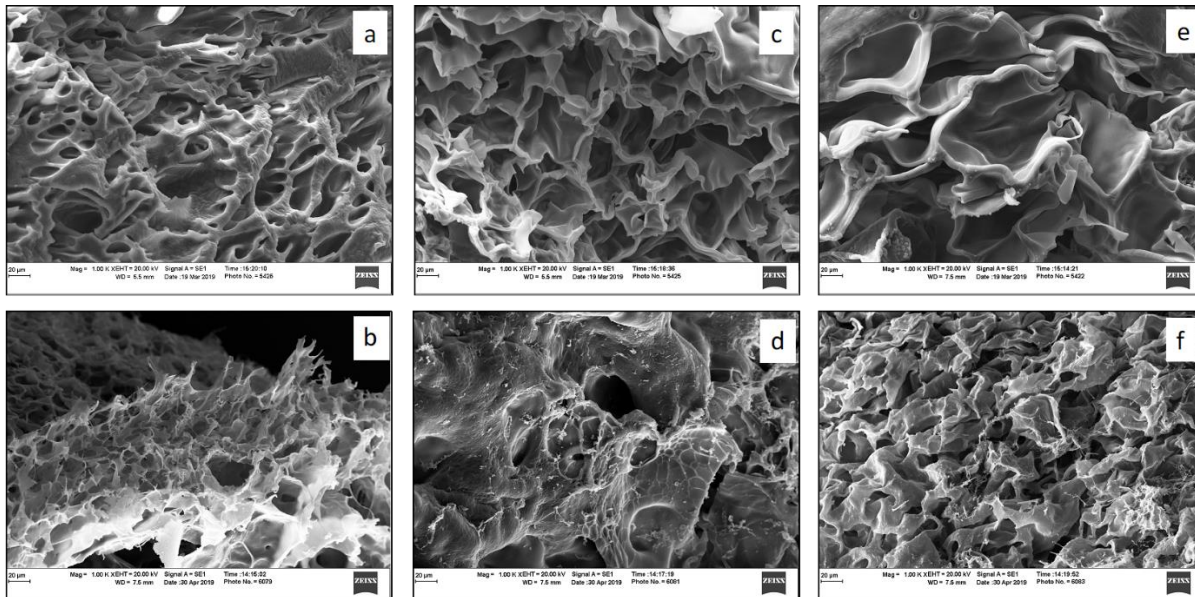


Figure 2.7: Effect on the morphological characterization after degradation of a hydrogel. a) PEGDMA 4000 at 0th week, b) PEGDMA 4000 after 2nd week, c) PEGDMA 6000 at 0th week, d) PEGDMA 6000 after 2nd week, e) PEGDMA 8000 at 0th week, f) PEGDMA 8000 after 2nd week of degradation.

2.3.2 The proliferation of fibroblast cells in the presence of the hydrogels

Microscopic studies of fibroblast cells cultured on the hydrogels show cell growth up to 7 days.

Cells were stained with live/dead stain for visualization (Figure 2.8).

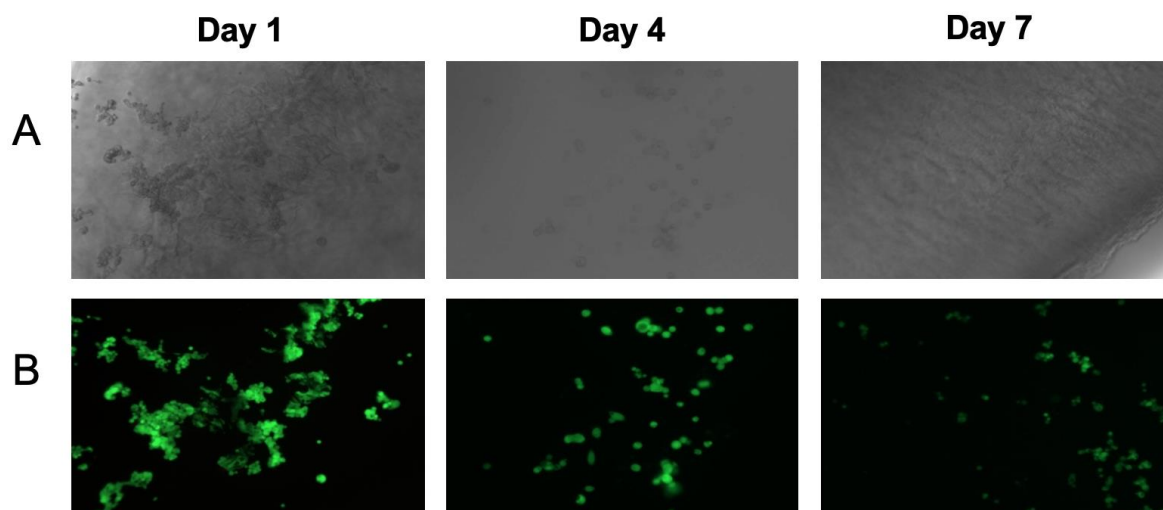


Figure 2.8: *Fibroblast Cell growth on PEGDMA 8000 hydrogels. A) Bright-field images of the cells B) Live/Dead Stain images of the cells*

Seeding efficiencies for our designed scaffold PEGDMA 4000, PEGDMA 6000, and PEGDMA 8000 were 96.8%, 93.7%, and 100%, respectively. Cell viability was estimated using MTT assay. Cell grown on scaffolds were viable for up to 7 days (Figure 2.9).

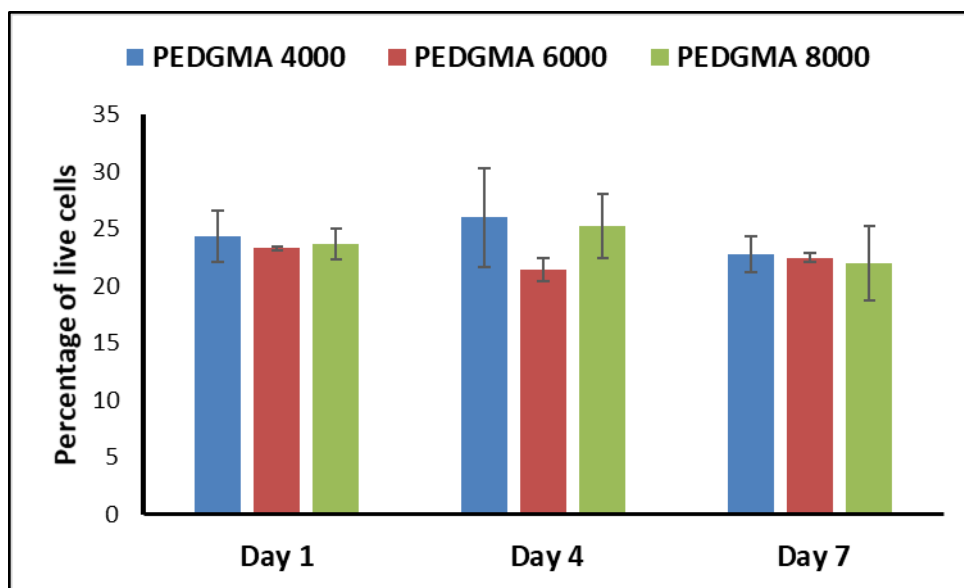


Figure 2.9: Cell viability of Fibroblast cells by MTT assay

2.4 Conclusion

PEGDMA hydrogels samples were synthesized using PEG with different molecular weights of PEG (4000 Da, 6000 Da, and 8000 Da) with the aid of microwaves assisted polymerization. Further, PEGDMA samples were photocured in the presence of Irgacure 184 to obtain crosslinked PEGDMA hydrogels via free radical polymerization. The characterization of hydrogels illustrated their biocompatibility and mechanical strength for their applications in tissue engineering. Cellular studies in our research work supported cell growth suggesting, poly (ethylene glycol) based hydrogels have the potential for application for tissue regeneration inside the human body.

2.5 References

- (1) Ahmed, E. M. Hydrogel: Preparation, Characterization, and Applications: A Review. *J. Adv. Res.* **2015**, *6* (2), 105–121. <https://doi.org/10.1016/j.jare.2013.07.006>.
- (2) Lee, C. Y.; Teymour, F.; Camastral, H.; Tirelli, N.; Hubbell, J. A.; Elbert, D. L.; Papavasiliou, G.; Kousar, F.; Malana, M. A.; Chughtai, A. H.; et al. Synthesis and Characterization of Methacrylamide-Acrylic Acid-N-Isopropylacrylamide Polymeric Hydrogel: Degradation Kinetics and Rheological Studies. *Biomed. Mater.* **2018**, *155* (2), 1275–1298. <https://doi.org/10.1088/1748-605X/aa9ad2>.
- (3) Caló, E.; Khutoryanskiy, V. V. Biomedical Applications of Hydrogels: A Review of Patents and Commercial Products. *Eur. Polym. J.* **2015**, *65*, 252–267. <https://doi.org/10.1016/j.eurpolymj.2014.11.024>.
- (4) Hoare, T. R.; Kohane, D. S. Hydrogels in Drug Delivery: Progress and Challenges. *Polymer (Guildf)*. **2008**, *49* (8), 1993–2007. <https://doi.org/10.1016/j.polymer.2008.01.027>.
- (5) Fu, Y.; Xu, K.; Zheng, X.; Giacomini, A. J.; Mix, A. W.; Kao, W. J. 3D Cell Entrapment in Crosslinked Thiolated Gelatin-Poly(Ethylene Glycol) Diacrylate Hydrogels. *Biomaterials* **2012**, *33* (1), 48–58. <https://doi.org/10.1016/j.biomaterials.2011.09.031>.
- (6) Gopinathan, J.; Noh, I. Recent Trends in Bioinks for 3D Printing. **2018**, 1–15.
- (7) Khademhosseini, A.; Langer, R. Microengineered Hydrogels for Tissue Engineering. *Biomaterials* **2007**, *28* (34), 5087–5092. <https://doi.org/10.1016/j.biomaterials.2007.07.021>.
- (8) Peppas, N. A.; Hilt, J. Z.; Khademhosseini, A.; Langer, R. Hydrogels in Biology and Medicine: From Molecular Principles to Bionanotechnology. *Adv. Mater.* **2006**, *18* (11),

- 1345–1360. <https://doi.org/10.1002/adma.200501612>.
- (9) Baolin, G.; Ma, P. X. Synthetic Biodegradable Functional Polymers for Tissue Engineering: A Brief Review.
- (10) Cheng, Y.; Lu, J.; Liu, S.; Zhao, P.; Lu, G.; Chen, J. The Preparation, Characterization and Evaluation of Regenerated Cellulose/Collagen Composite Hydrogel Films. *Carbohydr. Polym.* **2014**, *107* (1), 57–64. <https://doi.org/10.1016/j.carbpol.2014.02.034>.
- (11) Wang, C.; Liu, H.; Gao, Q.; Liu, X.; Tong, Z. Alginate-Calcium Carbonate Porous Microparticle Hybrid Hydrogels with Versatile Drug Loading Capabilities and Variable Mechanical Strengths. *Carbohydr. Polym.* **2008**, *71* (3), 476–480. <https://doi.org/10.1016/j.carbpol.2007.06.018>.
- (12) Monteiro, N.; Thirivikraman, G.; Athirasala, A.; Tahayeri, A.; França, C. M.; Ferracane, J. L.; Bertassoni, L. E. Photopolymerization of Cell-Laden Gelatin Methacryloyl Hydrogels Using a Dental Curing Light for Regenerative Dentistry. *Dent. Mater.* **2018**. <https://doi.org/10.1016/j.dental.2017.11.020>.
- (13) Lin, C. C.; Metters, A. T. Hydrogels in Controlled Release Formulations: Network Design and Mathematical Modeling. *Adv. Drug Deliv. Rev.* **2006**, *58* (12–13), 1379–1408. <https://doi.org/10.1016/j.addr.2006.09.004>.
- (14) Biondi, M.; Borzacchiello, A.; Mayol, L.; Ambrosio, L. Nanoparticle-Integrated Hydrogels as Multifunctional Composite Materials for Biomedical Applications. *Gels* **2015**, *1* (2), 162–178. <https://doi.org/10.3390/gels1020162>.
- (15) Vanderhoff, J. L.; Alcoutlabi, M.; Magda, J. J.; Prestwich, G. D. Rheological Properties of Cross-Linked Hyaluronan-Gelatin Hydrogels for Tissue Engineering. *Macromol. Biosci.* **2009**, *9* (1), 20–28. <https://doi.org/10.1002/mabi.200800141>.

- (16) Costa-Pinto AR, Martins AM, Castelhana-Carlos MJ, Correlo VM, Sol PC, Longatto-Filho A, Battacharya M, R. R. and N. N. In Vitro Degradation and in Vivo Biocompatibility of Chitosan– Poly(Butylene Succinate) Fiber Mesh Scaffolds. *J. Bioact. Compat. Polym.* **2014**, 29 (2), 137–151.
- (17) Saraiva Sofia M, Miguel Sonia P, Ribeiro Maximiano P, Coutinho Paula, C. I. J. Synthesis and Characterization of a Photocrosslinkable Chitosan-Gelatin Hydrogel Aimed for Tissue Regeneration. *RSC Adv.* **2015**, 5, 63478–63488.
- (18) Tan G.X., Wang Y.J., G. Y. X. Synthesis and Properties of Polyethylene Glycol Diacrylate /2-Hydroxyethyl Methacrylate Hydrogels. *Key Eng. Mater.* **2008**, 368–372, 1175.
- (19) Tan, G.; Wang, Y.; Li, J.; Zhang, S. Synthesis and Characterization of Injectable Photocrosslinking Poly (Ethylene Glycol) Diacrylate Based Hydrogels. *Polym. Bull.* **2008**, 61, 91–98. <https://doi.org/10.1007/s00289-008-0932-8>.
- (20) Wang Q.F., Ren L., Wang Y.J., Yao Y.C., Hou S.R. No Title. *J. South China Univ. Technol. (Natural Sci. Ed.* **2013**, 41 (7), 62.
- (21) Morris, V. B.; Nimbalkar, S.; Younesi, M.; McClellan, P.; Akkus, O. Mechanical Properties, Cytocompatibility and Manufacturability of Chitosan:PEGDA Hybrid-Gel Scaffolds by Stereolithography. *Ann. Biomed. Eng.* **2017**, 45 (1), 286–296. <https://doi.org/10.1007/s10439-016-1643-1>.
- (22) Escudero-Castellanos, A.; Ocampo-García, B. E.; Domínguez-García, M. V.; Flores-Estrada, J.; Flores-Merino, M. V. Hydrogels Based on Poly(Ethylene Glycol) as Scaffolds for Tissue Engineering Application: Biocompatibility Assessment and Effect of the Sterilization Process. *J. Mater. Sci. Mater. Med.* **2016**, 27 (12).

<https://doi.org/10.1007/s10856-016-5793-3>.

- (23) Racine, L.; Costa, G.; Bayma-Pecit, E.; Texier, I.; Auzély-Velty, R. Design of Interpenetrating Chitosan and Poly(Ethylene Glycol) Sponges for Potential Drug Delivery Applications. *Carbohydr. Polym.* **2017**, *170*, 166–175.
<https://doi.org/10.1016/j.carbpol.2017.04.060>.
- (24) Oh, Y.; Cha, J.; Kang, S. G.; Kim, P. A Polyethylene Glycol-Based Hydrogel as Macroporous Scaffold for Tumorsphere Formation of Glioblastoma Multiforme. *J. Ind. Eng. Chem.* **2016**, *39*, 10–15. <https://doi.org/10.1016/j.jiec.2016.05.012>.
- (25) Melchels, F. P. W.; Dhert, W. J. A.; Hutmacher, D. W.; Malda, J. Development and Characterisation of a New Bioink for Additive Tissue Manufacturing. *J. Mater. Chem. B* **2014**, *2* (16), 2282. <https://doi.org/10.1039/c3tb21280g>.
- (26) Van Hove, A. H.; Wilson, B. D.; Benoit, D. S. W. Microwave-Assisted Functionalization of Poly(Ethylene Glycol) and On-Resin Peptides for Use in Chain Polymerizations and Hydrogel Formation. *J. Vis. Exp.* **2013**, No. 80, 1–15. <https://doi.org/10.3791/50890>.
- (27) Sperling, L. H. *INTRODUCTION TO PHYSICAL POLYMER*.
- (28) Blaine, R. L.; Ph, D. Determination of Polymer Crystallinity by DSC. 1–3.
- (29) Pielichowski, K.; Flejtuch, K. Differential Scanning Calorimetry Studies on Poly (Ethylene Glycol) with Different Molecular Weights for Thermal Energy Storage Materials †. **2003**, *696* (November 2001), 690–696. <https://doi.org/10.1002/pat.276>.
- (30) ASTM D695-15. Standard Test Method for Compressive Properties of Rigid Plastics. *ASTM Int.* **2015**.
- (31) Lončarević, A.; Ivanković, M.; Rogina, A. Lysozyme-Induced Degradation of Chitosan: The Characterisation of Degraded Chitosan Scaffolds. *J. Tissue Repair Regen.* **2017**, *19*

- (1), 177.
- (32) *Handbook of Polymers for Pharmaceutical Technologies, Biodegradable Polymers*; Thakur Vijay Kumar, T. M. K., Ed.; Scrivener Publishing, 2015.
- (33) Guo X, Wang W, Wu G, Zhang J, Mao C, D. Y. et al. Controlled Synthesis of Hydroxyapatite Crystals Templated by Novel Surfactants and Their Enhanced Bioactivity. *New J Chem.* **2011**, *35*, 663–671.
- (34) Cheing BW, Ibrahim NA, Yunus WMZW, H. M. Poly (Lactic Acid)/Poly (Ethylene Glycol) Polymer Nanocomposites: Effects of Graphene Nanoplatelets. *Polymers (Basel)*. **2013**, *6*, 93–104.

CHAPTER 3

Synthesis of polysaccharide-based hydrogels for biomedical applications

3.1 Introduction

Tissue engineering is a discipline that is continuously evolving with the intent to reproduce cellular tissues^{1,2}. According to the US department of health and human services³, over the last decades, the number of patients on the waiting list of centers for organ donation is continuously increasing. For example, organ donors in 2019 were reported to be approximately 12,742 as compared to ~112,923 people who are still waiting for a donation³. This is the reason for ongoing research in materials and methods to improve the repair and regeneration of damaged tissues and organ replacement. Hydrogels have been extensively studied for their applications in biomedicine, and it has been observed that chemical and the network structure determine their final properties⁴. Polymeric systems like poly (ethylene glycol) and acrylic acid-based hydrogels perform very well in terms of mechanical properties but are hard for cell-binding and degradation⁵. These traditional hydrogel materials have low cell-responsivity and limited biodegradability due to the limitation of pores. Moreover, there are voids in biomaterials research considering the mechanical performance along with the good control of the pore geometry of the hydrogels.

Among all of the potential systems that are used, or have been proposed, for the biomedical applications^{5,6}, natural polysaccharides^{7,8} and their derivatives⁹⁻¹² are indeed the most versatile polymeric materials. Polysaccharides have applications ranging from their intrinsic biological activity to their ability in living cell encapsulation, as well as from bone and cartilage repair to the

preparation of friendly scaffolds for tissue engineering^{13,14,8,15}. The distinctive and multi-faceted properties of polysaccharides are dependent on the different molecular weights and chemical composition that these macromolecules possess¹⁶. Also, the types and number of reactive groups present on every single unit control the biological and physicochemical properties that make them attractive for cell interaction. The 3D porous structures needed for tissue-engineered scaffold purposes can be obtained using various polysaccharide hydrogels because of their versatility in producing external shapes that can be customized according to specific needs and, at the same time, well-defined networks with appropriate porosity capable of hosting cells¹⁶.

Gelatin is a hydrophilic protein obtained from denatured collagen¹⁷ obtained from various sources. Due to its biodegradability¹⁸, biocompatibility¹⁹, and ability to form hydrogels, gelatin has an essential role in research related to biomedical materials, specifically for cell culture structures in tissue engineering applications²⁰. Gelatin can form covalently crosslinked hydrogels^{18,19} with enhanced biocompatibility and tensile strength. In previous studies, gelatin-chitosan scaffolds made from thermal gelation (physical crosslinking) were tested in the regeneration of tissues of the body such as skin^{21,22}, cartilage^{23,24}, and bone^{24,25}. These hydrogels were not stable and dissolved at times.

Chitosan is a linear polysaccharide derivative of chitin with a distribution of N-acetyl glucosamine and glucosamine units^{2,26}. Due to its significant properties such as biocompatible, biodegradable, hemostatic activity, antimicrobial, and mucoadhesive, it has been extensively used in the development of tissue scaffolds. According to Racine et al.²⁶, chitosan can be adapted into diverse structures such as spongy-like scaffolds or films, which makes it potential for biomedical

applications like wound dressing²², drug delivery²⁷, and tissue scaffolds^{8,28}. However, the limited solubility of chitosan in aqueous solutions tightens its applicability in regenerative medicine. As a solution to this, methacrylate groups can be added to primary amine groups of chitosan to make them hydrophilic.

The proposed idea is to modify the structure of gelatin and chitosan to make them undergo chemical crosslinking, to improve the hydrogel's mechanical properties such as the strength while enhancing the biodegradability and biocompatibility. This work focuses on the incorporation of methacrylate functionality in gelatin and chitosan polysaccharides by chemically transforming the primary amine groups present in the polysaccharides. The resulting materials were then crosslinked using UV photocuring in the presence of Irgacure 184 (365nm wavelength). Mechanical, chemical, rheological, and morphological properties were investigated, and degradability was monitored for the produced hydrogels. Hydrogels cultured with fibroblast cells confirms the cell growth on designed hydrogel scaffolds.

3.2 Materials and Methods

3.2.1 Materials

In this research work, Gelatin powder (Type A, ~300 bloom) was purchased from Electron Microscopy Sciences (US), and chitosan ($\geq 85\%$ deacetylated) was obtained from Alfa Aesar (US). Methacrylic anhydride was purchased from Thermofisher Scientific Inc. (US). Dulbecco's phosphate buffered saline (DPBS), acetic acid, and phenylamine were purchased from VWR (US). Photoinitiator, 1-hydroxycyclohexyl phenyl ketone (Irgacure 184), was purchased from TCI (US),

while the UV light source used (UVLS-28 EL Series UV Lamp) was manufactured by Analytik Jena (US). For the degradation studies, lysozyme (chicken egg white) was purchased from Thermofisher Scientific Inc. (US). Deuterated water (D₂O) and deuterated acetic acid (CD₃COOD) were purchased from Acros Organics (US). Fibroblast cells were brought commercially (CCL 110; ATCC, VA). Cells were cultured in DMEM (Gibco, Gaithersburg, MD) supplemented with 10% v/v fetal bovine serum (Gibco, Gaithersburg, MD). MTT (3-(4,5-Dimethylthiazol-2-yl)-2,5-Diphenyltetrazolium Bromide) salt was brought from Invitrogen (NY) and Live and Dead Double Staining Kit was bought (Abbkine, China).

3.2.2 Methods

3.2.2.1 Preparation of gelatin methacrylate

The synthesis of gelatin methacrylate (GelMA) was performed following the procedure reported by Nichol et al.¹. Gelatin 5% (w/v) was dissolved in Dulbecco's phosphate buffered saline (DPBS) at 60°C and stirred for 2 hours for complete dissolution. The required amount of methacrylic anhydride (MA) (7.1, 21.4, and 35.67 molar excess) was then added dropwise into the gelatin solution under vigorous stirring to get different varieties of GelMA. Later, the methacrylation reaction was continuously monitored for 5 hours under a nitrogen atmosphere. In the end, additional DPBS (10x) was added after 5 hours to end the reaction. The resultant mixture was dialyzed using a membrane (MWCO 12-14K Da) at 40°C against ultrapure water for a week. Finally, the solution was freeze-dried and stored at -80°C until further use. Figure 3.1-a shows the chemical modification of amine functionalities in gelatin to produce gelatin methacrylated (GelMA).

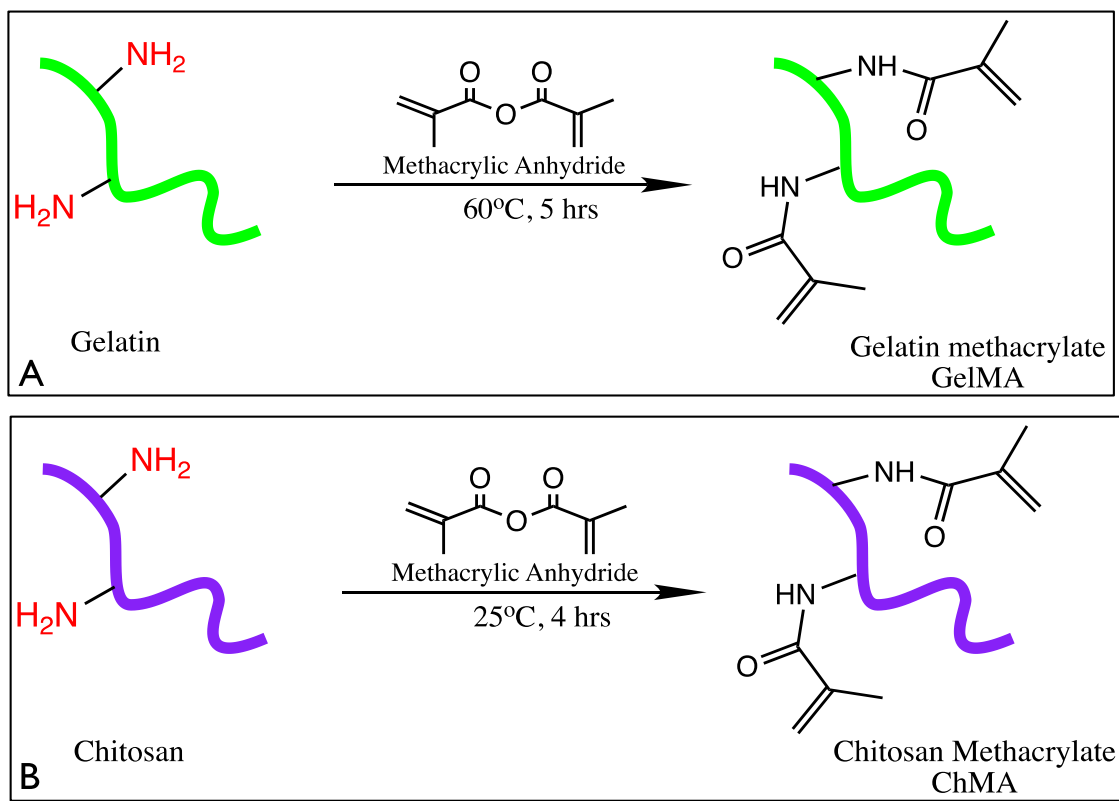


Figure 3.1: Methacrylation of a) gelatin and b) chitosan to obtain GelMA and ChMA, respectively.

3.2.2.2 Preparation of chitosan methacrylate

The synthesis of chitosan methacrylate (*ChMA*) was performed following the work of Saraiva et al.² with slight modifications. Figure 3.1-b shows the modification of amine functionality in chitosan towards the end of methacrylation. Chitosan 3% (w/v) was dissolved in 1-2% (w/v) acetic acid aqueous solution at 25°C and stirred overnight for complete dissolution. The required amount of methacrylic anhydride (MA) (35.67 molar excess) was then added dropwise into the chitosan solution under vigorous stirring. The methacrylation reaction was continued for 4 hours at 25°C. The resultant mixture was dialyzed using a membrane (MWCO 12-14K Da) at 25°C against

ultrapure water for a week. Finally, the solution was freeze-dried and stored at -80°C until further use. The resulting macromeres, *GelMA* and *ChMA*, have chain ending with $-\text{C}=\text{C}-$ bonds, which are easily photo-crosslinked among themselves by free radical polymerization, forming crosslinked network after.

3.2.2.3 Preparation of hydrogel using modified polysaccharide

10% (w/v) vacuum dried GelMA (7%, 16% and 21%) and 10% (w/v) vacuum dried ChMA (40%) macromer were mixed separately into DPBS containing 2% (w/v) 1-hydroxycyclohexyl phenyl ketone (Irgacure 184) as a photo-initiator until fully dissolved. Then, the solution was placed in small aluminum dishes and photo-polymerized at room temperature for 5-10 mins under UV-radiation (365 nm). The resulting crosslinked hydrogels were stored in distilled water for further testing. Figure 3.2 shows the reaction scheme occurring with end double bonds in modified polysaccharides to obtain crosslinked hydrogels.

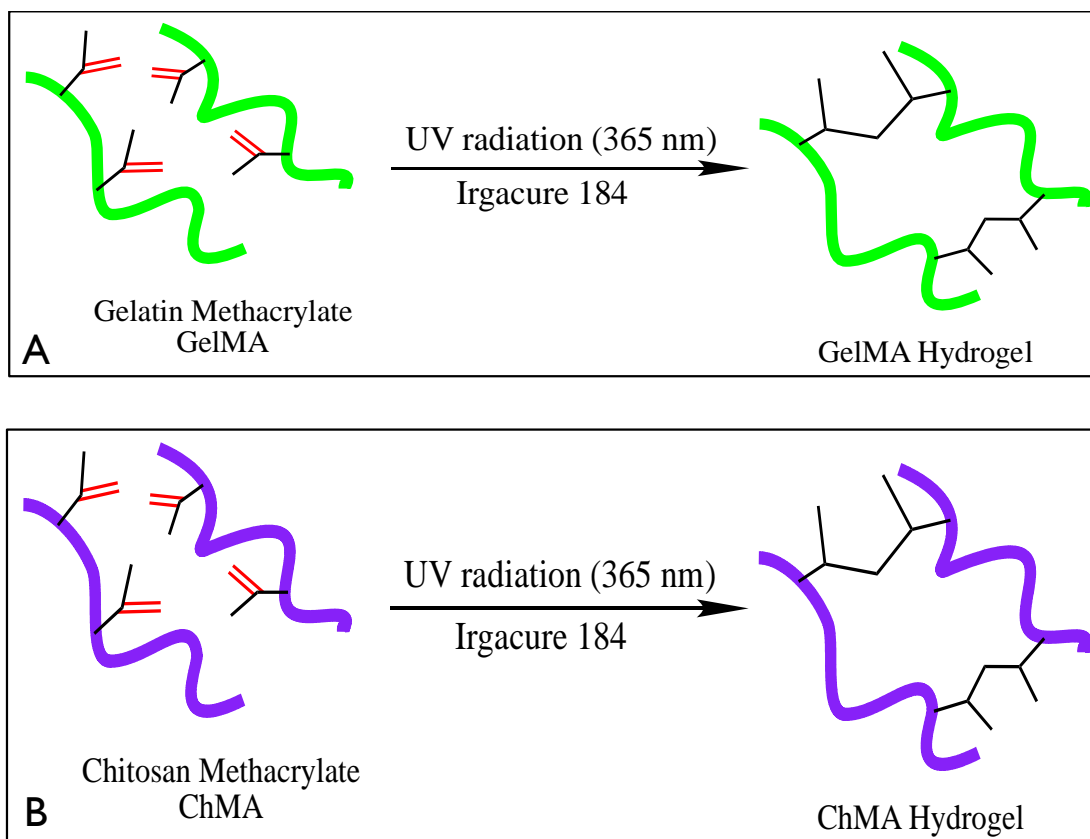


Figure 3.2: Photo-crosslinking of a) GelMA to obtain the GelMA hydrogel, and b) ChMA to ChMA hydrogel via free radical polymerization

3.2.2.4 Characterization of polysaccharide hydrogels samples

Infrared spectra of the starting materials- gelatin, chitosan and the products- GelMA, ChMA were obtained by attenuated total reflection (ATR) method using a Thermo Nicolet 6700 Fourier transform infrared spectrometer. The spectrums were analyzed using OMNIC 7.3 software to study the functionality of chemical structures. All spectra were recorded between 400 and 4000 cm^{-1} over 256 scans with a resolution of 4 cm^{-1} .

$^1\text{H-NMR}$ spectra were obtained using a 600 MHz spectrometer, at room temperature. 1-1.5 mL of deuterated water (D_2O) (with phenylamine as reference) was used as the solvent for 10-15 mg of dry GelMA, gelatin, and ChMA samples preparation. For chitosan, deuterated acetic acid (CD_3COOD) was used as the solvent. Each spectrum was phase-corrected, baseline subtracted and integrated by Mest Re Nova software. The degree of methacrylation (DM)² was measured using the NMR spectrum using the following equation:

$$[\text{DM}]_{\text{GelMA}} (\%) = \left[\frac{a}{b}\right]*100 \quad \text{Equation 1}$$

$$[\text{DM}]_{\text{ChMA}} (\%) = \left[\frac{c}{d}\right]*100 \quad \text{Equation 2}$$

Where ‘a’ is the integral of amine signal in GelMA, ‘b’ is the integral of phenylalanine signal in gelatin, ‘c’ is the integral of amine signal in ChMA and ‘d’ is the integral of methylene signal in chitosan.

The morphological structure of the hydrogels was investigated by scanning electron microscopy (SEM, Zeiss EVO 50 VP-SEM, Carl Zeiss Microscopy, LLC, White Plains, NY) to obtain the topological characteristics of the hydrogels. After photo-crosslinking, swollen hydrogels were lyophilized in a freeze dryer. The fractured surfaces of pre-chilled hydrogels in liquid nitrogen were studied by SEM. The samples were mounted on aluminium support stubs with double stick tape or fingernail polish. Then the stubs were sputtered with gold (EMS Q150R sputter coating device) prior to SEM observations. The average pore size of the samples was quantified using ImageJ software.

The swelling analysis was performed in hydrogel samples lyophilized in a freeze dryer and weighed to obtain dry sample weight (W_d). Then, samples were immersed in distilled water at

room temperature for 48 hours to reswell. The swollen hydrogels were removed from the water, and after wiping the excess water on the surface were weighed to obtain the weight of the wet sample (W_w). Swelling ratios were calculated using the following equation:

$$\text{Mass Swelling (\%)} = \left(\frac{W_w - W_d}{W_d} \right) * 100 \quad \text{Equation 3}$$

The mechanical properties of the hydrogels were tested with the help of a dynamic mechanical analyzer (DMA) TA Instrument RSAIII, US. Compression testing analysis was carried out according to the ASTM D695-15²⁹ on the specimens with 5 mm diameter and extension rate -0.067 mm/s at room temperature using the cylindrical compression geometry, performed for 3-6 replicates. From this data, the compression modulus was determined. Rheological measurements were obtained using a TA Instruments Rheology Advantage AR, US, using parallel plate geometry fitted with 25 mm aluminum plate at room temperature. Cylindrical samples (15 μ m diameter and 1000 μ m thickness) were cut and placed for strain sweep and frequency sweep experiments. From the strain sweep experiment performed at 1 Hz, 0.5% strain was selected (in the linear elastic range), which was then used as the constant strain in the oscillatory frequency sweep experiments. Comparative shear storage modulus (G') and shear loss modulus (G'') values for each were measured for polysaccharide hydrogels individually, and the average shear modulus was reported at 1 Hz.

The in-vitro biodegradation analysis of GelMA and ChMA hydrogels was performed in distilled water containing 600-900 mg/L of lysozyme^{30,31} at 37°C. In these experiments, a lysozyme solution served as the medium for biodegradation studies, which is similar to the physiological conditions found in the human body, which undergo normal metabolism of degradation.

Enzymatic degradation was monitored for four (4) weeks, while the enzyme solution was refreshed once. At predetermined times, 1, 2, 3, and 4 weeks, samples were removed from the medium and dried completely. The weight of samples, before (m_1) and after (m_2) in-vitro degradation, were calculated, and the degree of degradation (%) was determined using Equation 4:

$$\text{Degree of Degradation (\%)} = \left(\frac{m_1 - m_2}{m_1} \right) * 100 \quad \text{Equation 4}$$

3.2.2.5 Fibroblast cell attachment and proliferation on the hydrogel scaffolds

Fibroblast cells were cultured in DMEM media with 10% FBS and 1% Penicillin-Streptomycin antibiotic solution at 37°C in a 5% CO₂ incubator. The scaffolds were sterilized under UV for 30 minutes, followed by placement in a sterile plate with DMEM-10 media overnight. Following day fibroblast cells were seeded (50,000/well) on scaffolds. The scaffolds plated with cells were maintained in 5% CO₂ incubator at 37°C. The cells were regularly monitored by using an optical microscope and fluorescent microscope after staining with live/dead stain according to manufacturer protocol.

Cell viability of cells grown on scaffolds was measured by MTT (3-(4, 5-dimethyl-thiazol-2-yl)-2,5-diphenyl-tetrazolium bromide) dye reduction. Fibroblast cells were seeded in a 96-well plate at a density of 20,000 cells per well in DMEM containing 10% FBS and grown overnight. At periodic time intervals, 10 µL of MTT (0.5 mg/ml) in sterile-filtered PBS was added to each well and incubated for 3 h to allow the formation of formazan crystals at 37 °C. DMSO (200 µL) was added to each well after incubation to dissolve the MTT formazan crystals and incubated for another 60 min at 37°C The absorbance of formazan products was measured at 570 nm using a

microplate reader (Synergy LX, BioTek). The percentage of live cell death was obtained by the difference between the absorbance of control cells and cells grown on scaffolds.

The seeding efficiency of fibroblast cells on hydrogels was investigated by plating 20,000 cells on the surface of each scaffold in a 48 well cell culture plate in 100 μ l of media and incubated in 5% CO₂ incubator at 37 °C. After 30 min an additional 200 μ l of media was added and incubated. MTT assay was performed after 2 hours of incubation to calculate the number of seeded cells. A 96-well without scaffold was plated with cells and was used as a control. Seeding efficiency was calculated using the following equation where C is the absorbance of control cells and T is the absorbance of cells on the scaffold.

$$\text{Seeding efficiency (\%)} = \left(\frac{C-T}{C} \right) * 100 \quad \text{Equation 5}$$

3.3 Results and Discussion

3.3.1 Characterization of hydrogels

The degree of methacrylation for different varieties of polysaccharides was determined by proton nuclear magnetic resonance (¹H-NMR). Figure 3.3 gives the comparative NMR plots of gelatin, chitosan, and their respective modifications.

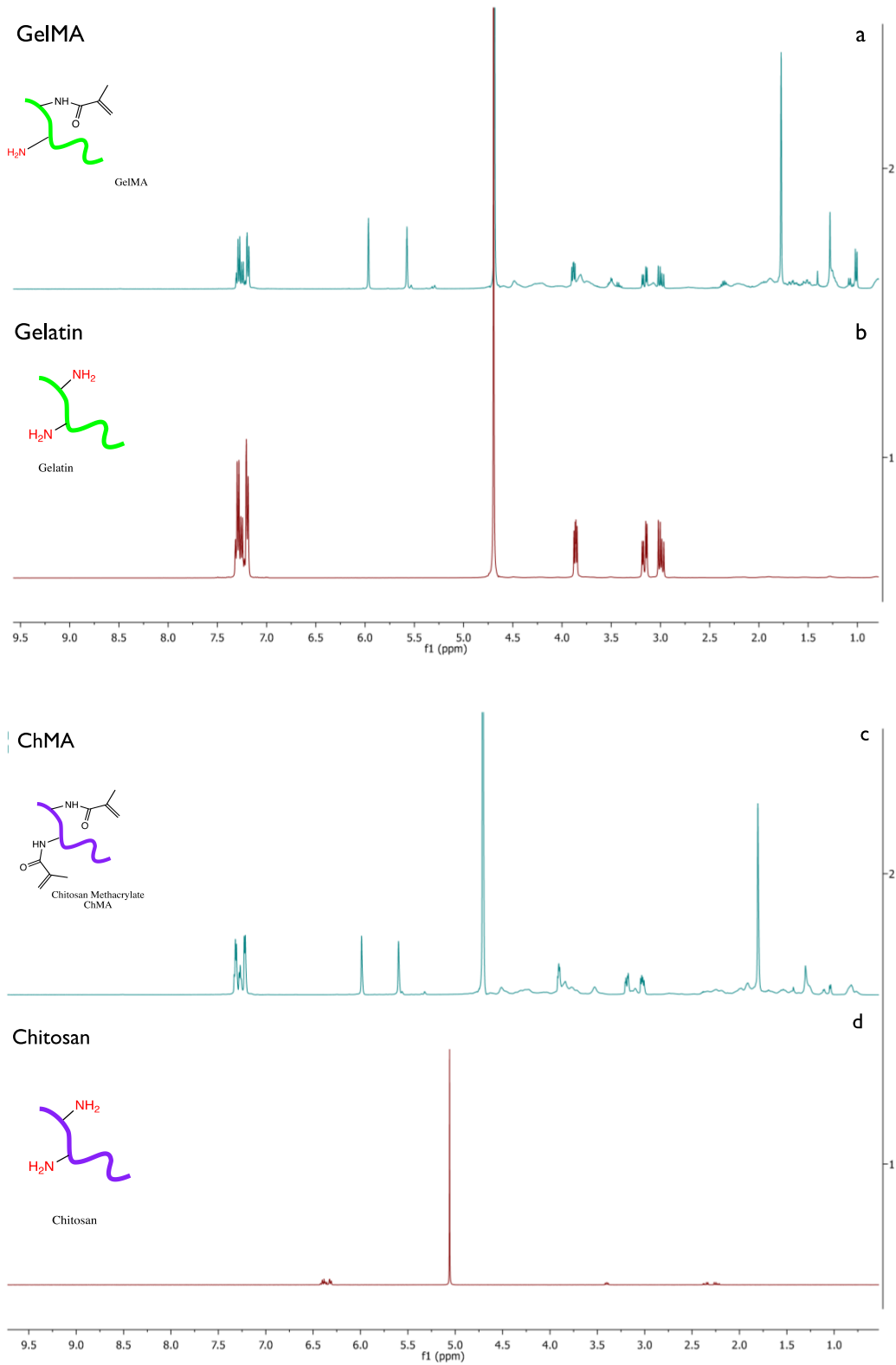


Figure 3.3: $^1\text{H-NMR}$ spectra of a) GelMA, b) Gelatin, c) ChMA and d) Chitosan

For GelMA, we observed the presence of peaks at 5.3 and 5.6 ppm (Figure 3.3.a), which represent the methacrylate groups obtained after the successful conversion of amine groups in gelatin to methacrylate groups (GelMA). On the other side, for ChMA, peaks 5.5-6.1 ppm (Figure 3.3.b) represents the binding of methacrylate groups to amine groups of chitosan. The degree of methacrylation of GelMA was calculated by Equations 1, by the ratio of the integrated area of amine groups of GelMA and gelatin. Similarly, for ChMA the degree of methacrylation was determined using Equation 2. The degree of methacrylation calculated is listed in Table 3.1 for the polysaccharide hydrogels. The degree of functionalization is similar to values reported in the literature³² for GelMA as 23% and ChMA as 33%.

Table 3.1: Characterization of different varieties of modified polysaccharide hydrogels

	Degree of Acrylation (%)	Pore Size (µm)	Swelling Ratio (%)	Compressive Modulus (kPa)	Shear Modulus (kPa)	Degradative weight loss (%)
GelMA (7%)	7	69.8	813 ± 24	10.4 ± 6.8	1.5 ± 0.2	22.3 ± 0.1
GelMA (16%)	16	37.3	617 ± 85	16.6 ± 6.9	2.1 ± 0.3	18.1 ± 3.2
GelMA (21%)	21	27.4	475 ± 122	30.4 ± 7.2	4.0 ± 0.6	15.9 ± 3.8
ChMA (40%)	40	68.1	2208 ± 240	33.0 ± 9.2	5.6 ± 0.9	35.2 ± 5.5

FTIR analysis of the freeze-dried GelMA and ChMA (macromer) was performed to characterize and confirm the methacrylation reaction. The FTIR spectrums comparing the characteristic bands of gelatin and chitosan powders to the modified polysaccharides, GelMA and ChMA, are displayed in Figure 3.4. For the GelMA spectrum (Figure 3.4.a), the absorption bands are similar to gelatin,

mainly, the peaks at 1529 and 1250 cm^{-1} correspond to N-H stretch of amide (II) and N-H stretch of amide (III). The broader peak at 3321 cm^{-1} also corresponds to N-H stretch of amide (II). The peaks at 2938 and 1633 cm^{-1} represent C-H stretch and C=O stretching vibrations in GelMA spectrum². The FTIR band of GelMA at 3321 cm^{-1} shows a decrease in the intensity of N-H, which indicates the methacrylation at the amine functionality. The FTIR spectrum of ChMA (Figure 3.4.b) depicts the peaks at ~ 3300 , 2930 and 1666 cm^{-1} that visualizes the O-H, C-H and C=O stretches of amide group, respectively. The 1055 cm^{-1} peak belongs to C-O stretch and the 1543 cm^{-1} represented N-H of amide (II) stretching mode. The FTIR spectrum of ChMA shows a decrease in intensities of N-H, C=O and O-H, which indicates the successful methacrylation of chitosan.

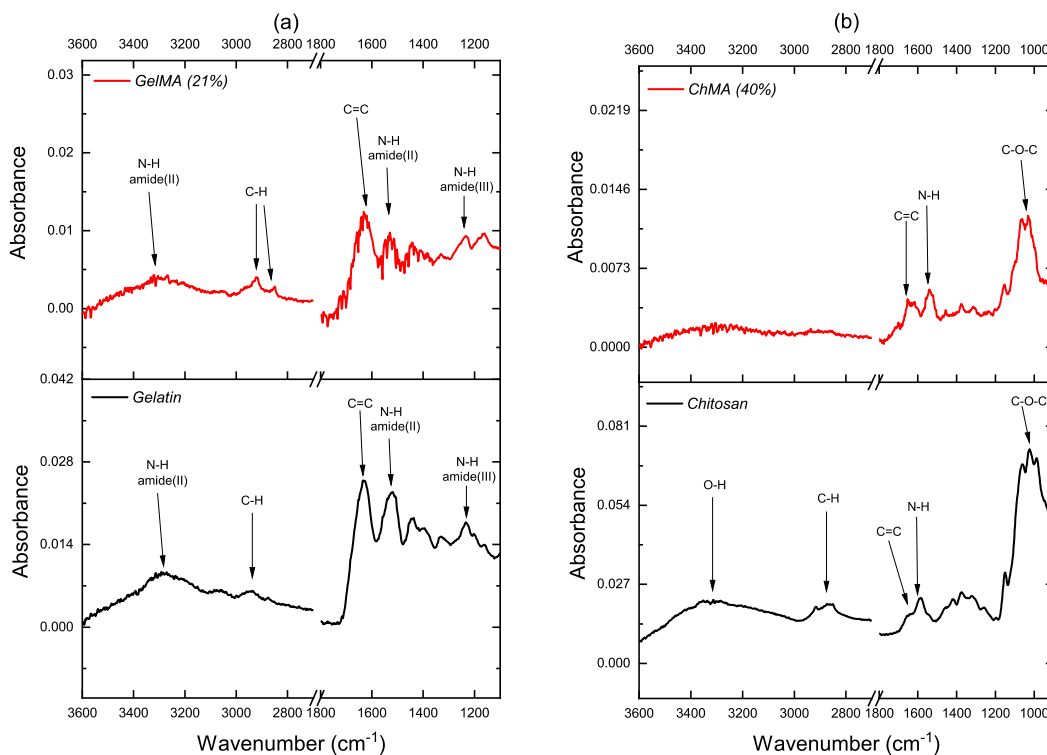


Figure 3.4: FT-IR spectrum for a) gelatin and GelMA and b) chitosan and ChMA

Figure 3.5 a, b, c and d shows the SEM micrograph of the freeze-dried GelMA and ChMA hydrogels. These pictures reveal a well-defined, 3D porous network structure of the hydrogel with an average pore size listed in Table-3.1. As the degree of methacrylation of GelMA increases from 7% (Figure 3.5-a) to 21% (Figure 3.5-c), the pore size decreases. As the molar excess of methacrylic anhydride is increased in the reaction, the degree of methacrylation increases. As a result, the crosslinking density of a hydrogel increases. This crosslinked network of hydrogel leads to a tighter network structure and therefore reduces pore size. The increase in the number of crosslinking points in GelMA (21%) during photo-crosslinking makes it a hydrogel with the smallest pore size. This trend is evident through the morphology of the different varieties of GelMA hydrogels.

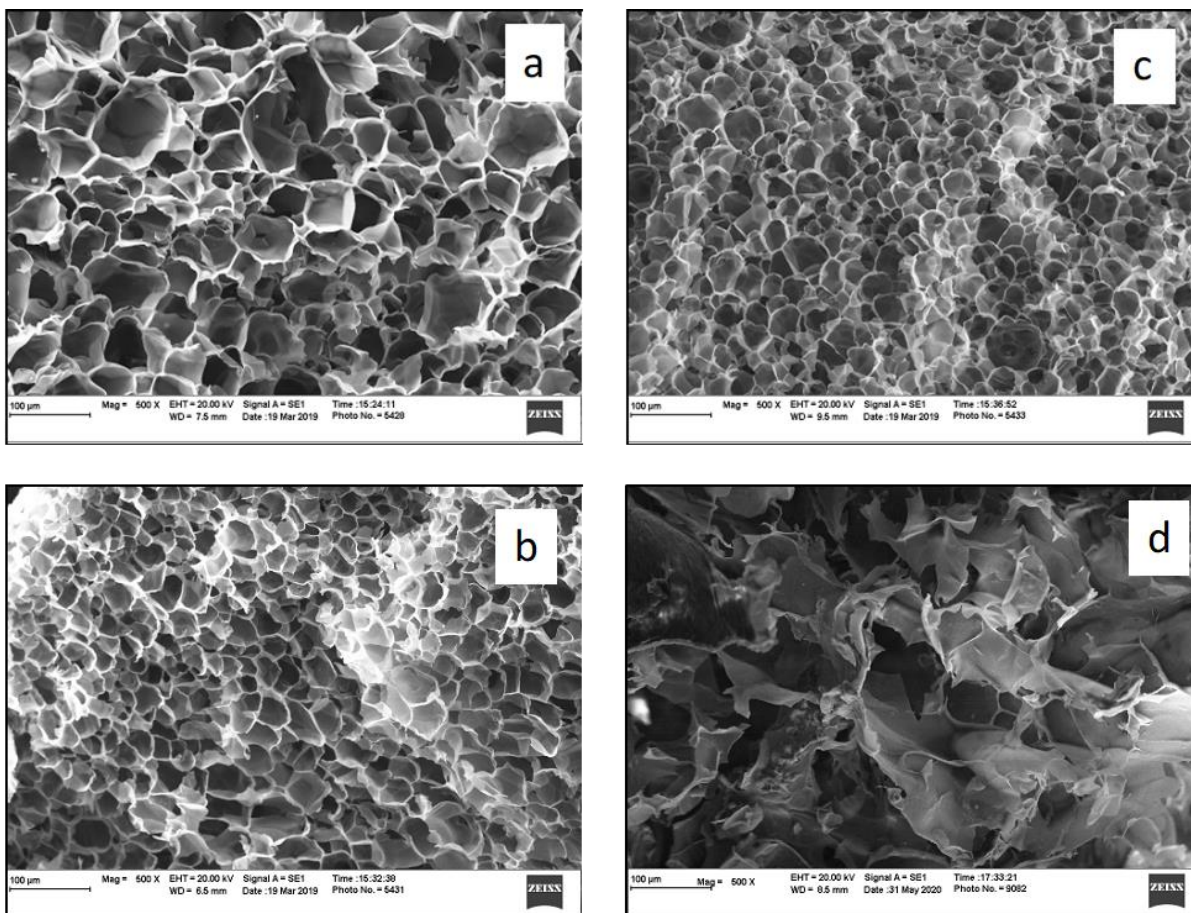


Figure 3.5: SEM image of a) GelMA (7%), b) GelMA (16%), c) GelMA (21%) and d) ChMA (40%) hydrogel

The porous structure is crucial for the cell dwelling, proliferation, and cell culture on polymer-based hydrogel; on the other side, this open architecture affects the swelling and mechanical properties of the hydrogel, as can be observed in the following section.

The water uptakes (%) of the synthesized polysaccharide hydrogels (GelMA and ChMA) were calculated using equation 3. The obtained water uptake percentages are reported (Table 3.1) for polysaccharide hydrogels. The observed trend shows that as the degree of methacrylation of GelMA is increased, the water uptake (or swelling ratio) decreases. This property also follows the

pore size trend explained before. As the degree of methacrylation of GelMA increases and indicates the increase in crosslinking, the number of pores (Figure 3.5) among the crosslinking points becomes small, which gives less room for absorption. Among the polysaccharide hydrogels, ChMA has the largest pore size. Therefore, the ChMA hydrogel has the highest ability to swell in water.

The mechanical behavior of the hydrogels is reported in Table 3.1. It can be observed that the compressive and shear modulus shows an increase, as the degree of methacrylation is increased. The crosslinking density is the main factor that is affecting the modulus of the hydrogel. As the molar excess of methacrylic anhydride is increased in the reaction, the degree of methacrylation increases. As a result, the crosslinking density of a hydrogel increases. This crosslinked network of hydrogel leads to a tighter network structure and enhances the mechanical performance by an increment in modulus.

Figure 3.6 shows the degradation behavior of synthesized GelMA and ChMA hydrogels with degradative weight loss for a specific variety for 4 weeks. As the exposure to the lysozyme enzyme solution increased, the degree of degradation was also increased. It can be observed in Figure 3.6, the hydrogel with the higher crosslinking density (GelMA-21%) degrades at a slower rate as compared to GelMA-7% due to a higher degree of methacrylation. Moreover, having the larger pore size, GelMA (7%) and ChMA (40%) allows a higher amount of the lysozyme solution to penetrate and degrade the hydrogel.

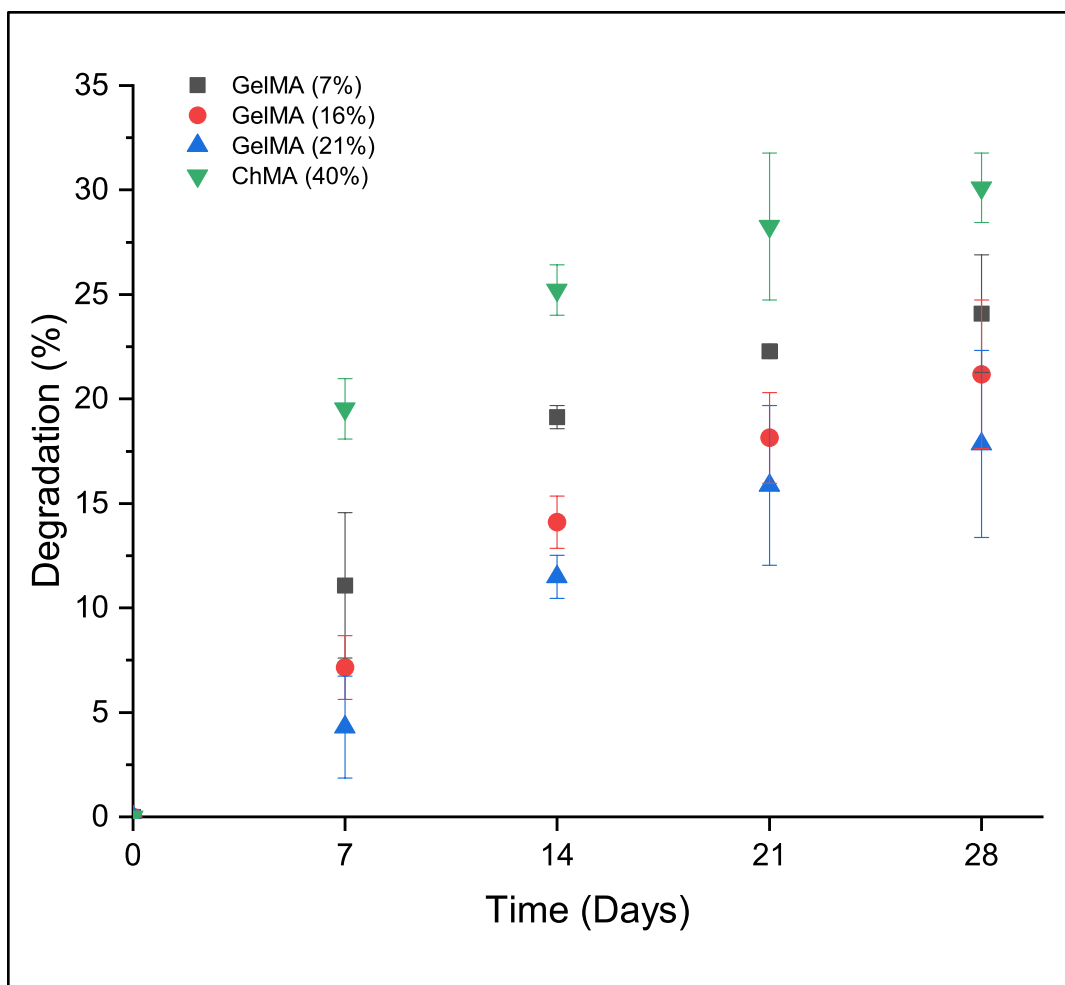


Figure 3.6: Degradation rate profile for different varieties of PEGDA with lysozyme

Figure 3.7 shows the morphology of hydrogel after 14 days of degradation. From the scanning electron microscopy (SEM), it is possible to observe the effect of the degradation process, as the porous structure collapses and fibrillar structures are formed. The clusters of fibrils are more prominent in ChMA, which indicates the evidence of the highest degradation.

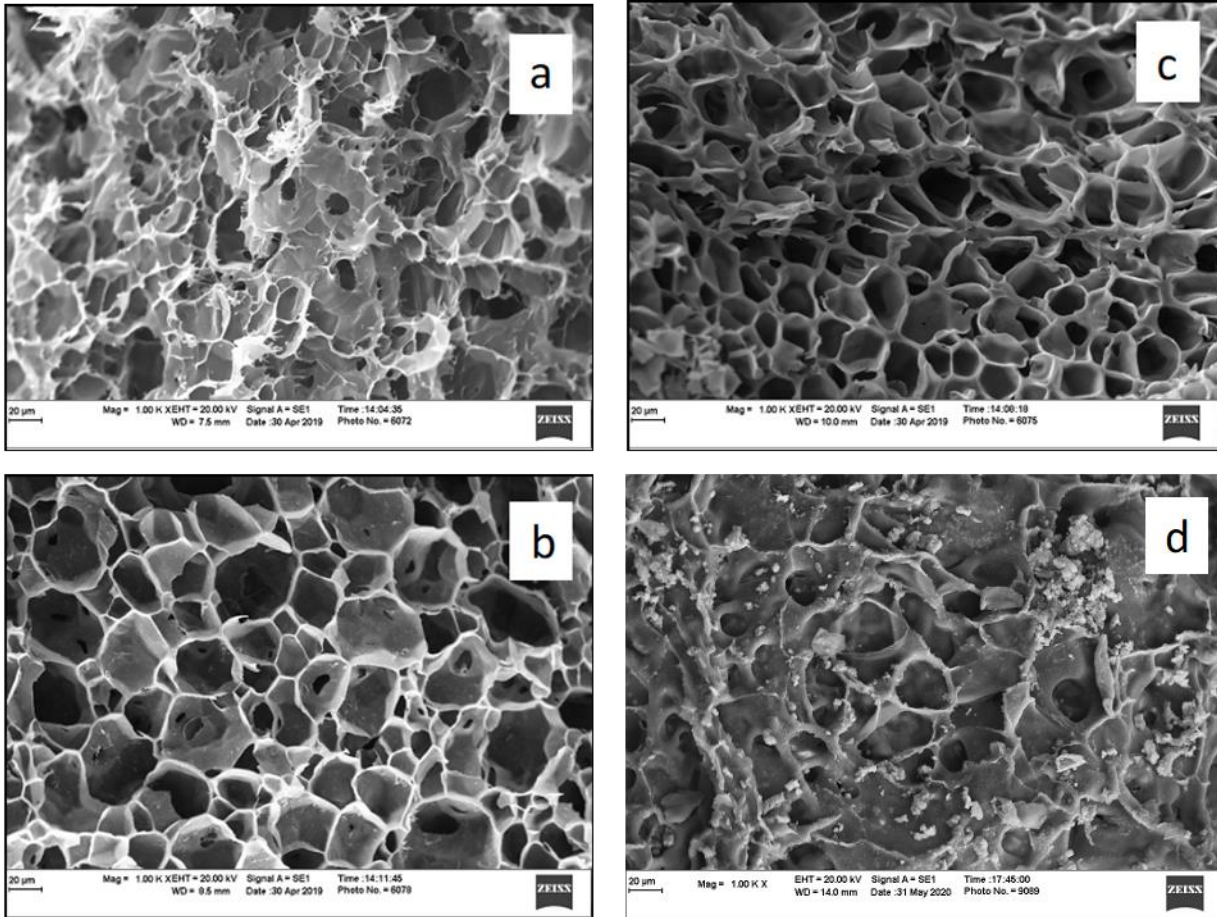


Figure 3.7: *Effect of enzymatic degradation on the morphology after 2 weeks of enzyme exposure on hydrogels a) GelMA (7%), b) GelMA (16%), c) GelMA (21%), d) ChMA (40%)*

3.3.2 Cell growth and proliferation on the hydrogel scaffolds

Our cell studies indicated fibroblast cell attachment and growth on the designed hydrogels for up to 7 days. Since the scaffolds are in the 3D architecture, the cells grown into the porous structures so that it becomes hard to count the actual number in the scaffolds. However, the cells in the scaffolds were confirmed by staining with Live/dead stain.

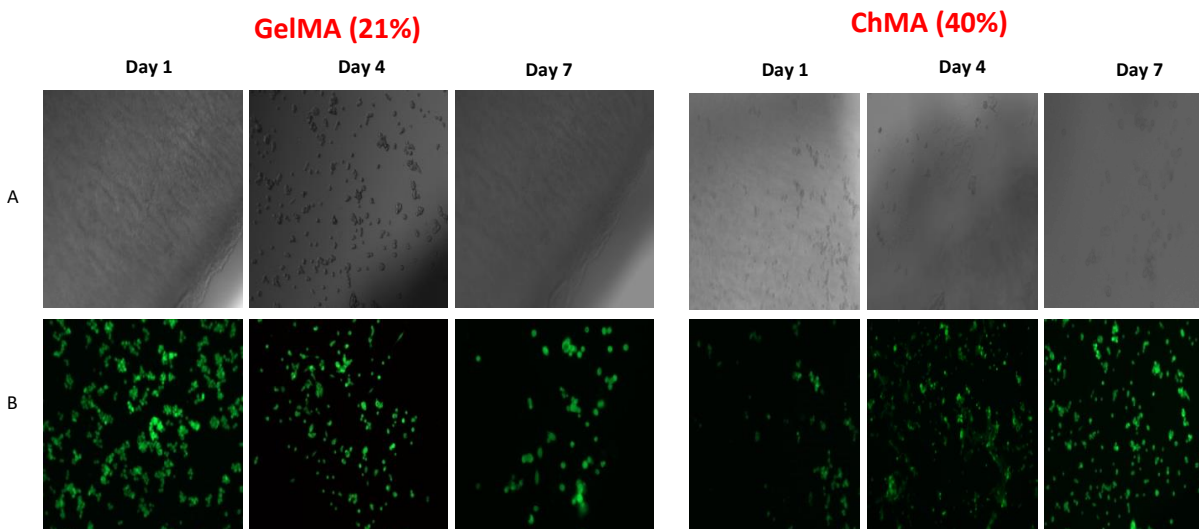


Figure 3.8: *Fibroblast Cell growth on GelMA (21%) and ChMA (40%). A) Bright-field images of the cells B) Live/Dead Stain images of the cells*

Seeding efficiencies for our designed scaffold GelMA (7%), GelMA (16%), GelMA (21%) and ChMA (40%) were 98.7%, 84.9%, 100% and 89.1%. Cell viability was estimated using MTT assay. Cell grown on scaffolds were viable for up to 7 days (Figure 3.9). We observed 6% increase in seven days in ChMA (40%) scaffold compared to 3% in GelMA (7%).

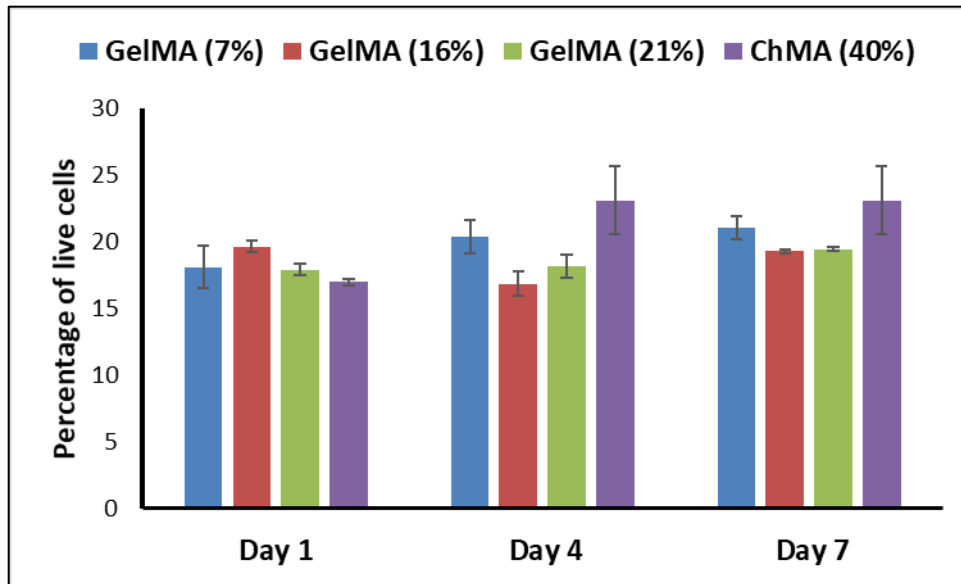


Figure 3.9: Cell viability of Fibroblast cells by MTT assay

3.4 Conclusion

GelMA and ChMA modified polysaccharide hydrogels were synthesized using gelatin and chitosan to get UV-polymerizable functionality. The polysaccharide solution was then photocured in the presence of Irgacure 184 to obtain hydrogels via free radical polymerization. The synthesized hydrogels showed biocompatibility for cell growth along with mechanical strength in their applications for tissue engineering. The obtained results show the evidence for increasing trend for mechanical performance as the degree of functionality increases. There is a range of properties corresponding to different polysaccharides synthesized, which gives more flexibility of its application in tissue regeneration.

3.5 References

- (1) Nichol, J. W.; Koshy, S.; Bae, H.; Hwang, C. M.; Khademhosseini, A. NIH Public Access. **2011**, *31* (21), 5536–5544.
<https://doi.org/10.1016/j.biomaterials.2010.03.064>. Cell-laden.
- (2) Saraiva Sofia M, Miguel Sonia P, Ribeiro Maximiano P, Coutinho Paula, C. I. J. Synthesis and Characterization of a Photocrosslinkable Chitosan-Gelatin Hydrogel Aimed for Tissue Regeneration. *RSC Adv.* **2015**, *5*, 63478–63488.
- (3) US department of health and human services <https://www.organdonor.gov/statistics-stories/statistics.html>.
- (4) Kim, S.; Kang, Y.; Mercado-Pagán, Á. E.; Maloney, W. J.; Yang, Y. In Vitro Evaluation of Photo-Crosslinkable Chitosan-Lactide Hydrogels for Bone Tissue Engineering. *J. Biomed. Mater. Res. - Part B Appl. Biomater.* **2014**, *102* (7), 1393–1406.
<https://doi.org/10.1002/jbm.b.33118>.
- (5) Du, Y.; Lo, E.; Ali, S.; Khademhosseini, A. Directed Assembly of Cell-Laden Microgels for Fabrication of 3D Tissue Constructs. *Proc Natl Acad Sci US A* **2008**, *105* (28), 9522–9527.
- (6) Tsang, V. L.; Chen, A. A.; Cho, L. M.; Jadin, K. D.; Sah, R. L.; DeLong, S.; West, J. L.; Bhatia, S. N. Fabrication of 3D Hepatic Tissues by Additive Photopatterning of Cellular Hydrogels. *FASEB J* **2007**, *21* (3), 790–801.
- (7) Croisier, F.; Jérôme, C. Chitosan-Based Biomaterials for Tissue Engineering. *Eur. Polym. J.* **2013**, *49* (4), 780–792. <https://doi.org/10.1016/j.eurpolymj.2012.12.009>.
- (8) Dragan, E. S. Design and Applications of Interpenetrating Polymer Network Hydrogels. A Review. *Chem. Eng. J.* **2014**, *243*, 572–590. <https://doi.org/10.1016/j.cej.2014.01.065>.

- (9) Giri, T. K.; Thakur, A.; Alexander, A.; Ajazuddin; Badwaik, H.; Tripathi, D. K. Modified Chitosan Hydrogels as Drug Delivery and Tissue Engineering Systems: Present Status and Applications. *Acta Pharm. Sin. B* **2012**, *2* (5), 439–449.
<https://doi.org/10.1016/j.apsb.2012.07.004>.
- (10) Peptu, A.; Savin, C. L.; Popa, M. *Chemically Modified Polysaccharides with Applications in Nanomedicine*; 2018. <https://doi.org/10.1016/B978-0-444-63774-1.00010-7>.
- (11) Lei, K.; Li, Z.; Zhu, D.; Sun, C.; Sun, Y.; Yang, C.; Zheng, Z.; Wang, X. Polysaccharide-Based Recoverable Double-Network Hydrogel with High Strength and Self-Healing Properties. **2020**, 794–802. <https://doi.org/10.1039/c9tb01679a>.
- (12) Vieira, E. F. S.; Cestari, A. R.; Airoidi, C.; Loh, W. Polysaccharide-Based Hydrogels: Preparation, Characterization, and Drug Interaction Behaviour. *Biomacromolecules* **2008**, *9* (4), 1195–1199. <https://doi.org/10.1021/bm7011983>.
- (13) Wang, Y.; Ma, M.; Wang, J.; Zhang, W.; Lu, W.; Gao, Y.; Zhang, B.; Guo, Y. Development of a Photo-Crosslinking , Biodegradable GelMA/PEGDA Hydrogel for Guided Bone Regeneration Materials. *Materials (Basel)*. **2018**, *11* (1345), 1–12.
<https://doi.org/10.3390/ma11081345>.
- (14) Kerscher, P. Human developing cardiac tissues for scale-up and disease. **2016**.
- (15) Rusanu, A.; Tamaş, A. I.; Vulpe, R.; Rusu, A.; Butnaru, M.; Vereştiuc, L. Biocompatible and Biodegradable Hydrogels Based on Chitosan and Gelatin with Potential Applications as Wound Dressings. *J. Nanosci. Nanotechnol.* **2017**, *17* (7).
<https://doi.org/10.1166/jnn.2017.14298>.
- (16) *Polysaccharide Hydrogels*; Matricardi, P., Alhaique, F., Coviello, T., Eds.; Taylor & Francis: Boca Raton, FL, 2016.

- (17) Russo, L.; Cipolla, L.; et al. VA-086 Methacrylate Gelatine Photopolymerizable Hydrogels : A Parametric Study for Highly ... A Parametric Study for Highly Biocompatible 3D Cell Embedding. **2014**, No. October.
<https://doi.org/10.1002/jbm.a.35346>.
- (18) Gopinathan, J.; Noh, I. Recent Trends in Bioinks for 3D Printing. **2018**, 1–15.
- (19) Gudapati, H.; Dey, M.; Ozbolat, I. A Comprehensive Review on Droplet-Based Bioprinting: Past, Present and Future. *Biomaterials* **2016**, *102*, 20–42.
- (20) Schuurman, W.; Levett, P. A.; Pot, M. W.; van Weeren, P. R.; Dhert, W. J. A.; Hutmacher, D. W.; Melchels, F. P. W.; Klein, T. J.; Malda, J. Gelatin-Methacrylamide Hydrogels as Potential Biomaterials for Fabrication of Tissue-Engineered Cartilage Constructs. *Macromol. Biosci.* **2013**, *13* (5), 551–561.
<https://doi.org/10.1002/mabi.201200471>.
- (21) Bressan, E.; Favero, V.; Gardin, C.; Ferroni, L.; Iacobellis, L.; Favero, L.; Vindigni, V.; Berengo, M.; Sivolella, S.; Zavan, B. Biopolymers for Hard and Soft Engineered Tissues: Application in Odontoiatric and Plastic Surgery Field. **2011**, 509–526.
<https://doi.org/10.3390/polym3010509>.
- (22) Miguel, S. P.; Ribeiro, M. P.; Brancal, H.; Coutinho, P.; Correia, I. J. Thermoresponsive Chitosan-Agarose Hydrogel for Skin Regeneration. *Carbohydr. Polym.* **2014**, *111*, 366–373. <https://doi.org/10.1016/j.carbpol.2014.04.093>.
- (23) Koch, L.; Kuhn, S.; Sorg, H.; Gruene, M.; Schlie, S.; Gaebel, R.; Polchow, B.; Reimers, K.; Stoelting, S.; Ma, N.; et al. Laser Printing of Skin Cells and Human Stem Cells. *Tissue Eng. Part C Methods* **2009**, *16* (5), 847–854.
- (24) Liu, M.; Zeng, X.; Ma, C.; Yi, H.; Ali, Z.; Mou, X.; Li, S.; Deng, Y.; He, N. Injectable

- Hydrogels for Cartilage and Bone Tissue Engineering. **2017**, No. November 2016.
<https://doi.org/10.1038/boneres.2017.14>.
- (25) Bae, M.; Ohe, J.; Lee, J.; Heo, D.; Byun, W. Photo-Cured Hyaluronic Acid-Based Hydrogels Containing Growth and Differentiation Factor 5 (GDF-5) for Bone Tissue Regeneration. *Bone* **2014**, *59*, 189–198.
- (26) Racine, L.; Costa, G.; Bayma-Pecit, E.; Texier, I.; Auzély-Velty, R. Design of Interpenetrating Chitosan and Poly(Ethylene Glycol) Sponges for Potential Drug Delivery Applications. *Carbohydr. Polym.* **2017**, *170*, 166–175.
<https://doi.org/10.1016/j.carbpol.2017.04.060>.
- (27) Bedel, N. S.; Tezcan, M.; Ceylan, O.; Gurdag, G.; Cicek, H. Effects of Pore Morphology and Size on Antimicrobial Activity of Chitosan/Poly(Ethylene Glycol) Diacrylate Macromer Semi-IPN Hydrogels. *J. Appl. Polym. Sci.* **2015**, *132* (43), 1–10.
<https://doi.org/10.1002/app.42707>.
- (28) Shimojo, A. A. M.; Galdames, S. E. M.; Perez, A. G. M.; Ito, T. H.; Luzo, Â. C. M.; Santana, M. H. A. In Vitro Performance of Injectable Chitosan-Tripolyphosphate Scaffolds Combined with Platelet-Rich Plasma. *Tissue Eng. Regen. Med.* **2016**, *13* (1), 21–30. <https://doi.org/10.1007/s13770-015-9111-9>.
- (29) ASTM D695-15. Standard Test Method for Compressive Properties of Rigid Plastics. *ASTM Int.* **2015**.
- (30) Lončarević, A.; Ivanković, M.; Rogina, A. Lysozyme-Induced Degradation of Chitosan: The Characterisation of Degraded Chitosan Scaffolds. *J. Tissue Repair Regen.* **2017**, *19* (1), 177.
- (31) *Handbook of Polymers for Pharmaceutical Technologies, Biodegradable Polymers*;

Thakur Vijay Kumar, T. M. K., Ed.; Scrivener Publishing, 2015.

- (32) Yu, L. M.; Kazazian, K.; Shoichet, M. S. Peptide Surface Modification of Methacrylamide Chitosan for Neural Tissue Engineering Applications. *J. Biomed. Mater. Res. Part A* **2007**, *82*, 243–255. <https://doi.org/10.1002/jbm.a>.

CHAPTER 4

Formulation of the polymeric double networks (DNs) for biomedical applications with physicochemical properties to resemble a biological tissue

4.1 Introduction

Polymeric hydrogels are hydrophilic crosslinked networks that acquire an expanded three-dimensional structure when at the swollen state¹. Although the physio-chemical properties of traditional hydrogels allow it to be valuable materials for biomedical applications like drug delivery²⁻⁴, tissue engineering⁵⁻⁷, molecular imprinting³, scaffolds⁸⁻¹⁰, yet they lack biocompatibility. The rapid evolution of tissue engineering is accelerating the research for biodegradable and biocompatible materials to make them appropriate for adhesion and proliferation of different types of cells^{5,11}. Among the synthetic and natural polymers which can be used for tissue engineering, polysaccharides applications have been of particular interest.

Most traditional hydrogels are generally having low mechanical strength, and elastic properties, and possesses biocompatibility issues which limits their biomedical application scope¹². In a hydrogel, the mechanical strength is a property which is used to maintain its original shape, and the biodegradability along with biocompatibility can allow its adaptation to tissue movement and reformation¹³. But, these two properties can be contradictory¹⁴ in the same hydrogels. Therefore, interpenetrating double networks are proposed to maintain synergy between mechanical properties and biocompatibility and obtain the desired performance.

The double network hydrogels are interpenetrating or interlaced polymer networks at the molecular scale with different properties¹⁵. The properties of double network hydrogels prepared from two or more different polymer chains were reported to be much better than single polymer hydrogels^{14,16,17}. Ordinary single network hydrogels, for example, poly(2-acrylamido-2-methylpropanesulfonic acid) (PAMPS) is said to have high hydrophilicity, good porosity, however, it has a compressive stress of only 0.4 MPa, which do not match the articular cartilage-like compressive strength (~36 MPa) as reported in the literature.¹² However, when a double network of poly(acrylamide) (PAAm) and PAMPS is produced, the authors indicate a 43 times higher compressive modulus than the PAMPS gel.

In particular, large numbers of hydrogel materials are from natural polysaccharides, such as gelatin, chitosan, hyaluronic acid, and many others. They have been rigorously researched for numerous biomedical applications due to their good biodegradability, biocompatibility, non-immunogenic performances, and abundant sources. The polysaccharides, gelatin, and chitosan have been widely used in the synthesis of hydrogels for tissue engineering due to its cell responsivity and biocompatibility¹⁸. The molecular chains of polysaccharides are linear so that the hydrogels are stiffer and less elastic, as reported by Li et al. On the contrary, poly(ethylene glycol)-based hydrogels are biocompatible hydrogels with outstanding elasticity, but its stiffness is low¹⁴. The three-dimensional porous structured double network hydrogel can be used to stimulate the combination of properties of both networks to mimic the cell-extracellular matrix. The good point to note is that the cartilage and other skeletal system tissues are high water-content materials and also employ crosslinking with a double-network strategy (e.g., highly crosslinked collagen plus proteoglycan gel) to achieve their mechanical properties along with biocompatibility.

In the current research, we focused on the synthesis of different double network hydrogels using poly(ethylene glycol)dimethacrylate, gelatin methacrylate and chitosan methacrylate macromere as an interpenetrating polymer network. Hence, an UV induced free radical polymerization was utilized to produce the double hydrogel networks. The physicochemical properties of the resulting samples were studied as well as fibroblast cell adhesion and proliferation.

4.2 Materials and Methods

4.2.1 Materials

For this research study, three varieties of linear poly (ethylene glycol) (PEG) were used: PEG (Mw ~ 4000 g/mol) purchased from Bean Town Chemicals (BTC) (US), PEG (Mw ~ 6000 g/mol) and PEG (Mw ~ 8000 g/mol) which were purchased from Acros Organics (US). Gelatin powder (Type A, ~300 bloom) purchased from Electron Microscopy Sciences (US). Chitosan ($\geq 85\%$ deacetylated) was purchased from Alfa Aesar (US). Methacrylic anhydride was purchased from Thermofisher Scientific Inc. (US). Dulbecco's phosphate buffered saline (DPBS) and acetic acid were purchased from VWR (US). Photoinitiator, 1-hydroxycyclohexyl phenyl ketone (Irgacure 184) was purchased from TCI (US), while the UV light source used (UVLS-28 EL Series UV Lamp) was manufactured by Analytik Jena (US). Lysozyme purchased from Thermofisher Scientific Inc. (US) was used for the degradation studies. Fibroblast cells were brought commercially (CCL 110; ATCC, VA). Cells were cultured in DMEM (Gibco, Gaithersburg, MD) supplemented with 10% v/v fetal bovine serum (Gibco, Gaithersburg, MD). MTT (3-(4,5-Dimethylthiazol-2-yl)-2,5-Diphenyltetrazolium Bromide) salt was brought from Invitrogen (NY), and Live and Dead Double Staining Kit was bought (Abbkine, China).

4.2.2 Methods

4.2.2.1 Preparation of hydrogel based on double networks (DN)

The individual polymeric systems (PEGDMA, GelMA and ChMA) were first synthesized separately. Briefly, poly(ethylene glycol) (PEG) was mixed with 10 molar excess of methacrylic anhydride via microwave synthesis to obtain the PEGDMA samples. Gelatin methacrylation was carried out using 5% (w/v) in Dulbecco's phosphate buffered saline (DPBS) and methacrylic anhydride (35.67 molar excess) at 60°C. It was then dialyzed for purification followed by lyophilization at 4 MPa and -50°C to obtain the pure gelatin methacrylate (GelMA) and stored at -80°C until further use. Chitosan methacrylation was carried out using 3% (w/v) in 1-2% (w/v) acetic acid aqueous solution and methacrylic anhydride (35.67 molar excess) at 25°C and was freeze-dried at 4 MPa and -50°C to obtain the pure chitosan methacrylate (ChMA) and stored at -80°C until further use.

The double network-based hydrogels were synthesized in two ways- (1) by dissolving 10% (w/v) of GelMA and 10% (w/v) of PEGDMA in DPBS buffer and (2) by dissolving 10% (w/v) ChMA and 10% (w/v) of PEGDMA in distilled water. Likewise, different varieties of PEGDMA-GelMA DN hydrogels were synthesized using three different PEGDMA samples with different molecular weight, 4000, 6000 and 8000 Da as shown in Table 4.1. Irgacure 184 (2% w/v) was used as a photo-initiator for free-radical photopolymerization reaction (Figure 4.1).

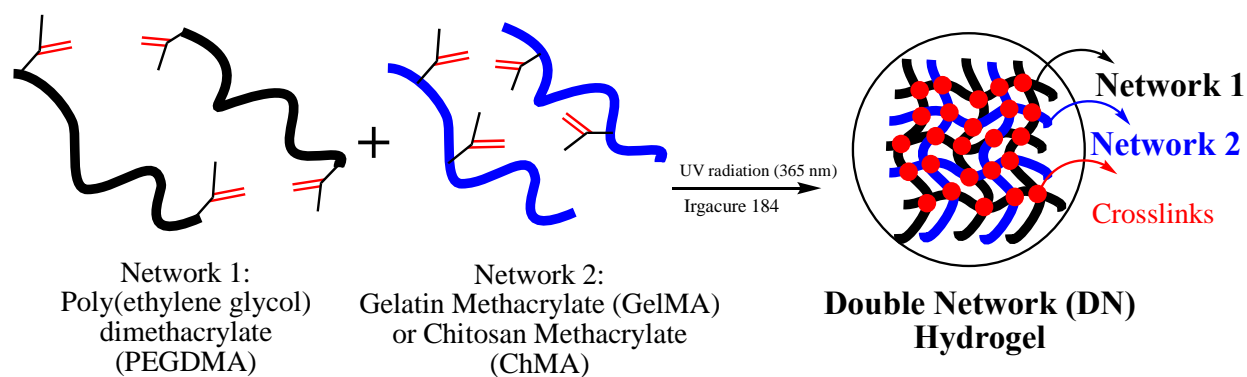


Figure 4.1: Photopolymerization reaction to obtain DN hydrogels

Table 4.1: Nomenclature of Double Network hydrogels

Double Network Hydrogels	PEGDMA 4000	PEGDMA 6000	PEGDMA 8000
GelMA (7%)	P4G7%	P6G7%	P8G7%
GelMA (16%)	P4G16%	P6G16%	P8G16%
GelMA (21%)	P4G21%	P6G21%	P8G21%
ChMA (40%)	NA	NA	P8C40%

4.2.2.2 Characterization of double networks

Infrared spectra of the starting materials- PEGDMA powder, GelMA and ChMA, and final products- PEGDMA-GelMA DN and PEGDMA-ChMA DN hydrogel were measured by attenuated total reflection (ATR) method using a Thermo Nicolet 6700 Fourier transform infrared spectrometer. The spectrums were analyzed using OMNIC 7.3 software. All spectra were recorded between 400 and 4000 cm^{-1} over 256 scans with a resolution of 4 cm^{-1} .

The morphological structure of the hydrogels was investigated by scanning electron microscopy (SEM, Zeiss EVO 50 VP-SEM, Carl Zeiss Microscopy, LLC, White Plains, NY) to obtain the topological characteristics of the hydrogels. After photo-crosslinking, swollen hydrogels were lyophilized in a freeze dryer. The fractured surfaces of pre-chilled hydrogels in liquid nitrogen were studied by SEM. The samples were mounted on aluminium support stubs with double stick tape or fingernail polish. Then the stubs were sputtered with gold (EMS Q150R sputter coating device) prior to SEM observations. The average pore size of the samples was quantified using ImageJ software.

Hydrogel samples were lyophilized in a freeze dryer and weighed to obtain dry sample weight (W_d). Then, samples were immersed in distilled water to swell at room temperature for about 48 hours. The swollen hydrogels were removed from the water after wiping excess water on the surface and weighed to obtain a wet sample (W_w). Swelling ratios were calculated using the following equation:

$$\text{Mass Swelling (\%)} = \left(\frac{W_w - W_d}{W_d} \right) * 100 \quad \text{Equation 1}$$

Modulated differential scanning calorimetry (DSC) (modulate $\pm 0.531^\circ\text{C}$ every 60 seconds using a heating rate $5^\circ\text{C}/\text{min}$) was carried out to observe the change in crystallization temperature (T_c), melting temperature (T_m) and enthalpy of melting (ΔH_m) of the polymer networks. Polymer crystallinity can be determined with DSC by quantifying the heat associated with melting (fusion) of the polymer. This heat is reported as percent crystallinity ($\% X_c$)¹⁹ by normalizing the observed heat of fusion (ΔH_m) to a 100% crystalline sample of the same polymer ($\Delta H_m^0 = 196.8 \text{ J/g}$)²⁰.

Table 4.3 gives the quantification of crystallinity (from equation 2, where $W_{\text{crystalline}}$ is the weight of crystalline part in the double network hydrogel) in the PEGDMA based on reversible heat flow.

$$X_c (\%) = [\Delta H_m / (\Delta H_m^0 * W_{\text{crystalline}})] * 100 \quad \text{Equation 2}$$

The mechanical properties of the hydrogels were tested with the help of a dynamic mechanical analyzer (DMA) TA Instrument RSAIII. Compression testing analysis was carried out according to the ASTM D695-15²¹ on the specimens with 5 mm diameter and extension rate -0.067 mm/s at room temperature using the cylindrical compression geometry, performed for 3-6 replicates. From this data, the compression modulus was determined. Rheological measurements were obtained using a TA Instruments Rheology Advantage AR parallel plate rheometer fitted with 25 mm aluminum plate in the presence of air and at room temperature. Cylindrical samples (15 μm diameter and 1000 μm thickness) were cut and placed for strain sweep and frequency sweep experiments. From the strain sweep experiment performed at 1Hz, 0.5% strain was selected (in the linear elastic range), which was then used as the constant strain in the oscillatory frequency sweep experiments. Tensile tests were performed according to the ASTM standards ASTM D1708-93²². The tensile analysis was carried out on rectangular swollen hydrogels specimens with 15 mm initial length, using an extension rate of 0.1667 mm/s, for 3-6 replicates. During tensile testing, data for any hydrogel that slipped off the clamped area or broke as a result of being next to the metallic surface was not considered. From this data, the tensile modulus was determined.

The biodegradation analysis of double networks was performed in distilled water containing 600-900 mg/L of lysozyme^{23,24} at 37°C. Enzymatic degradation was monitored for four (4) weeks, while the enzyme solution was refreshed once. At a predetermined time (1, 2, 3, and 4 weeks),

samples were removed from the medium and dried thoroughly. The weight of samples before (m_1) and after (m_2) the in-vitro degradation was measured and degree of degradation (%) was determined relative to respective weight loss to the initial weight of the sample as follows:

$$\text{Degree of Degradation (\%)} = \left(\frac{m_1 - m_2}{m_1} \right) * 100 \quad \text{Equation 3}$$

4.2.2.3 Fibroblast cell attachment and proliferation on the hydrogel scaffolds

Fibroblast cells were cultured in DMEM media with 10% FBS and 1% Penicillin-Streptomycin antibiotic solution at 37°C in a 5% CO₂ incubator. The scaffolds were sterilized under UV for 30 minutes, followed by placement in a sterile plate with DMEM-10 media overnight. Following day fibroblast cells were seeded (50,000/well) on scaffolds. The scaffolds plated with cells were maintained in 5% CO₂ incubator at 37°C. The cells were regularly monitored by using an optical microscope.

Cell viability of cells grown on scaffolds was measured by MTT (3-(4, 5-dimethyl-thiazol-2-yl)-2,5-diphenyl-tetrazolium bromide) dye reduction. Fibroblast cells were seeded in a 96-well plate at a density of 20,000 cells per well in DMEM containing 10% FBS and grown overnight. At periodic time intervals, 10 µL of MTT (0.5 mg/ml) in sterile-filtered PBS was added to each well and incubated for 3 h to allow the formation of formazan crystals at 37 °C. DMSO (200 µL) was added to each well after incubation to dissolve the MTT formazan crystals and incubated for another 60 min at 37°C The absorbance of formazan products was measured at 570 nm using a microplate reader (Synergy LX, BioTek). The percentage of live cell death was obtained by the difference between the absorbance of control cells and cells grown on scaffolds.

The seeding efficiency of fibroblast cells on hydrogels was investigated by plating 20,000 cells on the surface of each scaffold in a 48 well cell culture plate in 100 μ l of media and incubated in 5% CO₂ incubator at 37 °C. After 30 min, an additional 200 μ l of media was added and incubated. MTT assay was performed after 2 hours of incubation to calculate the number of seeded cells. A 96-well without scaffold was plated with cells and was used as a control. Seeding efficiency was calculated using the following equation where C is the absorbance of control cells and T is the absorbance of cells on the scaffold.

$$\text{Seeding efficiency (\%)} = \left(\frac{C-T}{C} \right) * 100 \quad \text{Equation 4}$$

4.3 Results and Discussion

4.3.1 Characterization of double networks

FTIR analysis of the PEGDMA-GelMA and PEGDMA-ChMA double networks after the free radical polymerization was performed, and the resulting FTIR spectra comparing the final networks with the original counterparts are displayed in Figure 4.2 (a-f).

In the GelMA spectrum (Figure 4.2a), particularly, the peaks 1529 cm⁻¹ and the broader peak of 3321 cm⁻¹ corresponds to N-H stretch of amide (II)²⁵⁻²⁷. The peaks visualized at 2938 and 1633 cm⁻¹ represent C-H stretch and C=O stretching vibrations in GelMA spectrum²⁶. The peaks corresponding to N-H and C=O are also seen in the spectrum of PEGDMA-GelMA DN, which gives the evidence for the presence of GelMA polymer in the double network hydrogel. Similarly, the FTIR spectrum of ChMA (Figure 4.2b) depicts the peaks at 2930 and 1666 cm⁻¹ that visualizes the C-H and C=O stretches of amide group, respectively^{26,28}. Moreover, the 1055 cm⁻¹ peak

belongs to C-O-C stretch and the 1543 cm^{-1} represented N-H of amide (II) stretching mode²⁶ in ChMA spectrum. The peaks corresponding to N-H, C=O and C-O-C are also seen the spectrum of PEGDMA-ChMA DN, which gives the evidence for the presence of ChMA polymer in the double network hydrogel. Also, PEGDMA marks its presence in both of these double networks as the strong bands at $\sim 2880\text{ cm}^{-1}$ and $\sim 1466\text{ cm}^{-1}$ represents C-H bonds^{29,30} are present in the spectra of PEGDMA as well as DNs. The bands at $\sim 1140\text{ cm}^{-1}$ and $\sim 960\text{ cm}^{-1}$ represent the asymmetrical C-O-C stretching mode³¹ are clearly seen in PEGDMA-GelMA, PEGDMA-ChMA and PEGDMA spectra.

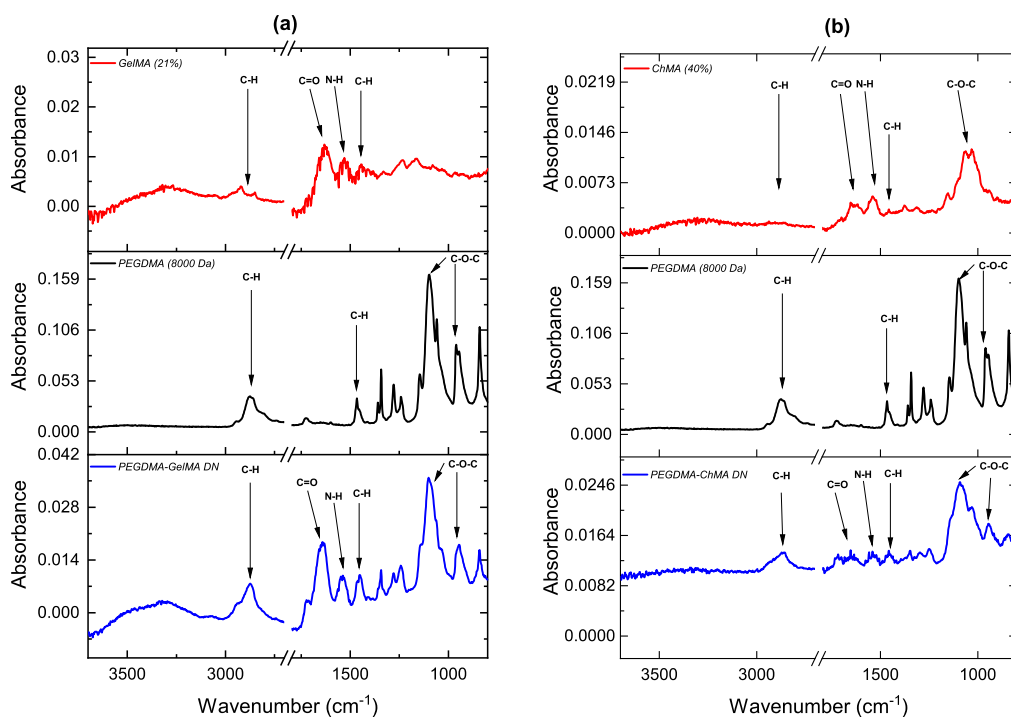


Figure 4.2: FT-IR spectrum for a) GelMA (21%), PEGDMA (8000 Da) and PEGDMA-GelMA DN, b) ChMA (40%), PEGDMA (8000 Da) and PEGDMA-ChMA DN

Figures 4.3 (a-d) show the SEM micrograph of the freeze-dried DN hydrogels. These pictures reveal a well-defined 3D porous network of the hydrogel with an average pore size $\sim 76\text{ }\mu\text{m}$ (Table

4.2) for DN hydrogels. The average pore sizes of PEGDMA 4000Da, 6000Da, 8000Da, GelMA (21%) and ChMA (40%) are listed in Table 4.2 for the comparison of single networks with the DN hydrogels. It shows pore size decreases, followed by an increase as we change the molecular weight of PEGDMA from 4000 Da to 8000 Da. The observed trend is the result of two effects, molecular weight of PEGDMA and degree of methacrylation of GelMA. As the molecular weight of PEGDMA increases, there is an increase in the molecular weight between the crosslinking points, which increases the pore size. However, as the degree of methacrylation of GelMA increases, the number of pores among the crosslinking points becomes small, which gives a smaller pore size.

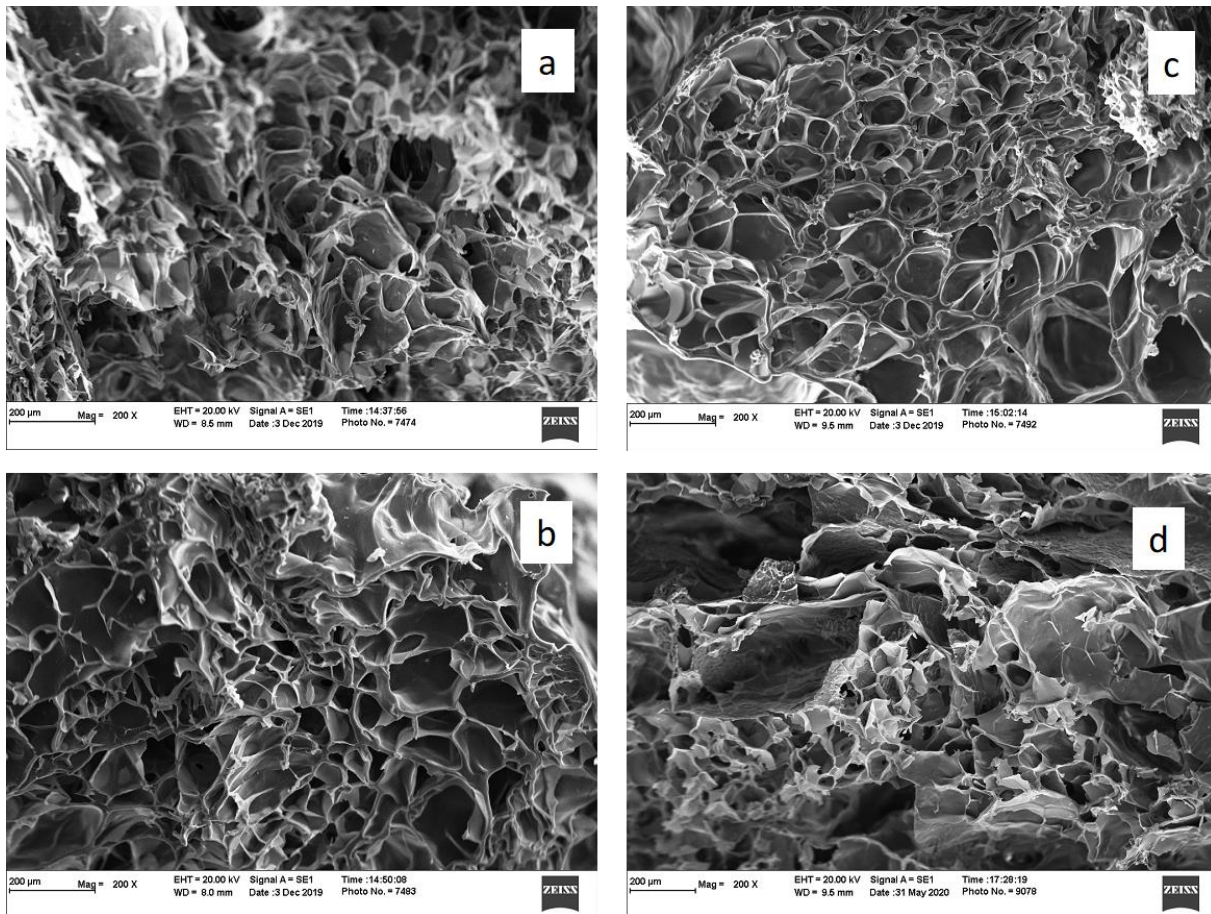


Figure 4.3: SEM image of a) P4G21%, b) P6G21%, c) P8G21% and d) P8C40% DN hydrogels

The porous structure is crucial for the cell dwelling, proliferation and cell culture on polymer-based hydrogel; on the other side, this open architecture affects the swelling and mechanical properties of the hydrogel, as can be observed in the following section.

Table 4.2: Comparison of morphology and swelling behavior for DN hydrogels

	Pore Size (μm)	Swelling Ratio (%)
PEGDMA 4000	61	1400 \pm 230
PEGDMA 6000	72	1500 \pm 64
PEGDMA 8000	87	1900 \pm 140
GelMA (21%)	27.4	475 \pm 122
ChMA (40%)	68.1	2208 \pm 240
P4G21%	74.1	708 \pm 39
P6G21%	64	588 \pm 20
P8G21%	79.5	678 \pm 30
P8C40%	88.2	2033 \pm 463

The water uptakes (%) of the synthesized DN hydrogels were calculated using equation 2. The obtained water uptake percentages are reported in Table 4.2 shows a decrease followed by an increasing effect. The observed trend is the result of two effects, molecular weight of PEGDMA and degree of methacrylation of GelMA or ChMA. As the molecular weight of PEGDMA is increased, the water uptake (or swelling ratio) is also increased. As the molecular weight of PEGDMA increases, there is an increase in the molecular weight between the crosslinking points, which increases the ability to swells. Nevertheless, the increase in the degree of methacrylation of GelMA decreases the water uptake. As the degree of methacrylation of GelMA increases, the number of pores among the crosslinking points becomes small, which gives less room for absorption.

Table 4.3: Characterization of the crosslinked DN hydrogels

	T_m (°C)	Δ H_m (J/g)	Crystallinity (%)	Compressive Modulus (kPa)	Shear Modulus (kPa)	Tensile Modulus (kPa)	Degradative weight loss (%)
P4G21%	22.83	17.93	18.2	8.41 ± 1.1	3.67 ± 0.05	8.4 ± 2.3	39 ± 1.6
P6G21%	29.57	25.37	25.8	10.8 ± 2.3	6.42 ± 0.86	13.9 ± 2.6	34 ± 1.2
P8G21%	44.23	27.79	28.2	9.97 ± 1.2	4.04 ± 0.85	16.1 ± 3.7	32 ± 1.1
P8C40%	27.33	7.15	7.3	77.6 ± 11.0	13.8 ± 1.1	21.2 ± 6.7	37 ± 1.3
GelMA (21%)	NA	NA	NA	30.4 ± 7.2	4.0 ± 0.6	NA	16 ± 3.8
ChMA (40%)	NA	NA	NA	33.0 ± 9.2	5.6 ± 0.9	NA	35 ± 5.5
PEGDMA 4000	48.42	70.57	35.9	17 ± 7	2.7 ± 0.73	13.1 ± 6.5	23 ± 1.1
PEGDMA 6000	56.31	109.3	55.5	18.8 ± 6	4.31 ± 0.68	20.7 ± 6.1	24 ± 1.2
PEGDMA 8000	57.93	151.6	77.0	16.5 ± 4	1.9 ± 0.43	31.3 ± 9.7	28 ± 1.4

Table 4.3 summarizes the heat of melting (ΔH_m) and melting temperatures (T_m) of the synthesized DN hydrogels. As the molecular weight of PEGDMA increases in the DN hydrogel, the crystallinity increases. Due to the increase in the molecular weight of PEG between crosslinking points, the linear PEG structure crystallized. As a result, the heat of melting increases and the melting temperature elevates hence. This tendency is the result of the reduced segmental mobility of the network due to the crystalline phase. Similar results have also been reported in the literature^{20,32}.

The mechanical behavior of the hydrogels is reported in Table 4.3. It can be observed that the compressive and shear modulus show an increase followed by a decreased effect, as the molecular weight of PEGDMA is increased. As explained, two factors are affecting modulus of the network, the crosslinking density, and the induced crystallinity. As we increase the molecular weight of PEGDMA, the molecular weight of the linear PEG increases the ability of the linear chains to crystallize, thus, increases the modulus. However, at higher molecular weight, the decrease of the crosslinking densities overpowers the effect of the crystallinity, reducing the modulus.

Moreover, from Table 4.3, it can be concluded that the trend of tensile modulus of DN hydrogels is similar to what we observe in different PEGDMA networks. Hence, to conclude, the tensile property in DN hydrogels is governed by the PEGDMA network in the double network hydrogels.

Figure 4.4 shows the degradation behavior of synthesized DN hydrogels with degradative weight loss for specific variety over a period of 8 weeks. In these experiments, a lysozyme solution served as the medium for biodegradation studies, which is similar to the physiological conditions found in the human body, which undergo normal metabolism of degradation. As the exposure to the lysozyme enzyme solution increased, the degree of degradation was also increased. It can be observed in figure 5, the DN hydrogel with the higher crosslinking density (lower molecular weight between crosslinking points) degrades at a slower rate as compared to PEGDMA 8000 Da. Moreover, having the larger pore size, PEGDMA 8000 allows a higher amount of the lysozyme solution to penetrate and degrade of the hydrogel.

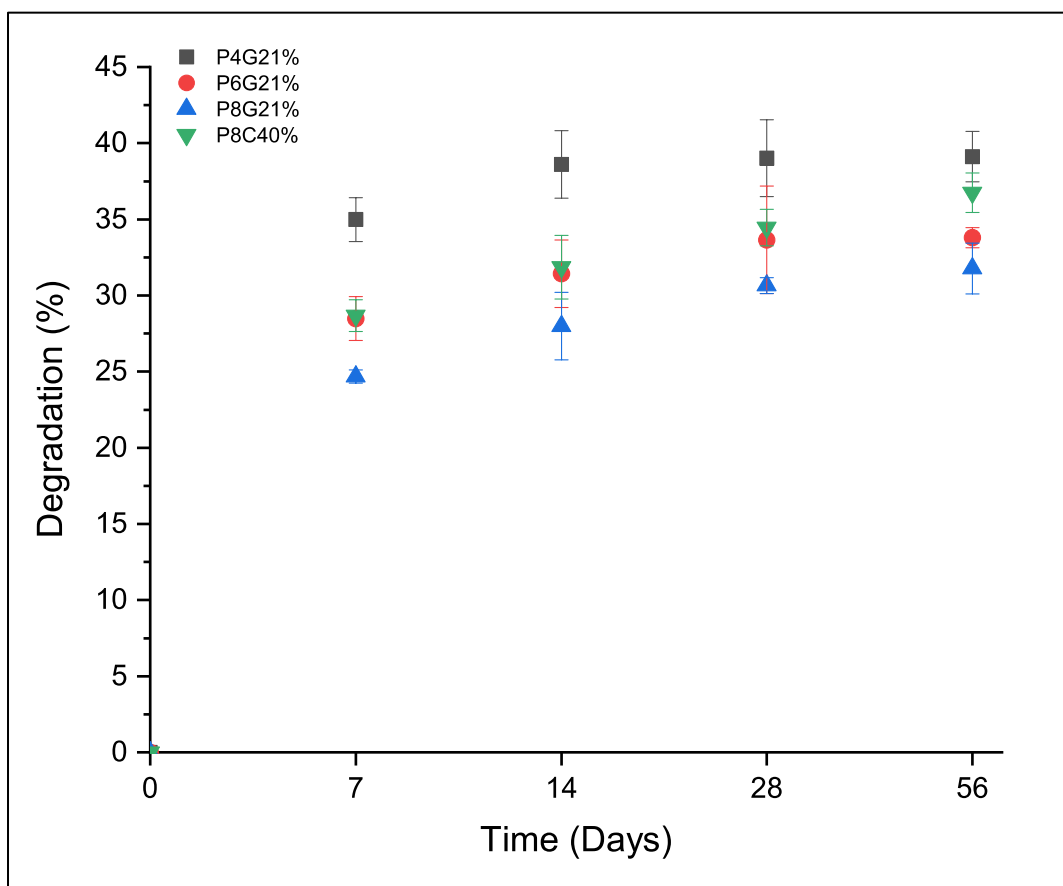


Figure 4.4: Degradation rate profile for different varieties of DN hydrogels with lysozyme

Figure 4.5 shows the morphology of DN hydrogels after 21 days of degradation. From the scanning electron microscopy (SEM), it is possible to observe the effect of the degradation process, as the porous structure collapses and fibrillar structures are formed.

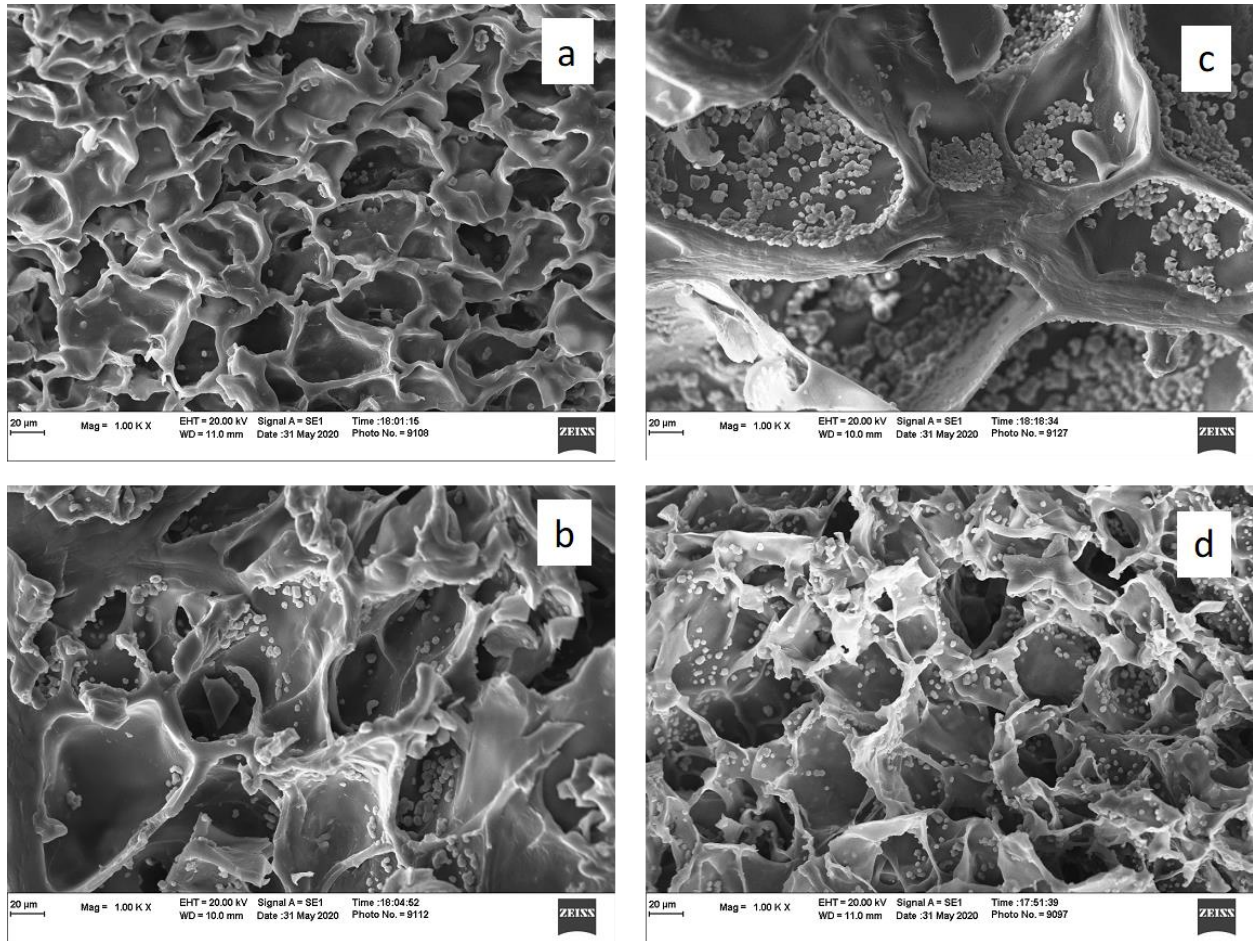


Figure 4.5: *Effect on the morphology after 3 weeks of degradation of following DN hydrogels a) P4G21%, b) P6G21%, c) P8G21%, and d) P8C40%*

4.3.2 Cell growth and proliferation on the hydrogel scaffolds

Our cell studies indicated fibroblast cell attachment and growth on the designed hydrogels for up to 7 days. Since the scaffolds are in the 3D architecture, the cells grown into the porous structures so that it becomes hard to count the actual number in the scaffolds. However, the cells in the scaffolds were confirmed by staining with Live/dead stain. Seeding efficiencies for our designed scaffold P4G21%, P6G21%, P8G21% and P8C40% were 76.4%, 78.8%, 61.8% and 72.9% respectively. Cell viability was estimated using MTT assay and showed viable cells up to 7 days

(Figure 4.6). However, the viability of cells decreased almost by 42-46% in 7 days on the designed scaffolds.

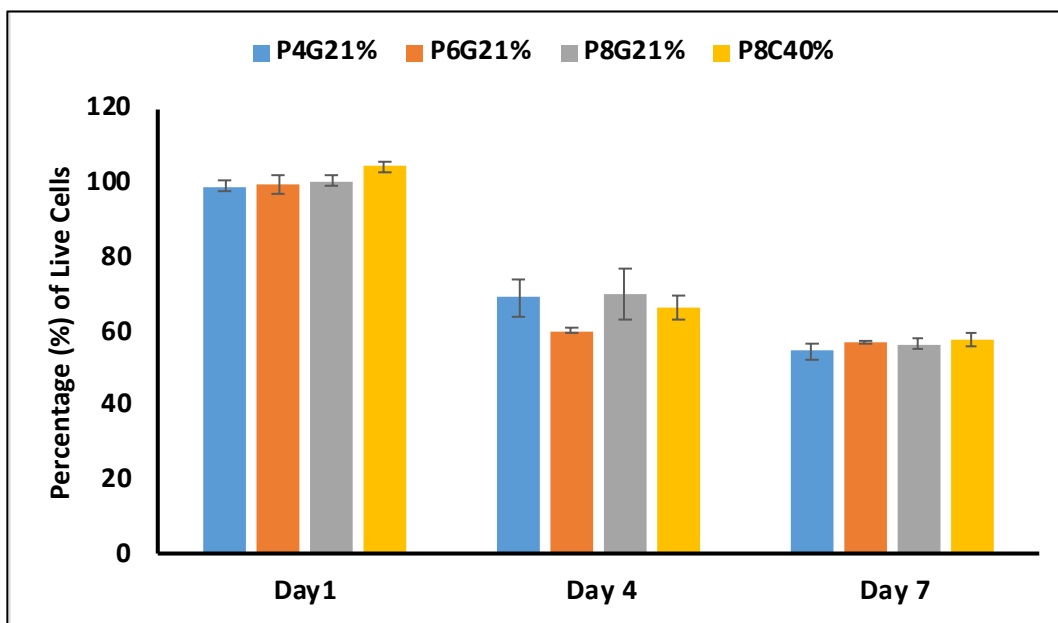


Figure 4.6: Cell viability of Fibroblast cells by MTT assay

4.4 Conclusion

PEGDMA-GelMA and PEGDMA-ChMA double network hydrogels were synthesized using PEGDMA macromer of different molecular weights (4000 Da, 6000 Da and 8000 Da) and modified polysaccharides such as GelMA and ChMA. Hydrogel samples undergo simultaneous free radical polymerization reaction in the presence of Irgacure 184 to obtain crosslinked double network (DN) hydrogels. The characterization of hydrogels illustrated their viability, biocompatibility, and mechanical strength for their applications in tissue engineering. Biodegradability and mechanical properties both are obtained synergistically using double networks (DN), thus making it more like living tissues. Also, performed for cell culture and

proliferation studies in our research work suggest, double network hydrogels have the potential to become functional for tissue regeneration inside the human body.

4.5 References

- (1) Ahmed, E. M. Hydrogel: Preparation, Characterization, and Applications: A Review. *J. Adv. Res.* **2015**, *6* (2), 105–121. <https://doi.org/10.1016/j.jare.2013.07.006>.
- (2) Lee, C. Y.; Teymour, F.; Camastral, H.; Tirelli, N.; Hubbell, J. A.; Elbert, D. L.; Papavasiliou, G.; Kousar, F.; Malana, M. A.; Chughtai, A. H.; et al. Synthesis and Characterization of Methacrylamide-Acrylic Acid-N-Isopropylacrylamide Polymeric Hydrogel: Degradation Kinetics and Rheological Studies. *Biomed. Mater.* **2018**, *155* (2), 1275–1298. <https://doi.org/10.1088/1748-605X/aa9ad2>.
- (3) Caló, E.; Khutoryanskiy, V. V. Biomedical Applications of Hydrogels: A Review of Patents and Commercial Products. *Eur. Polym. J.* **2015**, *65*, 252–267. <https://doi.org/10.1016/j.eurpolymj.2014.11.024>.
- (4) Hoare, T. R.; Kohane, D. S. Hydrogels in Drug Delivery: Progress and Challenges. *Polymer (Guildf)*. **2008**, *49* (8), 1993–2007. <https://doi.org/10.1016/j.polymer.2008.01.027>.
- (5) Fu, Y.; Xu, K.; Zheng, X.; Giacomini, A. J.; Mix, A. W.; Kao, W. J. 3D Cell Entrapment in Crosslinked Thiolated Gelatin-Poly(Ethylene Glycol) Diacrylate Hydrogels. *Biomaterials* **2012**, *33* (1), 48–58. <https://doi.org/10.1016/j.biomaterials.2011.09.031>.
- (6) Gopinathan, J.; Noh, I. Recent Trends in Bioinks for 3D Printing. **2018**, 1–15.
- (7) Khademhosseini, A.; Langer, R. Microengineered Hydrogels for Tissue Engineering. *Biomaterials* **2007**, *28* (34), 5087–5092. <https://doi.org/10.1016/j.biomaterials.2007.07.021>.
- (8) Peppas, N. A.; Hilt, J. Z.; Khademhosseini, A.; Langer, R. Hydrogels in Biology and Medicine: From Molecular Principles to Bionanotechnology. *Adv. Mater.* **2006**, *18* (11),

- 1345–1360. <https://doi.org/10.1002/adma.200501612>.
- (9) Baolin, G.; Ma, P. X. Synthetic Biodegradable Functional Polymers for Tissue Engineering: A Brief Review.
- (10) Cheng, Y.; Lu, J.; Liu, S.; Zhao, P.; Lu, G.; Chen, J. The Preparation, Characterization and Evaluation of Regenerated Cellulose/Collagen Composite Hydrogel Films. *Carbohydr. Polym.* **2014**, *107* (1), 57–64. <https://doi.org/10.1016/j.carbpol.2014.02.034>.
- (11) Matricardi, P.; Di Meo, C.; Coviello, T.; Hennink, W. E.; Alhaique, F. Interpenetrating Polymer Networks Polysaccharide Hydrogels for Drug Delivery and Tissue Engineering. *Adv. Drug Deliv. Rev.* **2013**, *65* (9), 1172–1187. <https://doi.org/10.1016/j.addr.2013.04.002>.
- (12) Arnold, M. P.; Daniels, A. U.; Ronken, S.; García, H. A.; Friederich, N. F.; Kurokawa, T.; Gong, J. P.; Wirz, D. Acrylamide Polymer Double-Network Hydrogels : Candidate Cartilage Repair Materials with Cartilage-Like Dynamic Stiffness and Attractive Surgery-Related Attachment Mechanics. **2011**. <https://doi.org/10.1177/1947603511402320>.
- (13) Li, H.; Wang, H.; Zhang, D.; Xu, Z.; Liu, W. A Highly Tough and Stiff Supramolecular Polymer Double Network Hydrogel. *Polymer (Guildf)*. **2018**, *153*, 193–200. <https://doi.org/10.1016/j.polymer.2018.08.029>.
- (14) Li, Z.; Wu, C.; Liu, Z.; Li, Z.; Peng, X.; Huang, J.; Ren, J.; Wang, P. A Polypropylene Mesh Coated with Interpenetrating Double Network Hydrogel for Local Drug Delivery in Temporary Closure of Open Abdomen †. **2020**, 1331–1340. <https://doi.org/10.1039/c9ra10455k>.
- (15) Haque, M. A.; Kurokawa, T.; Gong, J. P. Super Tough Double Network Hydrogels and Their Application as Biomaterials. *Polymer*. Elsevier Ltd April 17, 2012, pp 1805–1822.

- <https://doi.org/10.1016/j.polymer.2012.03.013>.
- (16) Lei, K.; Li, Z.; Zhu, D.; Sun, C.; Sun, Y.; Yang, C.; Zheng, Z.; Wang, X. Polysaccharide-Based Recoverable Double-Network Hydrogel with High Strength and Self-Healing Properties. **2020**, 794–802. <https://doi.org/10.1039/c9tb01679a>.
 - (17) Haque Md. Anamul, Kurokawa Takayuki, G. J. P. Super Tough Double Network Hydrogels and Their Application as Biomaterials. *Polymer (Guildf)*. **2012**, 53, 1805–1822.
 - (18) Monteiro, N.; Thirivikraman, G.; Athirasala, A.; Tahayeri, A.; França, C. M.; Ferracane, J. L.; Bertassoni, L. E. Photopolymerization of Cell-Laden Gelatin Methacryloyl Hydrogels Using a Dental Curing Light for Regenerative Dentistry. *Dent. Mater.* **2018**. <https://doi.org/10.1016/j.dental.2017.11.020>.
 - (19) Blaine, R. L.; Ph, D. Determination of Polymer Crystallinity by DSC. 1–3.
 - (20) Pielichowski, K.; Flejtuch, K. Differential Scanning Calorimetry Studies on Poly (Ethylene Glycol) with Different Molecular Weights for Thermal Energy Storage Materials †. **2003**, 696 (November 2001), 690–696. <https://doi.org/10.1002/pat.276>.
 - (21) ASTM D695-15. Standard Test Method for Compressive Properties of Rigid Plastics. *ASTM Int.* **2015**.
 - (22) ASTM D1708-93. Standard Test Method for Tensile Properties of Plastics by Use of Microtensile Specimens. *ASTM Int.* **1993**.
 - (23) Lončarević, A.; Ivanković, M.; Rogina, A. Lysozyme-Induced Degradation of Chitosan: The Characterisation of Degraded Chitosan Scaffolds. *J. Tissue Repair Regen.* **2017**, 19 (1), 177.
 - (24) *Handbook of Polymers for Pharmaceutical Technologies, Biodegradable Polymers*; Thakur Vijay Kumar, T. M. K., Ed.; Scrivener Publishing, 2015.

- (25) Sarem, M.; Moztaarzadeh, F.; Mozafari, M.; Shastri, V. P. No Title. *Mater. Sci. Eng. C* **2013**, *33*, 4777–4785.
- (26) Saraiva Sofia M, Miguel Sonia P, Ribeiro Maximiano P, Coutinho Paula, C. I. J. Synthesis and Characterization of a Photocrosslinkable Chitosan-Gelatin Hydrogel Aimed for Tissue Regeneration. *RSC Adv.* **2015**, *5*, 63478–63488.
- (27) Yang C, Xu L, Zhou Y, Zhang X, Huang X, Wang M, Han YK, Zhai M, Wei S, L. J. A Green Fabrication Approach of Gelatin/CM-Chitosan Hybrid Hydrogel for Wound Healing. *Carbohydr. Polym.* **2010**, *82*, 1297–1305.
- (28) Monier, M.; Wei, Y.; Sarhan, A. A.; Ayad, D. M. No Title. *Polymer (Guildf)*. **2010**, *51*, 1002–1009.
- (29) Escudero-Castellanos, A.; Ocampo-García, B. E.; Domínguez-García, M. V.; Flores-Estrada, J.; Flores-Merino, M. V. Hydrogels Based on Poly(Ethylene Glycol) as Scaffolds for Tissue Engineering Application: Biocompatibility Assessment and Effect of the Sterilization Process. *J. Mater. Sci. Mater. Med.* **2016**, *27* (12).
<https://doi.org/10.1007/s10856-016-5793-3>.
- (30) Guo X, Wang W, Wu G, Zhang J, Mao C, D. Y. et al. Controlled Synthesis of Hydroxyapatite Crystals Templated by Novel Surfactants and Their Enhanced Bioactivity. *New J Chem.* **2011**, *35*, 663–671.
- (31) Cheing BW, Ibrahim NA, Yunus WMZW, H. M. Poly (Lactic Acid)/Poly (Ethylene Glycol) Polymer Nanocomposites: Effects of Graphene Nanoplatelets. *Polymers (Basel)*. **2013**, *6*, 93–104.
- (32) Yasmin, M.; Gupta, M. Thermodynamical Study of Alcoholic Solutions of Poly (Ethylene Glycol) Diacrylate and Poly (Ethylene Glycol) Dimethacrylate. **2012**, *15* (2),

111–117. <https://doi.org/10.5541/ijot.371>.

CHAPTER 5

Design and synthesis of stereolithography (SLA) 3D printed poly (ethylene glycol) diacrylate (PEGDMA) based hydrogels for biomedical applications

5.1 Introduction

Additive manufacturing is a new technique utilized to produce complex-structured. In the medical field, it has the potential to be used to repair or replace damaged or diseased human tissues and organs. The flexibility and the level of control available by these computer-aided technologies to design and fabricate tissue scaffold expedite our understanding of tissue formation and function¹.

The fundamental concept underlying tissue engineering is to develop complex tissue structures to mimic native organs and tissues^{1,2}. Besides the physicochemical properties of the scaffold, the micro-architecture of the constructs is essential for the tissue formation process. Three-dimensional (3D) printing technique is reported to have precise control over the developed structures than other methods^{2,3}. Therefore, customization of very complex structures such as tissue scaffolds with required porosity, permeability, and other required properties is made possible². The significant advantages of 3D printing in the medical field have been made possible the creation of complex structures within a short period, with high precision, and patient-specific designs. Among the different 3D printing techniques, fused deposition modeling (FDM), direct ink writing (DIW), selective laser sintering (SLS), and stereolithography (SLA) are the most commonly considered for medical applications. In particular, SLA method is used in manufacturing scaffolds where the curing process takes place without affecting the sharpness and resolution of the printed material³.

Stereolithography (SLA) is one of the most commonly used technique where the 3D object is fabricated by selective photo-initiated cure reaction of a polymer in a layer by layer way¹⁻⁴. Although it is one of the few techniques with accuracies comparable to the size of a cell, yet the system has not been developed enough that enables handling materials³ with different compositions. Significant advances in work have been made using other techniques like DIW^{5,6} and inkjet printing^{6,7}. However, these techniques had issues with dispensing of highly viscous liquid from cartridges or syringes through a nozzle².

Photo-crosslinkable biopolymers, including hyaluronic acid⁸⁻¹⁰, chitosan^{11,12}, and gelatin¹³ derivatives, have been considered as one of the many biomaterials for SLA printing. Although natural polymers or hydrogels allows the desired microenvironment for simulating the native extracellular matrix for cell attachment and proliferation, there is a limitation in tuning properties of these polymers. Therefore, it is recommended to combine these natural polymers with synthetic polymers to obtain a more stable entity with synergy in properties. The synthetic polymers based on poly(ethylene glycol)¹⁴⁻¹⁶ are the most commonly used in 3D printing. Sometimes a single network may not promote adequate cellular adhesion or mechanical performance, but if combined with other polymeric systems can help in tuning the properties such as performance, printability adhesion, etc².

In this work, we focused on the synthesis of different types of bioink formulations from biopolymers like poly(ethylene glycol)diacrylate (PEGDA), poly(ethylene glycol)dimethacrylate (PEGDMA), gelatin methacrylate (GelMA) and chitosan methacrylate (ChMA). The bioinks were 3D printed in the presence of a photoinitiator (Darocure TPO) using the stereolithography

technique. Chemical, mechanical, and physical characteristics of these hydrogels were studied to create medical scaffolds.

5.2 Materials and Methods

5.2.1 Materials

In this study, linear poly (ethylene glycol) (PEG) was used: PEG (Mw ~ 8000 g/mol) purchased from Acros Organics (US). Gelatin powder (Type A, ~300 bloom) was purchased from Electron Microscopy Sciences (US), and chitosan ($\geq 85\%$ deacetylated) was obtained from Alfa Aesar (US). Methacrylic anhydride was purchased from Thermofisher Scientific Inc. (US). Dichloromethane (DCM) and anhydrous diethyl ether were purchased from VWR International LLC (US). Poly (ethylene glycol) diacrylate (PEGDA) (575 Da) was purchase from Sigma Aldrich (US). Acrylic acid (AA) and trimethylolpropane triacrylate (TT) were purchased from Alfa Aesar (US). Dulbecco's phosphate buffered saline (DPBS) and acetic acid were purchased from VWR (US). Photoinitiator, 2,4,6-Trimethylbenzoyl-diphenyl-phosphineoxide (Darocure TPO) was purchased from TCI (US), while the UV light source used (UVLS-28 EL Series UV Lamp) was manufactured by Analytik Jena (US). The photon stereolithography (SLA) 3D printer was purchased from Shenzhen ANYCUBIC Technology Co., Ltd (China).

5.2.2 Methods

5.2.2.1 Preparation of the bioink formulation

The individual polymeric systems PEGDMA, GelMA, and ChMA were first synthesized as described in the previous chapters. Briefly, poly(ethylene glycol) (PEG) was mixed with 10 molar excess of methacrylic anhydride via microwave synthesis to obtain the PEGDMA samples. Gelatin methacrylation was carried out using 5% (w/v) in Dulbecco's phosphate buffered saline (DPBS) and methacrylic anhydride (35.67 molar excess) at 60°C. It was then dialyzed for purification followed by lyophilization at 4 MPa and -50°C to obtain the pure gelatin methacrylate (GelMA) and stored at -80°C until further use. Chitosan methacrylation was carried out using 3% (w/v) in 1-2% (w/v) acetic acid aqueous solution and methacrylic anhydride (35.67 molar excess) at 25°C and was freeze-dried at 4 MPa and -50°C to obtain the pure chitosan methacrylate (ChMA) and stored at -80°C until further use. Finally, four types of bioink formulation based on multiple polymer network hydrogels were synthesized; the composition are summarized in Table 5.1. Darocure TPO, 2% (w/v) was used as a photoinitiator in the final mixture of bioink before proceeding to the SLA 3D printing step.

Table 5.1: Composition of Bioink formulation

	PEGDMA 8000	PEGDA 575	GelMA (21%)	ChMA (40%)	Acrylic Acid	TT*
100% (weight)	70%				30%	
Type 1- PEGDA 575	0	70%	0	0	25%	5%
Type 2- PEGDMA- PEGDA (1:1)	35%	35%	0	0	25%	5%
Type 3- PEGDMA- PEGDA-GelMA (1:1:2)	17.5%	17.5%	35%	0	25%	5%
Type 4- PEGDMA- PEGDA-ChMA (1:1:2)	17.5%	17.5%	0	35%	25%	5%
* <i>trimethylolpropane triacrylate (TT)</i>						

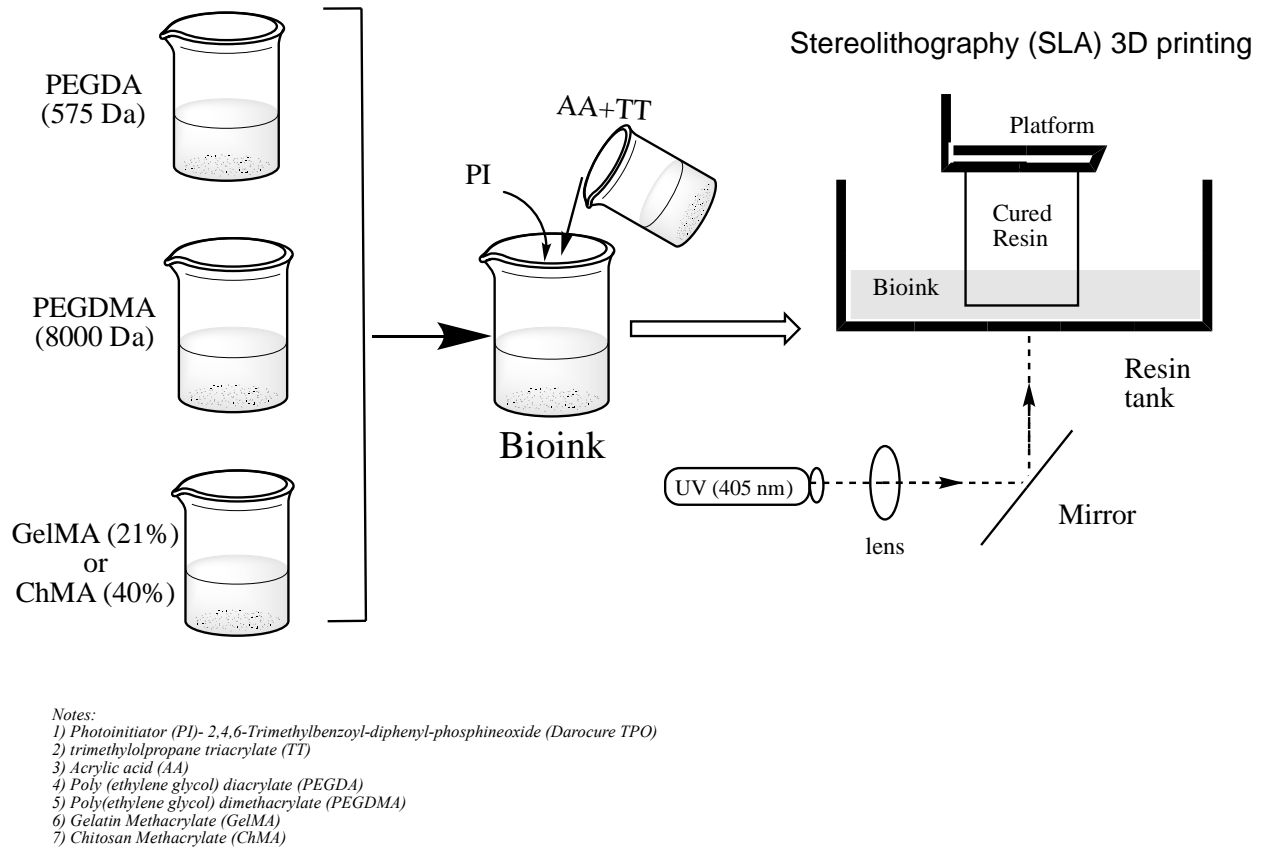


Figure 5.1: Bioink formulation for SLA 3D printing.

5.2.2.2 SLA 3D printing

3D hydrogel samples were printed using stereolithography technique (SLA), as explained in Figure 1. Initially, the bioink was mixed with the Darocure TPO photoinitiator (decomposition wavelength of 405nm) and then was poured into the resin tank. Then, the bioink was exposed to a UV laser of 405nm and cured in a layer-by-layer fashion. Finally, the cured resin in the form of 3D printed part is removed from the platform and cleaned to remove excess bioink. The STL file of the 3D-cellular structure was sliced using photon software (Photon_workshop_V1.0.0_Basic_Edition) to get a photon file ready to feed the SLA 3D printer. For SLA 3D printing of cellular structure; the exposure time utilized was 16s/layer over 853 layers

total, off time was 5s, bottom exposure was 80 s/layer for eight (8) bottom layers, Z lift distance: 4mm, Z lift speed: 3mm/s and Z retract speed: 3mm/s.

5.2.2.3 SLA 3D printed Samples

The following pictures represent different 3D printed structures developed in our laboratory. The synthesized bioink formulations were 3D printed in different shapes and sizes, such as cellular ring, complex structure, etc.

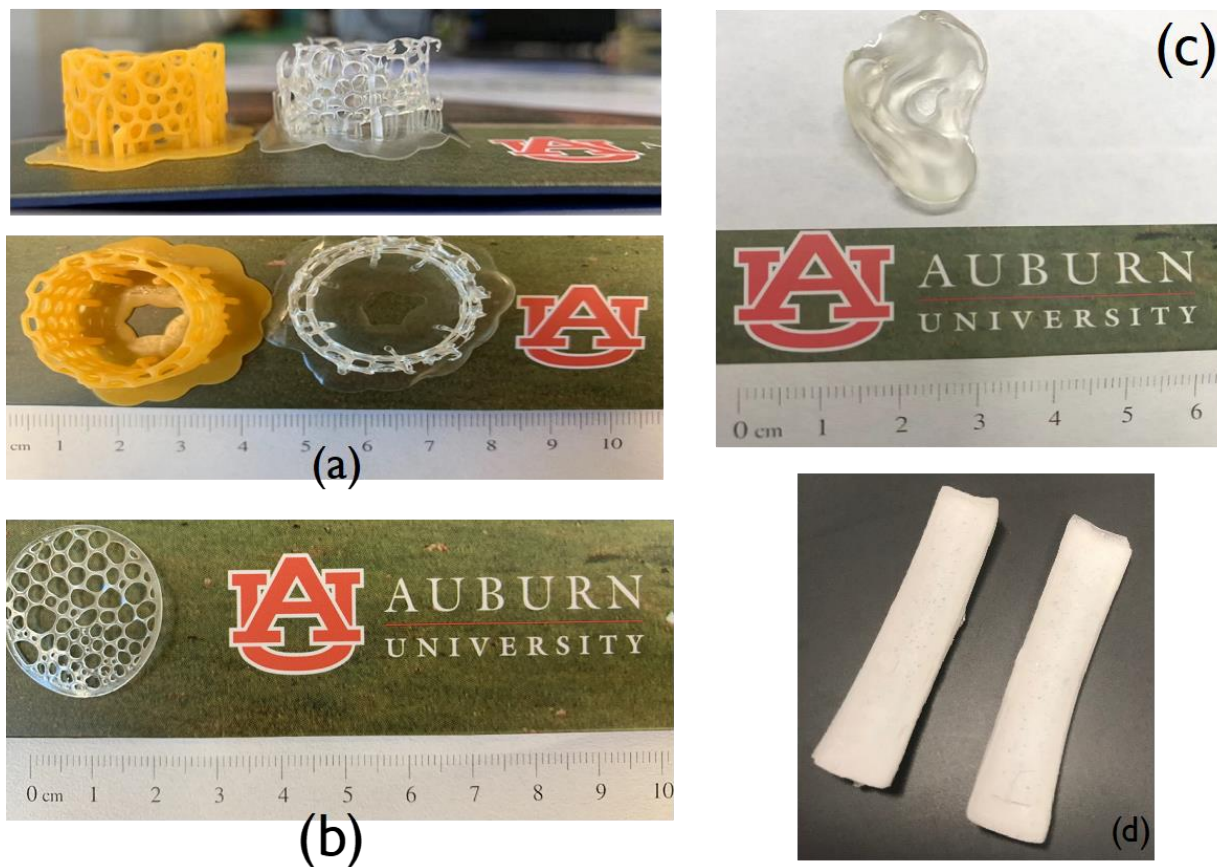


Figure 5.2: 3D printed structures. a) cellular ring (using Type 2 bioink), b) cellular structure (using Type 2 bioink), c) human ear (using Type 2 bioink), and d) rectangular strips (using Type 3 bioink)

5.2.2.4 Characterization of 3D printed samples

Infrared spectra of the PEGDMA (8000 Da), PEGDA (575 Da), GelMA (21%), ChMA (40%) and the 3D printed parts from the four different types were measured by attenuated total reflection (ATR) method using a Thermo Nicolet 6700 Fourier transform infrared spectrometer. The spectrums were analyzed using OMNIC 7.3 software to study the functionality of chemical structures. All spectra were recorded between 400 and 4000 cm^{-1} over 256 scans with a resolution of 4 cm^{-1} .

The swelling analysis was performed in hydrogel samples lyophilized in a freeze dryer and weighed to obtain dry sample weight (W_d). Then, samples were immersed in distilled water at room temperature for 48 hours to reswell the samples. The swollen hydrogels were removed from the water and after wiping the excess water on the surface were weighed to obtain the weight of the wet sample (W_w). Swelling ratios were calculated using the following equation:

$$\text{Mass Swelling (\%)} = \left(\frac{W_w - W_d}{W_d} \right) * 100 \quad (1)$$

The mechanical properties of the hydrogels were tested with the help of a dynamic mechanical analyzer (DMA) TA Instrument RSAIII. Tensile tests were performed according to the ASTM standards ASTM D1708-93¹⁷. The tensile analysis was carried out on rectangular swollen hydrogels specimens with 15 mm initial length, using an extension rate of 0.1667 mm/s, for 3-6 replicates. During tensile testing, data for any hydrogel that slipped off the clamped area or broke as a result of being next to the metallic surface was not considered. From this data, the tensile modulus was determined.

5.3 Results and Discussion

5.3.1 FTIR

FTIR analysis of the 3D printed parts (Type-1, 2 and PEGDMA 8000) was performed to characterize and confirm the chemical crosslinking among the different polymer chains after the free radical polymerization occurred through stereolithography. The FTIR spectrum (Figure 5.2a) displays the comparison of characteristic bands at 1722 cm^{-1} in all 3D printed hydrogels in Figure 5.2a, which represent C=O stretching mode of ester groups^{18,19}. The strong bands at $\sim 2880\text{ cm}^{-1}$ and $\sim 1466\text{ cm}^{-1}$ represents the $-\text{CH}_2$ bonds^{18,19}. The peaks at $\sim 1092\text{ cm}^{-1}$ and $\sim 946\text{ cm}^{-1}$ represent the asymmetrical C-O-C stretching mode²⁰.

Figure (5.2b and c) depicts FTIR analysis of the Type-3 and 4 of the multinetwork bioink after 3D printing and its comparison with the GelMA and ChMA counterparts. In the GelMA spectrum (Figure 2b), the peak at 1589 cm^{-1} corresponds to N-H stretch of amide (II)²¹⁻²³. The peaks at 2938 and 1633 cm^{-1} represent C-H stretch and C=C stretching vibrations in GelMA spectrum, respectively²². Similarly, the FTIR spectrum of PEGDMA-PEGDA-ChMA (Figure 5.2c) depicts the peaks at 2930 and 1666 cm^{-1} corresponding to the C-H and C=C stretches of the amide group, respectively^{22,24}. Moreover, the 1055 cm^{-1} peak belongs to C-O-C stretch and the 1543 cm^{-1} represented N-H of amide (II) stretching mode²² in the ChMA spectrum.

To summarize, the peaks corresponding to N-H and C=C are seen with small intensity in the PEGDMA-PEGDA-GelMA and PEGDMA-PEGDA-ChMA spectra, which gives the evidence for the disappearance of the C=C functionality present in PEGDMA, GelMA, and PEGDA for the UV-curing of the bioink to fabricate the 3D printed hydrogel. To highlight, the peak at 1636 cm^{-1} ,

assigned to the C=C, which is seen as a small peak or disappears in all of the spectra, shows the success of the free radical polymerization reaction carried out in stereolithography process as the bioink is cured.

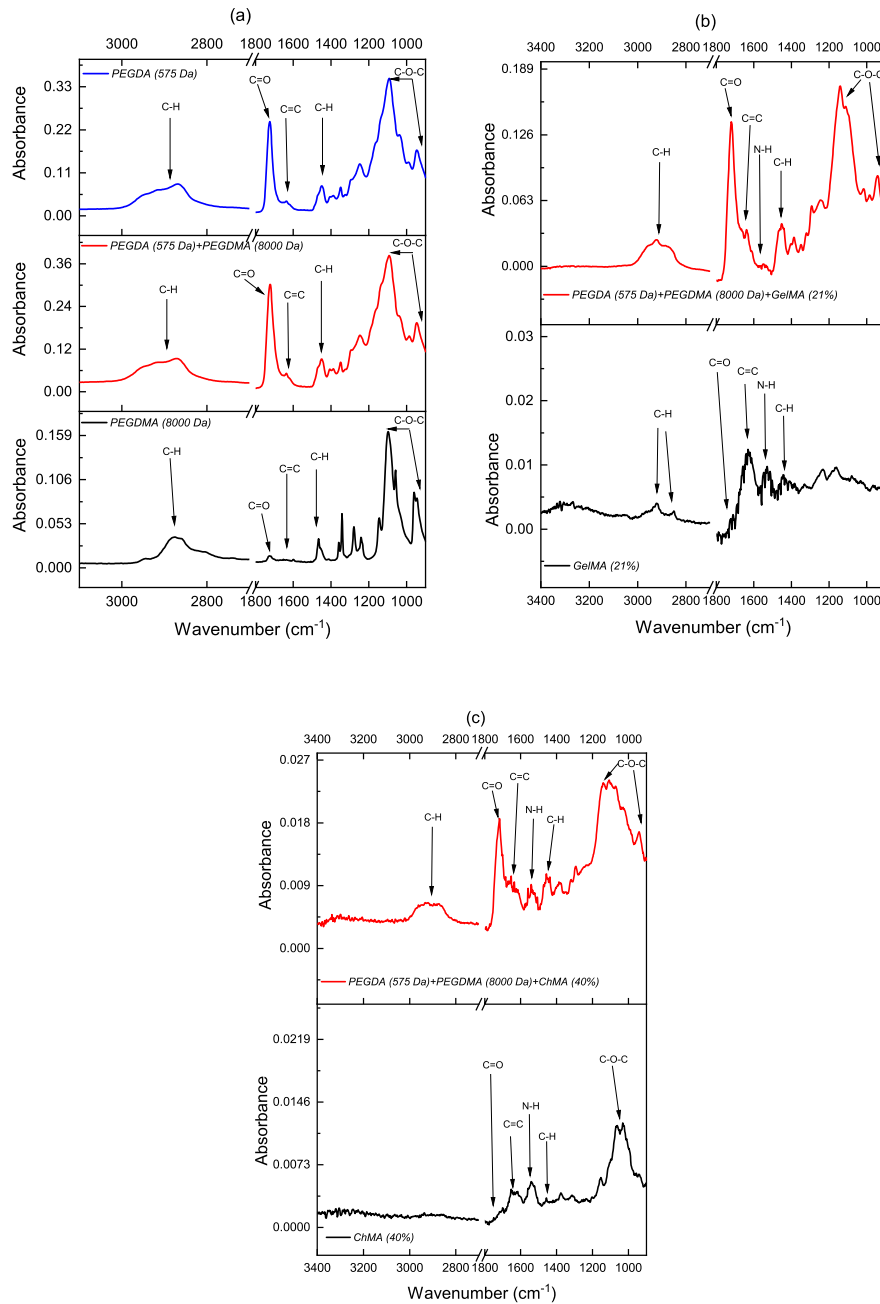


Figure 5.3: FT-IR spectrum for a) Type 1 (PEGDA) and Type 2 (PEGDMA-PEGDA) bioink formulations, b) Type 3 (PEGDMA-PEGDA-GelMA) bioink, c) Type 4 (PEGDMA-PEGDA-ChMA) bioink formulation

5.3.2 Mass Swelling

The water uptakes (%) of the synthesized DN hydrogels were calculated using equation 2. The obtained water uptake percentages are reported in Table 5.2. It can clearly be observed that there is a considerable increase as the polysaccharides like GelMA and ChMA are utilized in the bioink formulation. From Chapter 3, we have reported that the GelMA and ChMA have larger pore sizes. Therefore, the 3D printed structures from Type 3 and 4 bioinks give more swelling tendency. Moreover, the crosslinking is higher in the case of Type 1 and 2, which determines that the swelling behavior is low. PEGDMA 8000 swells the most when it is printed in the absence of crosslinking system (acrylic acid-AA and trimethylolpropane triacrylate-TT), as the hydrogel is least crosslinked in that case which allows maximum room for absorption.

Table 5.2: Characterization of 3D printed hydrogels

SLA 3D printing	Swelling (%)	Elastic Modulus (kPa)
PEGDMA 8000 (absence of AA and TT)	1937 ± 141	21.3 ± 9.5
Type 1- PEGDA 575	32 ± 3	1151.7 ± 484.8
Type 2- PEGDMA-PEGDA (1:1)	40 ± 6	2056.3 ± 654.8
Type 3- PEGDMA-PEGDA-GelMA (1:1:2)	93 ± 19	1505.5 ± 406.3
Type 4- PEGDMA-PEGDA-ChMA (1:1:2)	309 ± 14	1611.2 ± 716.6

5.3.3 Tensile Modulus

The mechanical behavior of the hydrogels is also reported in Table 5.2. It can be observed that the trend of tensile elastic modulus of 3D printed hydrogels is majorly dependent on the crosslinking process. The trimethylolpropane triacrylate (TT) and acrylic acid (AA) acts as a crosslinking

monomer for the bioink; its presence increases the mechanical performance of the hydrogels. From the swelling behavior, we can observe that the presence of GelMA and ChMA tend to increase the swelling. Therefore, the 3D printed structures from Type 3 and 4 bioinks give low elastic modulus. Moreover, the crosslinking is higher in the case of Type 2, which determines that the modulus is highest when both PEGDMA and PEGDA get crosslinked along with the crosslinking system. PEGDMA 8000 swells the most when it is printed in the absence of a crosslinking system (AA and TT), as the hydrogel is least crosslinked in that case, which explains the lowest mechanical property for PEGDMA 8000.

5.4 Conclusion

PEGDMA, GelMA and ChMA based hydrogels samples were synthesized and utilized in formulating different bioinks. Further, the bioinks were 3D printed in the presence of UV radiation (405 nm) via stereolithography to obtain crosslinked hydrogels. The characterization of hydrogels illustrated their mechanical strength in the range 20 kPa- 2000 kPa for their potential applications in tissue engineering.

5.5 References

- (1) Melchels, F. P. W.; Domingos, M. A. N.; Klein, T. J.; Malda, J.; Bartolo, P. J.; Huttmacher, D. W. Additive Manufacturing of Tissues and Organs. *Prog. Polym. Sci.* **2012**, *37* (8), 1079–1104. <https://doi.org/10.1016/j.progpolymsci.2011.11.007>.
- (2) Gopinathan, J.; Noh, I. Recent Trends in Bioinks for 3D Printing. **2018**, 1–15.
- (3) Lee, J. M.; Yeong, W. Y. Design and Printing Strategies in 3D Bioprinting of Cell-Hydrogels: A Review. *Adv. Healthc. Mater.* **2016**, *5* (22), 2856–2865. <https://doi.org/10.1002/adhm.201600435>.
- (4) Billiet, T.; Vandenhaute, M.; Schelfhout, J.; Van Vlierberghe, S.; Dubruel, P. A Review of Trends and Limitations in Hydrogel-Rapid Prototyping for Tissue Engineering. *Biomaterials* **2012**, *33* (26), 6020–6041. <https://doi.org/10.1016/j.biomaterials.2012.04.050>.
- (5) Miri, A. K.; Khalilpour, A.; Cecen, B.; Maharjan, S.; Shin, S.-R.; Khademhosseini, A. Multiscale Bioprinting of Vascularized Models. *Biomaterials* **2018**. <https://doi.org/10.1016/j.biomaterials.2018.08.006>.
- (6) Derakhshanfar, S.; Mbeleck, R.; Xu, K.; Zhang, X.; Zhong, W.; Xing, M. 3D Bioprinting for Biomedical Devices and Tissue Engineering: A Review of Recent Trends and Advances. *Bioact. Mater.* **2018**, *3* (2), 144–156. <https://doi.org/10.1016/j.bioactmat.2017.11.008>.
- (7) Los Angeles Poly (Ethylene Glycol) -Based Photo-Curable Bioink in Inkjet 3D Printing of Pharmaceutical Tablets for Hydrophobic Drugs A Thesis Submitted in Partial Satisfaction of the Requirements for the Degree Master of Science in Bioengineering by Tim. **2017**.

- (8) Prestwich, G. D. Molecule Delivery in Regenerative Medicine. **2013**, *155* (2), 193–199.
<https://doi.org/10.1016/j.jconrel.2011.04.007.Hyaluronic>.
- (9) Schuurman, W.; Levett, P. A.; Pot, M. W.; van Weeren, P. R.; Dhert, W. J. A.; Hutmacher, D. W.; Melchels, F. P. W.; Klein, T. J.; Malda, J. Gelatin-Methacrylamide Hydrogels as Potential Biomaterials for Fabrication of Tissue-Engineered Cartilage Constructs. *Macromol. Biosci.* **2013**, *13* (5), 551–561.
<https://doi.org/10.1002/mabi.201200471>.
- (10) Ouyang, L.; Highley, C. B.; Rodell, C. B.; Sun, W.; Burdick, J. A. 3D Printing of Shear-Thinning Hyaluronic Acid Hydrogels with Secondary Cross-Linking. **2016**.
<https://doi.org/10.1021/acsbiomaterials.6b00158>.
- (11) Croisier, F.; Jérôme, C. Chitosan-Based Biomaterials for Tissue Engineering. *Eur. Polym. J.* **2013**, *49* (4), 780–792. <https://doi.org/10.1016/j.eurpolymj.2012.12.009>.
- (12) Morris, V. B.; Nimbalkar, S.; Younesi, M.; McClellan, P.; Akkus, O. Mechanical Properties, Cytocompatibility and Manufacturability of Chitosan:PEGDA Hybrid-Gel Scaffolds by Stereolithography. *Ann. Biomed. Eng.* **2017**, *45* (1), 286–296.
<https://doi.org/10.1007/s10439-016-1643-1>.
- (13) Wang, Y.; Ma, M.; Wang, J.; Zhang, W.; Lu, W.; Gao, Y.; Zhang, B.; Guo, Y. Development of a Photo-Crosslinking , Biodegradable GelMA/PEGDA Hydrogel for Guided Bone Regeneration Materials. *Materials (Basel)*. **2018**, *11* (1345), 1–12.
<https://doi.org/10.3390/ma11081345>.
- (14) Son, K. H.; Lee, J. W. Synthesis and Characterization of Hydrogels for Cell Sheet Engineering. **2016**. <https://doi.org/10.3390/ma9100854>.
- (15) Kerscher, P. Human developing cardiac tissues for scale-up and disease. **2016**.

- (16) Tan, F.; Xu, X.; Deng, T.; Yin, M.; Zhang, X.; Wang, J. Fabrication of Positively Charged Poly(Ethylene Glycol)-Diacrylate Hydrogel as a Bone Tissue Engineering Scaffold. *Biomed. Mater.* **2012**, 7 (5). <https://doi.org/10.1088/1748-6041/7/5/055009>.
- (17) ASTM D1708-93. Standard Test Method for Tensile Properties of Plastics by Use of Microtensile Specimens. *ASTM Int.* **1993**.
- (18) Escudero-Castellanos, A.; Ocampo-García, B. E.; Domínguez-García, M. V.; Flores-Estrada, J.; Flores-Merino, M. V. Hydrogels Based on Poly(Ethylene Glycol) as Scaffolds for Tissue Engineering Application: Biocompatibility Assessment and Effect of the Sterilization Process. *J. Mater. Sci. Mater. Med.* **2016**, 27 (12). <https://doi.org/10.1007/s10856-016-5793-3>.
- (19) Guo X, Wang W, Wu G, Zhang J, Mao C, D. Y. et al. Controlled Synthesis of Hydroxyapatite Crystals Templated by Novel Surfactants and Their Enhanced Bioactivity. *New J Chem.* **2011**, 35, 663–671.
- (20) Cheing BW, Ibrahim NA, Yunus WMZW, H. M. Poly (Lactic Acid)/Poly (Ethylene Glycol) Polymer Nanocomposites: Effects of Graphene Nanoplatelets. *Polymers (Basel)*. **2013**, 6, 93–104.
- (21) Sarem, M.; Moztarzadeh, F.; Mozafari, M.; Shastri, V. P. No Title. *Mater. Sci. Eng. C* **2013**, 33, 4777–4785.
- (22) Saraiva Sofia M, Miguel Sonia P, Ribeiro Maximiano P, Coutinho Paula, C. I. J. Synthesis and Characterization of a Photocrosslinkable Chitosan-Gelatin Hydrogel Aimed for Tissue Regeneration. *RSC Adv.* **2015**, 5, 63478–63488.
- (23) Yang C, Xu L, Zhou Y, Zhang X, Huang X, Wang M, Han YK, Zhai M, Wei S, L. J. A Green Fabrication Approach of Gelatin/CM-Chitosan Hybrid Hydrogel for Wound

Healing. *Carbohydr. Polym.* **2010**, 82, 1297–1305.

- (24) Monier, M.; Wei, Y.; Sarhan, A. A.; Ayad, D. M. No Title. *Polymer (Guildf)*. **2010**, 51, 1002–1009.

CHAPTER 6

General Conclusions and Future Work

Polymers, like poly(ethylene glycol), gelatin and chitosan, were modified using methacrylation reaction for allowing it to possess chemical functionality. The chemically modified polymers were utilized for the synthesis of hydrogels. The compositional information and confirmation for the presence of specific functional groups like C=C, C=O, O-H, C-H, N-H, and C-O-C were obtained using the chemical characterization of modified polymers, ¹H-NMR spectroscopy, and FTIR spectroscopy. The end functionality in the modified polymers reacted in the presence of UV and photoinitiator to produce desired hydrogels with porous structures.

In chapter two, the different varieties of poly(ethylene glycol) dimethacrylate (PEGDMA) were synthesized from poly(ethylene glycol) (PEG) of different molecular weights using microwave-assisted methacrylation reaction. The PEGDMA hydrogels were produced using different varieties of PEGDMA by free-radical polymerization in the presence of a photoinitiator (Irgacure 184). The characterization of these hydrogels suggested that the crystallinity of PEGDMA increases as the molecular weight increases, but modulus (compressive and shear) remains similar to the change of molecular weight. Cellular studies with fibroblast cells and enzymatic biodegradability confirm that PEGDMA hydrogels can be used as material for cell growth and application towards tissue engineering.

In chapter three, the polysaccharides like gelatin and chitosan were incorporated with methacrylate functionality. The modified gelatin and chitosan were synthesized by controlling the degree of

methacrylation of primary amine groups present in the polysaccharides. ¹H-NMR spectroscopy and FTIR spectroscopy proved the successful formation of methacrylate functionality. Methacrylated gelatin (GelMA) and methacrylated chitosan (ChMA) were photocured (365nm) in the presence of a photoinitiator (Irgacure 184) at room temperature to obtain the hydrogels of polysaccharide. From the characterization, we can report that increase in the degree of methacrylation decreases the pore size of hydrogels and mass swelling; but improves the mechanical and rheological performance of the hydrogel. Cellular studies with fibroblast cells and enzymatic biodegradability confirm that GelMA and ChMA hydrogels can be used as material for cell growth and application towards tissue engineering.

In chapter four, the properties of poly(ethylene glycol) dimethacrylate (PEGDMA) macromer and the modified polysaccharides were combined in double networks (DN) for synergistic effects of unique properties of both components resulting in the interpenetrating polymeric network for making it functional for replacement of injured tissues inside the human body. The different DNs were synthesized using PEGDMA, GelMA and ChMA with different combinations and were photocured (365nm) in the presence of a photoinitiator (Irgacure 184) at room temperature to obtain the double network hydrogels. FTIR spectroscopy confirmed the successful interpenetration of the double networks within a hydrogel. Excellent mechanical and morphological behavior, along with cellular studies with fibroblast cells and enzymatic biodegradability, confirms that DN hydrogels can be a good candidate for tissue-engineered scaffolds.

In the final chapter, the synthesized PEGDMA, GelMA, and ChMA were used to formulate different types of bioinks, which can be used for stereolithography (SLA) 3D printing. The

varieties of bioinks were fed to printed and then underwent layer-by-layer photocuring at 405 nm in the presence of photoinitiator, 2,4,6-Trimethylbenzoyl-diphenyl-phosphineoxide (Darocure TPO). Acrylic acid (AA) and trimethylolpropane triacrylate (TT) were used as a crosslinking system for better interlayer adhesion. The properties of the hydrogel allow it to undergo 3D fabrication for a complex-structured scaffold for particular tissue engineering.

In general, polymeric hydrogels materials can be used in medicine due to their similarity with the biological components of the body. These biocompatible materials like poly(ethylene glycol) and polysaccharides have the potential to promote cell proliferation and tissue support because of their hydrophilic nature, porous structure, and elastic properties. Controlling the chemical transformation (degree of methacrylation) and molecular structure, it can be observed that the hydrophilicity, mechanical properties, and cell responsivity of modified polysaccharides can be tuned for different tissue engineering applications. The results show that we have a range of elastic modulus and degradation rate of hydrogels, which can be targeted for various biomedical applications. The future of this research will involve a detailed understanding of bioprinting and feasibility for generating patient-specific tissue-engineered scaffolds. The understanding of these hydrogels for different drug delivery applications as well as with different cell lines is required for targeting the applications inside human body. In the field of additive manufacturing, it is required to consider the printability of SLA 3D printing along with hydrogel based bioinks. Moreover, challenges of interlayer adhesion, viscosity of bioink and improper printing needs more research for better applicability of these hydrogel based bioink in the biomedicine.